Alma Mater Studiorum · Università di Bologna

SCUOLA DI INGEGNERIA E ARCHITETTURA
Corso di Laurea Magistrale in Automation Engineering

Modelling, stability, and control of DAE numerical integration

Tesi in Control Engineering

Relatore:
Chiar.mo Prof.
LORENZO MARCONI

Co - Relatori:
Chiar.mo Prof.
THOMAS PARISINI
Chiar.mo Prof.
ALESSANDRO ASTOLFI
Dott.
PIERLUIGI DI FRANCO

Candidato:
FEDERICO OLIVA

III Sessione

Anno Accademico 2019/2020

"Quando uno scienziato non sa la risposta a un problema è ignorante; quando ha una vaga idea della possibile soluzione è incerto; e quando, dannazione, è sicuro del risultato, ha ancora qualche dubbio. Noi scienziati ci siamo abituati, e diamo per scontato che sia perfettamente coerente non essere sicuri, che si possa vivere e non sapere."

R. Feynman

A te, che stai leggendo; grazie,
perchè quando ti chiedo di fare con me un miglio,
tu ne fai due.

Abstract

This thesis deals with the integration of differential algebraic equations systems. Generally speaking the execution of numerical integration algorithms may introduce some errors, which could propagate ending up in a wrong description of system dynamics. This issue, named drifting, will be highlighted by dealing with a specific constrained mechanical system presenting. Such system consists of a looper, which is a mechanism used in the steel production to sense and control the tension acting on the material. The thesis unfolds as follows: a first section model the looper and inspects the main properties related to its joint space and singularities. A brief introduction to stability analysis on multidof systems is proposed. Then, the thesis proceeds analysing looper stability properties, eventually finding a globally asymptotic stable configuration. Lastly, the drifting is highlighted by numerical simulations. To solve this issue two control algorithms are proposed: the first is the Baumgarte algorithm [8] and the second consists of a nonlinear stabilizer [7]. A performance comparison of both algorithms is then presented at the end of the implementation description. All the code used for the symbolic analysis and the numerical simulations is available under request at Federico Oliva github page.

Contents

Chapter 1

Modelling of mechanical constrained systems

Differential Algebraic Equations (DAE) consist of a composite set of differential and algebraic equations. They are widely used in engineering as they accurately describe multiple set-up. DAEs can be both linear and nonlinear. In this thesis we mostly deal with nonlinear DAEs describing mechanical systems subject tp holonomic constraints.

1.1 Mechanical Systems - Lagrange modelling

Mechanical systems are usually composed by a set of rigid bodies interconnected through joints. The structure of the interconnection dictates the number of dof the system. Typically the joints are actuated and their position can be expressed through the set of variables $b = (b_1, \ldots, b_n)^T$. The number of joints is related to the number of dof. The kinematic chain defining the mechanical system is usually provided with an endpoint, namely a structure executing a specific action. Such endpoint is instead described through its Cartesian coordinates. With respect to this description, the following concepts are introduced.

1. **Joint space**. all the joint variables can be stacked in a single vector:

$$b = [b_1, \ldots, b_n]^T \in \mathcal{B} \subset \mathbb{R}^{N_{dof}} \tag{1.1}$$

   The set $\mathcal{B}$ is called joint space, and contains all the possible values that the joint variables may assume. Note that for each $b \in \mathcal{B}$, there is a unique configuration of the mechanical structure[1].

2. **Work-space**. The work-space is a subset of the Euclidean space $\mathbb{E}$ in which the robot executes its tasks. It is the set of all the points (configurations) that the mechanical structure may assume, and in general is a 3D (2D) subset of $\mathbb{E}$. Each point of the work-space is indicated by a vector x of proper dimension, that is $x \in \mathbb{R}^y$, where usually $y = \{3, 6\}$.

3. **Configuration**. It takes into account both the position and the orientation of a reference frame fixed to the system endpoint. Then, locally:

   a) $x \in \mathbb{R}^3$ if the system evolves in a plane

b) $x \in \mathbb{R}^6$ if the system evolves in space

In describing mechanical systems, two main problems have to be addressed, namely the direct and the inverse kinematic problem [1].

1. **Direct kinematic.** Once the position, velocity and acceleration of the joints are known, it is useful to determine the corresponding kinematic entities in the work-space. This problem is solved through the so called direct kinematic model, namely

$$x = f(b), \quad b \in \mathcal{B}, x \in \mathbb{R}^y. \tag{1.2}$$

2. **Inverse kinematic.** Once the position,velocity and acceleration of a point in the work-space, the inverse kinematic problem is about determining the corresponding entities in the joint space. This is done finding the inverse mapping of the direct kinematic model, namely

$$b = g(x) = f^{-1}(x), \quad b \in \mathcal{B}, x \in \mathbb{R}^y. \tag{1.3}$$

Note that it is possible to define different kinematic models for a given mechanism, although equivalent from a mathematical point of view. Mechanical systems are of particular interest when dealing with algebraic constraints. In fact, it is not unusual for system work-space and joint space to be limited in terms of kinematic entities such as position and velocity.

Roughly speaking mechanical constraints can be divided into two main types [2].

- *holonomic*. Affecting both the configuration and the velocity (instantaneous motion) of the system.
- *non-holonomic*. Affecting only the velocity (instantaneous motion) of the system.

Indeed, it is way easier to deal with an unconstrained system. However, in some cases it is impossible to avoid them or, even, it is preferable to have them. For instance, when non-holonomic constraints contain non-integrable velocity expressions or when holonomic constraints are described by a set of redundant coordinates. Recall that a general mapping $f : \mathbb{R} \to \mathbb{R}$ is said to be integrable on a specific interval $[a; b]$ if

$$\int_a^b f(\tau)d\tau = \overline{M} < \infty \tag{1.4}$$

For example, constrained systems are used to achieve specific trajectories. Consider a general mechanical system and its joint space variables $b \in \mathcal{B}$; as often happens, such variables are inconvenient to describe the configuration of the system. Therefore, a set of redundant variables can be defined in order to simplify system description. These variables are referred to as *generalised coordinates* and defined by the vector

$$q = \begin{bmatrix} q_1 \\ \vdots \\ q_n \end{bmatrix} \in: \mathbb{R}^n. \tag{1.5}$$

Such coordinates are uniquely related to the joint space variables b by means of a mapping, namely

$$q = \Psi(b), \quad \Psi : \mathbb{R}^{N_{dof}} \to \mathbb{R}^n. \tag{1.6}$$

Finally, the generalised coordinates are a redundant yet more convenient way to describe the behaviour of the system. They will be used in the proposed modelling procedure in subsection 1.2.2. Generalised velocities are defined as the time derivative of the generalised coordinates, namely

$$\dot{q} = \frac{dq}{dt} = \begin{bmatrix} \dot{q}_1 \\ \vdots \\ \dot{q}_n \end{bmatrix}. \tag{1.7}$$

Generally speaking, constraints are expressed both in *configuration* form and in *velocity* form. The former description uses the system generalised coordinates, while the latter uses the system generalised velocities. It follows that the configuration form refers to the effects of the constraint on the system position and orientation. The two forms have the following structure.

- *Configuration form*:
$$f(q_1, \ldots, q_n, t) = 0. \tag{1.8}$$
- *Velocity form*:
$$g(\dot{q}_1, \ldots, \dot{q}_n, t) = 0. \tag{1.9}$$

A constraint is said to be *holonomic* if it can be expressed in configuration form or in an integrable velocity form[1].

Mechanical constrained systems can be modelled through the *Lagrange Multipliers* method. This method is discussed in section 1.1.3. As it will be shown, it is derived as the unconstrained energetic Lagrange approach (subsection 1.1.1) but with some modifications.

1.1.1 Lagrange equations for unconstrained systems

This section describes the modelling procedure for general unconstrained mechanical systems via the Lagrange method. The *Lagrange equations* provide a simple method to model mechanical systems by using an energetic approach. In this section no constraints are considered. In order to develop this method two definitions are needed ([2] and [3]). Let $\mathbf{P} = P(q_1, \ldots, q_n, t)$ be a mapping of system position, and $v_p = \dot{\mathbf{P}}$ the correspondent system velocity. The vector $(q_1, \ldots, q_n)$ defines the system independent generalised coordinates.

[1] See Equation 1.4

Definition 1 (Virtual displacement)**.** *A virtual displacement consists of a infinitesimal quantity, consistent with system constraints and obtained by considering time as fixed and changing only the generalised coordinates. Namely, a virtual displacement is defined as:*

$$\delta \mathbf{P} = \sum_{k=1}^{n} \frac{\partial \mathbf{P}}{\partial q_k} \delta q_k. \tag{1.10}$$

Definition 2 (Virtual work)**.** *Consider a force F acting on the system over a virtual displacement $\delta \mathbf{P}$. Its virtual work is defined as*

$$\delta L = F \cdot \delta \mathbf{P}. \tag{1.11}$$

The main result developed over the defined framework above is the so called *virtual work principle.*

Theorem 1. *A system is in dynamic equilibrium if and only if the virtual work performed by the external forces and by the internal dissipative forces equals the virtual variation of the kinetic energy, namely:*

$$\delta L - \delta T = 0. \tag{1.12}$$

Considering that $\delta T = -\delta L_I$ the following equivalent statement holds:

$$\delta L + \delta L_I = 0, \tag{1.13}$$

where δL_I is the virtual work developed by system inertia forces. Moreover, if conservative and non-conservative external forces are distinguished, it holds:

$$\delta L_I + \delta L_{NC} - \delta U = 0, \tag{1.14}$$

where U stands for the potential energy of the system.

From the considerations above it holds that the total work done by a set of external forces acting on the system can be defined as

$$\delta \mathbf{L} = \sum_{k=1}^{n} Q_k \delta q_k, \tag{1.15}$$

where Q_k is defined as *generalised force* associated to the generalised coordinate q_k. Defining $\mathcal{L} = T - U$ as the *Lagrangian* function the following result can be proved [3].

$$\sum_{k=1}^{n} \left[\frac{d}{dt} \left(\frac{\partial \mathcal{L}}{\partial \dot{q}_k} \right) - \frac{\partial \mathcal{L}}{\partial q_k} - Q_{NC,k} \right] \delta q_k = 0, \tag{1.16}$$

which will be referred from now on as the *virtual work equation.* In this equation the term $Q_{NC,k}$ represents the generalised non-conservative force performing work due to the virtual displacement δ_{q_k} considered. By removing the virtual displacement terms a set of n equations is obtained. This set describes the mechanical system by means of the generalised coordinates $(q_1, \ldots, q_n)$.

Systems with friction If the system considered also has friction terms the previous formulation can be straightforwardly extended by adding a *friction energy* term. This term is added to the Lagrangian function and then differentiated with respect to the generalised coordinates. The additional term is in the general form

$$R = \frac{1}{2}\sum_{i=1}^{m} \mu_i x_i^2 + \frac{1}{2}\sum_{j=1}^{p} c_j \dot{\theta}_j^2 \tag{1.17}$$

where μ_i and c_j are the friction coefficients associated to the linear and torsional dampers. The new Lagrangian function is defined as $\mathcal{L} = T - U - R$ and the Lagrange equations are

$$\sum_{k=1}^{n} \left[\frac{d}{dt}\left(\frac{\partial T}{\partial \dot{q}_k}\right) - \frac{\partial T}{\partial q_k} + \frac{\partial U}{\partial q_k} + \frac{\partial R}{\partial \dot{q}_k} - Q_{NC,k} \right] \delta q_k = 0 \tag{1.18}$$

1.1.2 Constraints definition

This section defines the main guidelines for dealing with general constraints. Consider a system described by n generalised coordinates. Consider also a set of m equality constraints. Generally speaking the number of *dof* is $n - m$. This aspect will be clarified in subsection 1.2.1. For the time being assume the number of *dof* to be $p = n - m$.

The system constraints are described in velocity form as follows:

$$\sum_{k=1}^{n} a_{jk}\dot{q}_k + a_{j0} = 0 \quad j = \{1, 2, \ldots, m\}, \tag{1.19}$$

where a_{jk} and a_{j0} are scalar coefficients. Consider now the virtual displacements on the generalised coordinates. The variations of the constraints can be defined as

$$\sum_{k=1}^{n} a_{jk}\delta q_k = 0 \quad j = \{1, 2, \ldots, m\}. \tag{1.20}$$

All the description above are defined for a single constraint, identified by the index j. Clearly, considering this formulation for a general constraint, there is no longer any difference in the way holonomic and non-holonomic constraints are treated.

1.1.3 Lagrange multipliers method

This section describes a modification to the Lagrange equations approach in order to take into account also constraints acting on the system. Consider a set of constraints defined accordingly to subsection 1.1.2. The first step in the method consists in multiplying the constraint description in Equation 1.20 by a set of algebraic variables λ_j called *Lagrangian multipliers* and then sum up the whole result.

$$\sum_{j=1}^{m}\sum_{k=1}^{n} \lambda_j a_{jk}\delta q_k = 0 \quad j = \{1, 2, \ldots, m\}. \tag{1.21}$$

At this stage of the method no restrictions on the magnitude of the multipliers are imposed. Moreover, the summation order in Equation 1.21 is irrelevant.

The main difference between unconstrained and constrained systems is that the generalised coordinates q_k and their virtual displacements δq_k are not independent entities anymore. In fact, constraints define a precise algebraic relation between generalised coordinates q_k. Lagrangian multipliers are introduced specifically to force the constraints to be satisfied. Actually, their physical interpretation is strictly related to the constraint reactions, widely use in Newton modelling approach. However, as far as the model formulation, they can be treated as input for the system. Back to the magnitude consideration previously pointed out, it is clear that the higher the value of the multipliers, the stronger the force acting on the mechanism. Therefore, by looking at the magnitude of the multipliers it is possible to understand in which configurations the system is subject to excessive strain.

Recall the *virtual work equation* defined in Equation 1.11. By adding the multipliers to the former set of Lagrangian equations, a new model is obtained.

$$\begin{cases} \frac{d}{dt}\left(\frac{\partial \mathcal{L}}{\partial \dot{q}_k}\right) - \frac{\partial \mathcal{L}}{\partial q_k} - Q_{NC,k} + \sum_{k=1}^{n} \lambda_j a_{jk} & = 0 \quad k = \{1, 2, \dots, n\} \\ \sum_{k=1}^{n} a_{jk}\dot{q_k} + a_{j0} & = 0 \quad j = \{1, 2, \dots, m\} \end{cases} \tag{1.22}$$

Such system is a set of $n + m$ equations: the first n are differential equations while the last m are algebraic ones. Differential equations describe the dynamics of the system while the algebraic ones are in charge of the relations between the generalised coordinates imposed by the constraints. These kind of equations set can be solved in two ways:

- *algebraic manipulation.* Manipulating the system in order to eliminate the Lagrangian multipliers. By doing so the system boils down to a set of $n - m$ equations.
- *numerical integration.* Solve the system by using a numerical scheme specifically suited for such tasks.

Holonomic constraints - coefficient computation

Consider a system subject only to m holonomic constraints. Those can be assumed to be expressed in the form of Equation 1.8. Proceed by taking the derivative of the configuration form, in order to obtain the velocity form of the constraint.

$$\frac{df_j}{dt} = \sum_{k=1}^{n} \frac{\partial f_j}{\partial q_k}\dot{q}_k + \frac{\partial f_j}{\partial t} = 0 \quad j = \{1, \dots, m\}. \tag{1.23}$$

This equation coincides with the constraint velocity form described in Equation 1.19, whith the following coefficients:

$$\begin{cases} a_{jk} = \frac{\partial f_j}{\partial q_k}\dot{q}_k \\ a_{j0} = \frac{\partial f_j}{\partial t} \end{cases} \tag{1.24}$$

1.2 Mechanical Systems - case of study

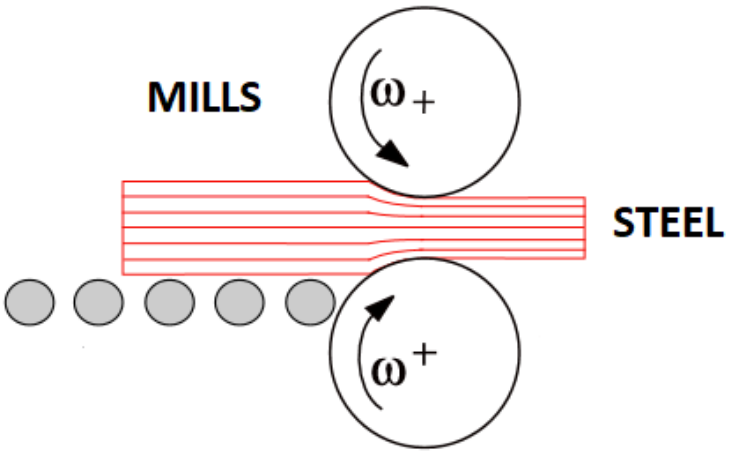

Figure 1.1: Lamination process - simplification model

The mechanism analysed in this thesis is a *looper* [4]. A looper is a mechanism widely used in steel production to sense and control the tension acting on the material. More precisely, the looper is used during the hot-rolling procedure of steel. This procedure aims to turn reheated steel into strips which will be further processed later on. Basically, the reheated steel passes through a set of mills being eventually thickened. The process is simplified in Figure 1.1.

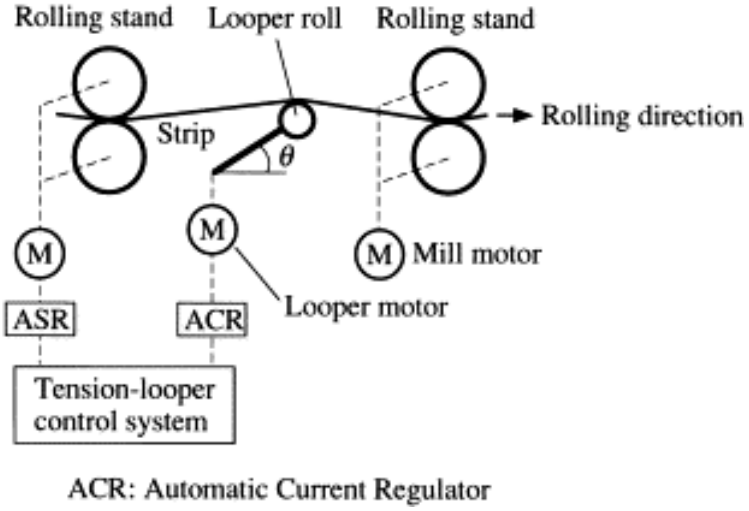

Figure 1.2: Looper configuration

It goes without saying that tension control has a huge role in this process. In fact, by keeping tension constant between the mills, folds and rips can be avoided in the material. The general structure of the hot-roller and of the looper can be seen in Figure 1.2. However, the structure of the mills is here oversimplified. In fact, the flow of reheated steel is initially processed by the so called *stands*, namely horizontal cages thickening the material. These stands are placed sequentially one after the other. The steel flows from a stand to the following one. During its path the looper is used to tight the material and to keep its tension constant. Such structure can be seen in Figure 1.3.

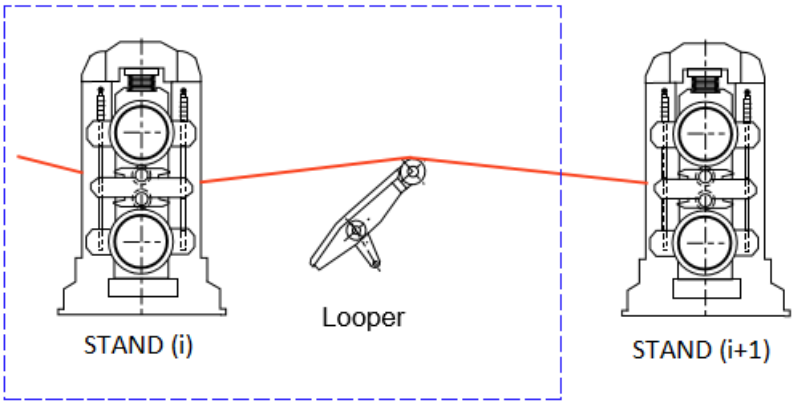

Figure 1.3: Structure of the lamination process - stands and looper

1.2.1 Looper - model description

The simplified model of looper showed in Figure 1.3 has been expanded ending up with the mechanism in Figure 1.4.

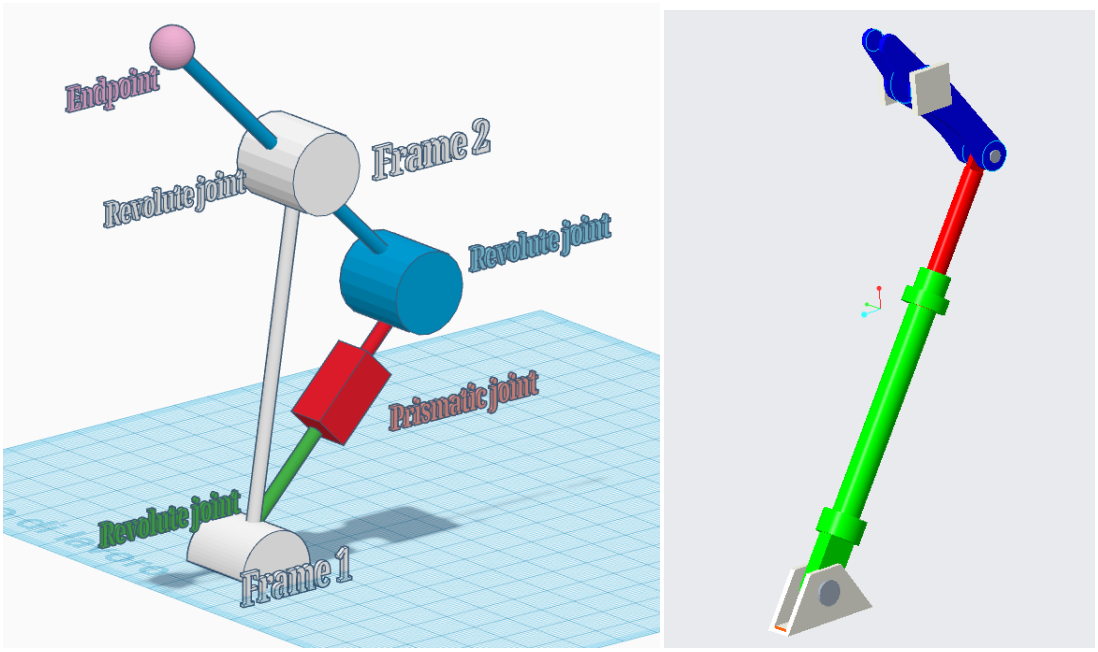

(a) Looper simplified 3D model (b) Looper CAD model

Figure 1.4: Lyapunov 3D models W

Such model consists of a fixed frame on which two revolute joints have been mounted and positioned respectively on **Frame 1** and on **Frame 2**. A first link (green in the model) is attached to the revolute joint in **Frame 1** and to a prismatic joint which is also connected to the second link (red in the model). Therefore the first two links of the mechanism define a 2-dof motion system. The second link is then connected to a second revolute joint as well as the third link (blue in the model). This third link is finally connected to the revolute joint in **Frame 2**. This link continues up to the endpoint (pink in the model). The steel strip is assumed to flow over the endpoint, pushing down on it. Indeed, the system can't assume any position in the workspace due to the connection between link 2 and link 3. Clearly, the blue revolute joint

is responsible for the algebraic constraints acting on the system. The third link is here represented as homogeneous but actually its weight is concentrated on the part near the blue revolute joint. This is done to limit the inertia forces on the endpoint, resulting in a more robust and reliable structure. Such structure is visible in the CAD 3D model (Figure 1.4).

The mechanism just described has been also modelled in a 3D CAD environment. However, its motion develops on a plane. Therefore a planar dof analysis can be performed by means of the *Grubler* formula for planar mechanisms:

1. The system is build up by 4 links (**frame**, first link, second link, third link).
2. Recall that Any joint with i dof is defined as a joint of class C_i. Both prismatic and revolute joints allow a single dof. Therefore they are all of class C_1.

The Grubler formula for planar mechanisms states:

$$N_{dof} = 3(m-1) - 2C_1 - C_2 \tag{1.25}$$

where N_{dof} stands for the number of dof of the system, m the number of links, C_1 the number of joints of class C_1, and C_2 the number of joints of class C_2. The looper has $m = 4$, $C_1 = 4$, $C_2 = 0$ and therefore $N_{dof} = 1$.

This mechanism includes a closed loop kinematic chain. Thus it's an example of parallel robot.

In order to model and analyse the system, parametric entities have been defined; they are all presented in Table 1.1 and they refer to the 2D model description in Figure 1.5[2]. Note that the origin is assumed to be placed on **Frame 1**, on the rolling point of the first revolute joint.

1.2.2 Looper - Lagrange modelling

This section goes through the looper model description and analysis. In the first paragraph the system is considered as unconstrained and the model equations are derived; in the second the algebraic constraints are described and added to the previous model.

Unconstrained system

Considering the Lagrange approach presented in subsection 1.2.2 the first step of the modelling procedure consists in describing the system in terms of generalised coordinates, namely:

$$\begin{cases} q_1 = \theta_1 \\ q_2 = s \\ q_3 = \theta_2 \end{cases} \tag{1.26}$$

The looper is made up by 3 moving elements, whose centres of mass will be defined as G_1, G_2, G_3. Their position can be instantly described as a function of the generalised coordinates.

[2]All the values has been estimated from the CAD model in Figure 1.4. The material considered material is steel ($\rho = 7827.082 Kg/M^3$).

Table 1.1: Model parameters

Variable	Value	Description
θ_1	-	angular position of the first/second link
s	-	elongation of the prismatic joint
θ_2	-	angular position of the third link
Geometric parameter	**Value**	**Description**
R_{G1}	0.703 m	position of first link's baricenter
R_{G2}	0.674 m	position of second link's baricenter
R_{G3}	0.182 m	position of third link's baricenter
R_{12}	0.29 m	first link's length
R_{23}	1.392 m	second link's length
R_{34}	0.55 m	distance from second revolute joint and Frame 2
R_3	0.85 m	third link's length
R_x	0.8 m	x coordinate of Frame 2
R_y	2.2 m	y coordinate of Frame 2
Dynamic parameter	**Value**	**Description**
M_1	130.6 Kg	first link mass
M_2	66.8 Kg	second link mass
M_3	86.71 Kg	third link mass
J_1	32.55 $Kg \cdot m^2$	first link inertia
J_2	10.18 $Kg \cdot m^2$	second link inertia
J_3	5.63 $Kg \cdot m^2$	third link inertia
C_1	10^5 Kg/s	first revolute joint friction
C_2	10^5 Kg/s	prismatic joint friction
C_3	10^5 Kg/s	second revolute joint friction
g	9.8 m/s^2	gravitational acceleration
F	0 N	external force magnitude
α	0°	external force orientation

$$\begin{cases} G_1 &= (R_{G1}\cos q_1, R_{G1}\sin q_1) \\ G_2 &= ((R_{12}+R_{G2}+q_2)\cos q_1, (R_{12}+R_{G2}+q_2)\sin q_1) \\ G_3 &= (R_x + R_{G3}\cos q_3, R_y - R_{G3}\sin q_3) \end{cases} \tag{1.27}$$

In order to proceed the kinetic and potential energy terms shall be computed. They are defined in the following general form.

$$T = \frac{1}{2}\sum_{k=1}^{n} M_k V_{Gk}^2 + \frac{1}{2}\sum_{k=1}^{n} J_k \omega_{Gk}^2, \tag{1.28}$$

$$U = g\sum_{k=1}^{n} M_k h_k + \frac{1}{2}\sum_{p=1}^{m} k_p x^2, \tag{1.29}$$

where V_{Gk} are the linear velocities of the center of mass, ω_{Gk} the angular velocities, M_k the masses, J_k the inertias with respect to the center of mass, h_k the center of masses height with respect to the origin, and k_p the spring capacities.

In order to compute these terms, the velocities of the centres of mass are needed. Both linear and angular velocities can be computed from Equation 1.27 through simple time differentiation.

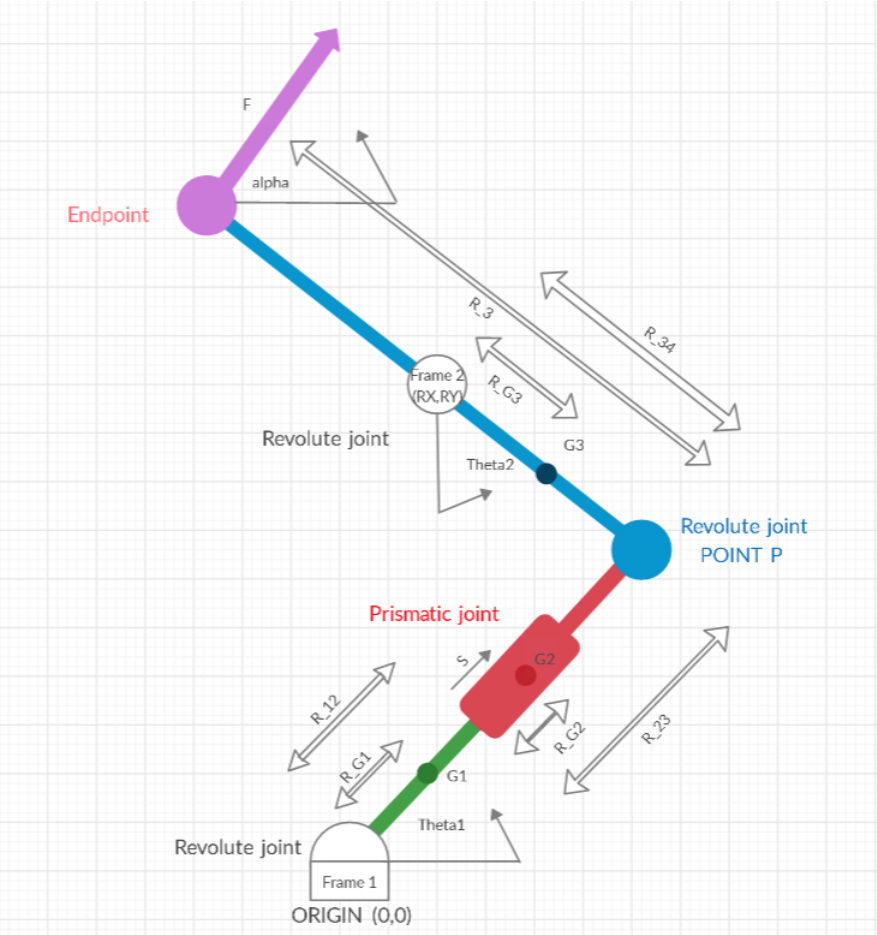

Figure 1.5: Looper 2D model

$$
\begin{aligned}
V_{G1} &= (-R_{G1}\dot{q}_1 \sin q_1, R_{G1}\dot{q}_1 \cos q_1), \\
V_{G2} &= (-(R_{12} + R_{G2} + q_2)\dot{q}_1 \sin q_1 + \dot{q}_2 \cos q_1, \\
&\quad (R_{12} + R_{G2} + q_2)\dot{q}_1 \cos q_1 + \dot{q}_2 \sin q_1), \\
V_{G3} &= (R_{G3}\dot{q}_2 \cos q_2, R_{G3}\dot{q}_2 \sin q_2), \\
\omega_{G1} &= \dot{q}_1, \\
\omega_{G3} &= \dot{q}_3.
\end{aligned} \tag{1.30}
$$

Moreover, the squared modules of the previous velocities are described as follows.

$$
\begin{aligned}
V_{G1}^2 &= R_{G1}^2 \dot{q}_1^2, \\
V_{G2}^2 &= (R_{12} + R_{G2} + q_2)^2 \dot{q}_1^2 + \dot{q}_2^2, \\
V_{G3}^2 &= R_{G3}^2 \dot{q}_3^2, \\
\omega_{G1}^2 &= \dot{q}_1^2, \\
\omega_{G3}^2 &= \dot{q}_3^2,
\end{aligned} \tag{1.31}
$$

From these considerations the kinetic energy turns out to be described by the following equations.

$$T = \frac{1}{2}M_1 R_{G1}^2 \dot{q}_1^2 + \frac{1}{2}M_2\big((R_{12} + R_{G2} + q_2)\dot{q}_1^2 + \dot{q}_2^2\big) + \\ + \frac{1}{2}M_3 R_{G3}^2 \dot{q}_3^2 + \frac{1}{2}J_1\dot{q}_1^2 + \frac{1}{2}J_2\dot{q}_1^2 + \frac{1}{2}J_3\dot{q}_3^2. \tag{1.32}$$

As for the potential energy, there won't be elastic terms due to the absence of springs in the model. Regarding the gravitational energy terms, the height of the centres of mass shall be retrieved from Equation 1.27. Therefore the total potential energy term is described by the following equation.

$$U = M_1 g R_{G1}\sin q_1 + M_2(R_{12} + R_{G2} + q_2)\sin q_1 + \\ + M_3 g(R_y - R_{G3}\cos q_2). \tag{1.33}$$

Ultimately, each joint is assumed to have friction. This aspect is modelled through the viscous friction coefficient c_i. Therefore, accordingly to section 1.1.1, the friction energy term is defined as

$$R = \frac{1}{2}c_1\dot{q}_1^2 + \frac{1}{2}c_2\dot{q}_2^2 + \frac{1}{2}c_3\dot{q}_3^2. \tag{1.34}$$

From the Lagrangian terms the model equations are derived as described in Equation 1.18:

- $q = q_1$: the terms obtained by derivation with respect to q_1 are the following.

$$\frac{d}{dt}\left(\frac{\partial T}{\partial \dot{q}_1}\right) = \Big(M_1 R_{G1}^2 + M_2(R_{12} + R_{G2} + q_2)^2 + J_1 + J_2\Big)\ddot{q}_1 + 2M_2(R_{12} + R_{G2} + q_2)\dot{q}_1\dot{q}_2, \tag{1.35}$$

$$\frac{\partial T}{\partial q_1} = 0,$$
$$\frac{\partial U}{\partial q_1} =, \Big(M_1 R_{G1} + M_2(R_{12} + R_{G2} + q_2)\Big)g\cos q_1,$$
$$\frac{\partial R}{\partial \dot{q}_1} = c_1\dot{q}_1.$$

- $q = q_2$: tthe terms obtained by derivation with respect to q_2 are the following.

$$\frac{d}{dt}\left(\frac{\partial T}{\partial \dot{q}_2}\right) = M_2\ddot{q}_2, \tag{1.36}$$
$$\frac{\partial T}{\partial q_2} = M_2(R_{12} + R_{G2} + q_2)\dot{q}_1^2,$$
$$\frac{\partial U}{\partial q_1} = M_2 g\sin q_1,$$
$$\frac{\partial R}{\partial \dot{q}_1} = c_2\dot{q}_2.$$

– $q = q_3$: the terms obtained by derivation with respect to q_3 are the following.

$$\begin{aligned}
\frac{d}{dt}\left(\frac{\partial T}{\partial \dot{q}_3}\right) &= (M_3 R_{G3}^2 + J_3)\ddot{q}_3, \\
\frac{\partial T}{\partial q_3} &= 0, \\
\frac{\partial U}{\partial q_3} &= M_3 R_{G3} g \sin q_3, \\
\frac{\partial R}{\partial \dot{q}_3} &= c_3 \dot{q}_3.
\end{aligned} \tag{1.37}$$

The looper doesn't move only due to its free dynamics. In fact it's subjected both to an external force and to an actuation. As described in Figure 1.5 the endpoint is subjected to a force F with an orientation α. This force models the action of the steel acting on the mechanism. Thus, such action creates a torque T_F on the system, describes as follows.

$$T_F = F(R_3 - R_{34} + R_{G3}) \sin(q_3 + \alpha). \tag{1.38}$$

Moreover, the system is assumed to be actuated on q_2. Namely, a force is applied on the prismatic joint causing the mechanism to move. A single actuation is needed as the system ha sonly 1 dof. This force is modelled as an input variable u directly acting on q_2 dynamics.

Therefore, the unconstrained model for the looper is described by the following equations.

$$\begin{aligned}
\Big(M_1 R_{G1}^2 + M_2(R_{12} + R_{G2} + q_2)^2 + J_1 + J_2\Big)\ddot{q}_1 = \\
-2M_2(R_{12} + R_{G2} + q_2)\dot{q}_1\dot{q}_2 + \\
-\Big(M_1 R_{G1} + M_2(R_{12} + R_{G2} + q_2)\Big) g \cos q_1 - c_1 \dot{q}_1,
\end{aligned} \tag{1.39}$$

$$M_2\ddot{q}_2 = M_2(R_{12} + R_{G2} + q_2)\dot{q}_1^2 - M_2 g \sin q_1 - c_2\dot{q}_2 + u,$$

$$(M_3 R_{G3}^2 + J_3)\ddot{q}_3 = -M_3 R_{G3} g \sin q_3 - c_3\dot{q}_3 + T_F.$$

These equations can be wrapped in the following compact form.

$$\begin{cases}
M_1^{tot}\ddot{q}_1 = F_1(q, \dot{q}) \\
M_2^{tot}\ddot{q}_2 = F_2(q, \dot{q}) \\
M_3^{tot}\ddot{q}_3 = F_3(q, \dot{q})
\end{cases} . \tag{1.40}$$

Constrained system

Recall now Figure 1.5. The intersection of the second and third link (point P) is supposed to lie on the circumference centred in $(0, 0)$ with radius $(R_{12} + R_{23} + q_2)$

but also on the one centred in (R_x, R_y) with radius R_{34}. These conditions limit the set of position the system can reach, namely they introduce 2 algebraic constraints. Indeed, point P is constrained both along the x axis and along the y axis. Therefore, as mentioned in subsection 1.2.1, the second revolute joint is responsible for the algebraic constraints acting on the system.

The two constraints can be described as follows.

$$\begin{cases} h_1(q) = (R_{12} + R_{23} + q_2)\cos q_1 - R_x - R_{34}\sin q_3 = 0 \\ h_2(q) = (R_{12} + R_{23} + q_2)\sin q_1 - R_y + R_{34}\cos q_3 = 0 \end{cases} \tag{1.41}$$

In order to consider these constraints the previous model shall be extended through the Lagrangian multipliers approach described in subsection 1.1.3. Both the introduced constraints are holonomic and expressed in configuration form. Therefore the Lagrangian coefficients can be computed as presented in section 1.1.3.

$$\begin{cases} a_{11} = \frac{\partial h_1}{\partial q_1} = -(R_{12} + R_{23} + q_2)\sin q_1 \\ a_{12} = \frac{\partial h_1}{\partial q_2} = \cos q_1 \\ a_{13} = \frac{\partial h_1}{\partial q_3} = -R_{34}\cos q_3 \end{cases} \tag{1.42}$$

$$\begin{cases} a_{21} = \frac{\partial h_2}{\partial q_1} = (R_{12} + R_{23} + q_2)\cos q_1 \\ a_{22} = \frac{\partial h_2}{\partial q_2} = \sin q_1 \\ a_{23} = \frac{\partial h_2}{\partial q_3} = -R_{34}\sin q_3 \end{cases} \tag{1.43}$$

From these coefficients the model described in Equation 1.40 can be extended to the constrained version below.

$$\begin{cases} M_1^{tot}\ddot{q}_1 = F_1(q,\dot{q}) + a_{11}(q)\lambda_1(q,\dot{q}) + a_{21}(q)\lambda_2(q,\dot{q}) \\ M_2^{tot}\ddot{q}_2 = F_2(q,\dot{q}) + a_{12}(q)\lambda_1(q,\dot{q}) + a_{22}(q)\lambda_2(q,\dot{q}) \\ M_3^{tot}\ddot{q}_3 = F_3(q,\dot{q}) + a_{13}(q)\lambda_1(q,\dot{q}) + a_{23}(q)\lambda_2(q,\dot{q}) \\ h_1(q) = 0 \\ h_2(q) = 0 \end{cases} \tag{1.44}$$

The pair of Lagrangian multipliers $\big(\lambda_1(q,\dot{q}), \lambda_2(q,\dot{q})\big)$ will be derived in section 2.3. The obtained model is defined by $n = 3$ dynamic equations and by $m = 2$ algebraic ones. Therefore, as reported in subsection 1.1.3 the system is expected to have $n - m = 1$ dof, that is exactly the case. In fact, also from the analysis carried on through Equation 1.25 it turns out that the system has a single *dof*. However, the model described in section 1.1 uses 3 different generalised coordinates, namely (q_1, q_2, q_3). Therefore only one of these will be used as independent variable in the description of the system. In order to understand the algebraic relation between those variables, consider again Figure 1.5. Assume $\theta_1 = q_1$ as the independent variable and consider the intersection point P. The coordinates of P are defined by the intersection of the following curves.

$$\begin{cases} y = (\tan q_1)x \\ (x - R_x)^2 + (y - R_y)^2 = R_{34}^2 \end{cases}, \tag{1.45}$$

namely the line with angular coefficient $\tan q_1$ and the circumference centred in (R_x, R_y) with radius R_{34}. Clearly, point P depends only on the slope of the line and therefore on the value of q_1, that is

$$P = (x_{int}(q_1), y_{int}(q_1)) \in \mathbb{R}^2. \tag{1.46}$$

Thus, the instantaneous relation between θ_1, s, and θ_2 is described by the following equations.

$$\begin{aligned} s = q_2 &= \sqrt{x_{int}^2 + y_{int}^2} - (R_{12} + R_{23}), \\ \theta_2 = q_3 &= \tan^{-1}\left(\frac{x_{int} - R_x}{R_y - y_{int}}\right). \end{aligned} \tag{1.47}$$

As previously mentioned the main effect of the constraints on the system is to limit the configurations the mechanism can reach, resulting in a specific range of values for q_1. Consider now the further simplified system described in Figure 1.6.

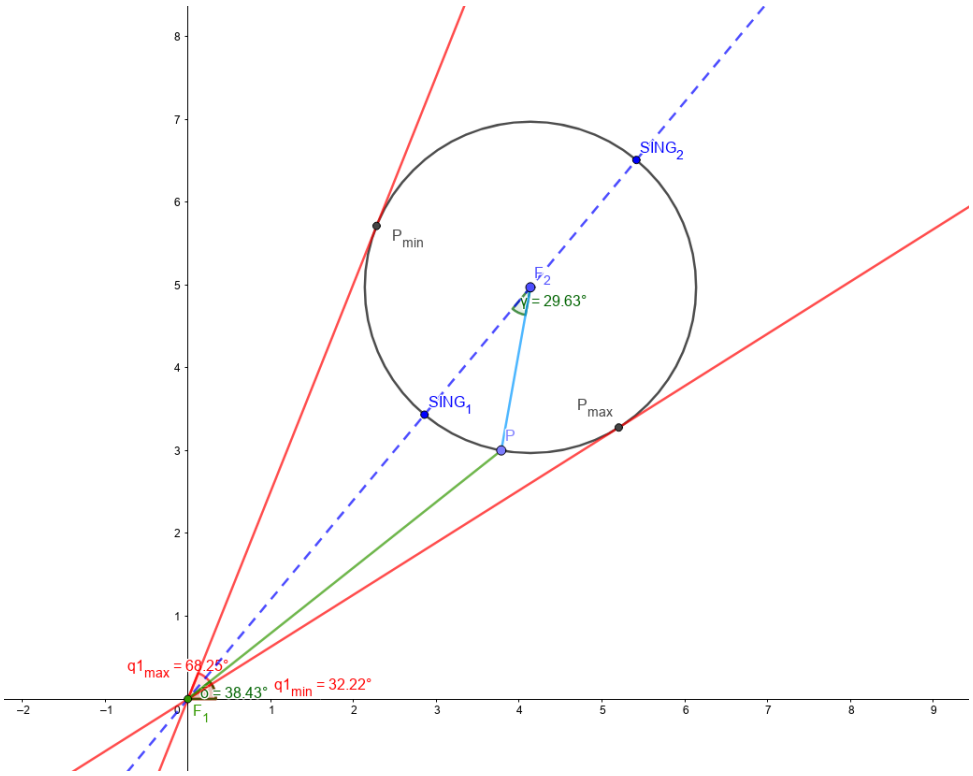

Figure 1.6: Limitations on q_1

The intersections between the circumference centred in F_2 with radius R_{34} and its tangents starting from F_1 represent two limit configurations of the mechanism. Actually, the slope of those tangents represents the maximum and minimum value that q_1 can assume during the motion. Moreover, they also coincides with the motion inversion of q_1, namely $\dot{q}_1 = 0$. Such workspace limitations are computed through the procedure reported below.

1. *Curves intersection.* The following system of equations imposes the intersection of the 2 curves

$$\begin{cases} y = \tan q_1 x = mx \\ (x - R_x)^2 + (y - R_y)^2 = R_{34}^2 \end{cases} \qquad m = \tan q_1, \tag{1.48}$$

ending up with a quadratic equation in x:

$$x^2(1+m^2) - 2x(R_x + mR_y) + (R_x^2 + R_y^2 - R_{34}^2) = 0 \tag{1.49}$$

2. *Tangency condition.* In order impose tangency on the computed intersections, Equation 1.49 Δ shall be put to zero, ending up with the following equation in m:

$$m^2(R_{34} - R_x^2) + 2mR_xR_y + (R_{34}^2 - R_y^2) = 0. \tag{1.50}$$

3. q_1 *limits solution.* The solution of Equation 1.50 results in

$$\begin{cases} m_1 = \frac{-R_xR_y - R_{34}\sqrt{R_x^2+R_y^2-R_{34}^2}}{R_{34}^2-R_x^2} \\ m_2 = \frac{-R_xR_y + R_{34}\sqrt{R_x^2+R_y^2-R_{34}^2}}{R_{34}^2-R_x^2} \end{cases} \rightarrow \begin{cases} q_1^{min} = \tan^{-1} m_1 \\ q_1^{max} = \tan^{-1} m_2 \end{cases} \tag{1.51}$$

This solution points out another constraint on the geometry of the mechanism, namely

$$(R_x^2 + R_y^2 - R_{34}^2) \geq 0. \tag{1.52}$$

This isn't an algebraic constraint to be added to the model, it's just a geometric condition allowing the system to be in a physically meaningful configuration.

Clearly, from Equation 1.49 2 intersections are possible. These are related to the initial configuration of the mechanism but they can also be crossed by the system during its motion. Assuming to know the initial position of the mechanism, this ambiguity won't affect the model in Equation 1.44 because the correct position is retrieved by integration on $(\ddot{q}_1, \ddot{q}_2, \ddot{q}_3)$. However, recalling Figure 1.5, from now on the system will be considered as working only in the lower configuration as this allows the endpoint to be correctly positioned under the steel strip. Little oscillations around a fixed position are required for the tension control described in section 1.2. The 2 different configurations are shown in Figure 1.7.

1.2.3 Singularity analysis

The mechanism can run in some critical points during its motion. These are called singular configurations as they change or limit the behaviour of the system. Consider again the system in Figure 1.2. The following geometric relations are imposed by the structure of the mechanism.

$$\begin{cases} x_{int}^2 + y_{int}^2 = (R_{12} + R_{23} + q_2)^2 \\ (x_{int} - R_x)^2 + (y_{int} - R_y)^2 = R_{34}^2 \end{cases}. \tag{1.53}$$

Time differentiation holds, therefore,

$$\begin{cases} 2x_{int}\dot{x}_{int} + 2y_{int}\dot{y}_{int} = 2(R_{12} + R_{23} + q_2)\dot{q}_2 \\ 2(x_{int} - R_x)\dot{x}_i nt + 2(y_{int} - R_y)\dot{y}_i nt = 0 \end{cases}. \tag{1.54}$$

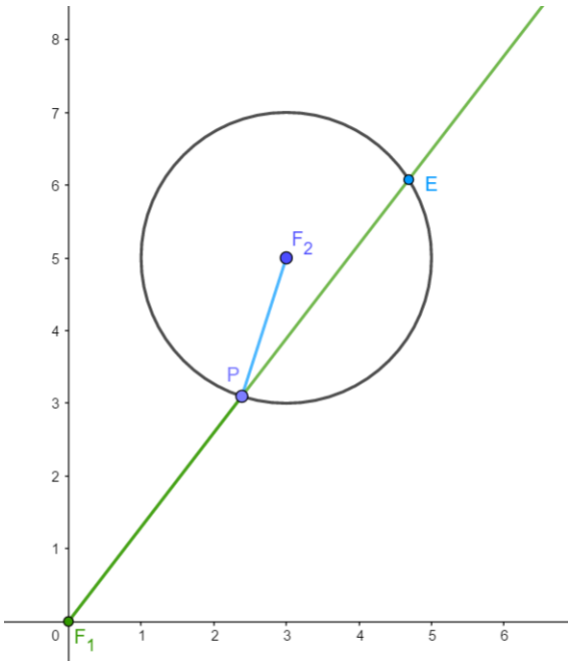

Figure 1.7: System's different configurations

These relations can be written in matrix form, namely

$$2J_{dir}\begin{bmatrix}\dot{x}_{int}\\ \dot{y}_{int}\end{bmatrix} = J_{inv}\dot{q}_2, \tag{1.55}$$

where

$$\begin{aligned} J_{dir} &= \begin{bmatrix} x & y \\ (x-R_x) & (y-R_y)\end{bmatrix}, \\ J_{inv} &= \begin{bmatrix} 2(R_{12}+R_{23}+q_2) \\ 0 \end{bmatrix}. \end{aligned} \tag{1.56}$$

This mapping defines a relation between the workspace (represented by point $P = (x_{int}, y_{int})$) and the joint-space (represented by the actuated variable q_2). Generally speaking, in parallel mechanism as the looper, singularities occur whenever J_{dir}, J_{inv} or both become singular.

1. J_{inv} **singularities**. These configurations occur whenever the inverse kinematic problem has multiple solutions for a specific set of workspace variables. Since J_{inv} is singular, it's possible to find non-zero values of $\dot{q}_2$ corresponding to null workspace velocities $(\dot{x}_{int}, \dot{y}_{int})$. Therefore, in these configurations non-zero actuation values don't correspond to any motion. The system loses a dof.

   In the system in analysis the only way for J_{inv} to be singular would be having $q_2 = -(R_{12}+R_{23})$. Consider Equation 1.47. It holds

   $$x_2 = \sqrt{x_{int}^2 + y_{int}^2} - (R_{12}+R_{23}). \tag{1.57}$$

   Therefore J_{inv} would be singular only if (x_{int}, y_{int}) coincided with the origin. This never happens for standard configurations of the mechanism. Therefore, the system in analysis never reaches a singularity related to the inverse kinematic problem.

2. J_{dir} **singularities**: these configurations occur whenever the direct kinematic problem has multiple solutions for a specific set of joint-space variables. Since J_{dir} is singular, its null-space is not empty. Therefore it's possible to find non-zero values of $(\dot{x}_{int}, \dot{y}_{int})$ corresponding to zero input velocities, namely $\dot{q}_2$. Therefore, in these configurations zero actuation values correspond to motion. The system gains a dof, meaning the endpoint to be locally movable even if all the joints are locked.

   In the system in analysis J_{dir} is singular if

$$\det(J_{dir}) = x_{int}(y_{int} - R_y) - y_{int}(x_{int} - R_x) = 0 \rightarrow y_{int} = \frac{R_y}{R_x} x_{int}. \quad (1.58)$$

This condition is satisfied in two points of the workspace, namely $SING_1$ and $SING_2$ in Figure 1.6. Indeed, when the mechanism is in these positions, R_{34} and $(R_{12}+R_{23})$ are aligned and therefore the prismatic joint is free to slide. Thus, locally the system has an additional dof.

Chapter 2

Introduction to DAE

This chapter goes through a general overview on DAE and their main properties. Then, the state space representation of the looper is presented, followed by the analysis of the system in.

2.1 DAE representation

DAE can be written both in general and in semi-explicit form, as described in Equation 2.1 and Equation 2.2.

$$F(\dot{y}, y, t) = 0 \tag{2.1}$$

$$\begin{aligned} \dot{x} &= f(x, u) + g(x)\lambda, \\ 0 &= h(x) \end{aligned} \tag{2.2}$$

Transformations between these two formulations can be achieved as reported in [5]. From now on the semi-explicit form will be used. Consider then Equation 2.2. The main elements present in the model are the following.

- $x(t) \in \mathbb{R}^n$. State vector.
- $\lambda(t) \in \mathbb{R}^m$. Algebraic variable.
- $u(t)$. Input variable.
- $f \ : \ \mathcal{U} \subseteq \mathbb{R}^n \to \mathbb{R}^n$. Free dynamics of the system.
- $g \ : \ \mathcal{U} \subseteq \mathbb{R}^n \to \mathbb{R}^{n \times m}$. Input dynamics of the system.
- $h \ : \ \mathcal{U} \subseteq \mathbb{R}^n \to \mathbb{R}^m$. Algebraic constraints acting on the system.

The mappings $f : \mathcal{U} \to \mathbb{R}^n$, $\quad g : \mathcal{U} \to \mathbb{R}^m$, and $h : \mathcal{U} \to \mathbb{R}^p$ with $\mathcal{U} \in \mathbb{R}^n$, are smooth, i.e. they have continuous partial derivative of any order and can be written as follows.

$$f = \begin{pmatrix} f_1 \\ \vdots \\ f_n \end{pmatrix}, \ g = (g_1, \ldots, g_m) = \begin{pmatrix} g_{11} \ldots g_{m1} \\ \vdots \quad \vdots \\ g_{1n} \ldots g_{mn} \end{pmatrix}, \ h = \begin{pmatrix} h_1 \\ \vdots \\ h_p \end{pmatrix}. \tag{2.3}$$

These mappings can be used to describe both linear and nonlinear systems. The set $\mathcal{U}$ is in general dictated by the specific application, for instance by the existence of physical limitations in the work space or in the joint space.

The mappings $f, g_{11}, \ldots, g_{nn}$ assign to each point in $\mathcal{U}$ a vector and for this reason they are called *vector fields*. They define a family of vectors, namely

$$\begin{aligned} v_f(\bar{x}) &= \Big(f_1(\bar{x}), \ldots, f_n(\bar{x}) \Big), \\ v_{g_i}(\bar{x}) &= \Big(g_{1i}(\bar{x}), \ldots, g_{ni}(\bar{x}) \Big). \end{aligned} \tag{2.4}$$

2.2 Looper state space representation

Consider the system described by Equation 1.44. As mechanical systems are described by a sequence of two integrators in the acceleration, the state variables for the looper are chosen to be $(x_1, x_2, x_3, x_4, x_5, x_6) = (q_1, q_2, q_3, \dot{q}_1, \dot{q}_2, \dot{q}_3)$. As a consequence, the model presented in Equation 1.44 can be written in the following form.

$$\begin{cases} \dot{x}_1 = x_4 \\ \dot{x}_2 = x_5 \\ \dot{x}_3 = x_6 \\ \dot{x}_4 = F_4(x) + a_{11}(x)\lambda_1(x) + a_{21}(x)\lambda_2(x) \\ \dot{x}_5 = F_5(x) + a_{12}(x)\lambda_1(x) + a_{22}(x)\lambda_2(x) \\ \dot{x}_6 = F_6(x) + a_{13}(x)\lambda_1(x) + a_{23}(x)\lambda_2(x) \end{cases}, \tag{2.5}$$

where the algebraic variables (λ_1, λ_2) represent the Lagrangian multipliers. Note that as for the model analysis, the algebraic variables are considered as input signals. The signal u is considered as an input too. However, from now on the system will be considered as non-actuated, that is, $u = 0$. Therefore only the pair (λ_1, λ_2) is considered as responsible for input signals. Thus, being $m = 2$ the system in analysis is *MIMO*.

Back to the previous model, in order to simplify the notation, the following quantities are defined.

$$\begin{cases} J_{tot_1} = (M_1 R_{G1}^2 + M_2 (R_{12} + R_{G2} + x_2)^2 + J_1 + J_2) \\ J_{tot_2} = (M_3 R_{G3}^2 + J_3) \end{cases} \tag{2.6}$$

Consider again the state space model in Equation 2.5: the set of coefficients

$$\Big(a_{11}(x),\ a_{21}(x),\ a_{12}(x),\ a_{22}(x),\ a_{13}(x),\ a_{23}(x) \Big)$$

is obtained from Equation 1.42 and Equation 1.43 through the following relation.

$$\begin{cases} a_{1k}(x) = \frac{a_{1k}(q)}{J_{tot_1}} \\ a_{2k}(x) = \frac{a_{2k}(q)}{M_2} \\ a_{3k}(x) = \frac{a_{3k}(q)}{J_{tot_2}} \end{cases} \qquad k = \{1, 2, 3\}. \tag{2.7}$$

Lastly, the triple $(F_1(x),\ F_2(x),\ F_3(x))$[1] describes system's free dynamics, namely

$$\begin{cases} F_4(x) = \frac{1}{J_{tot_1}}\Big(-2M_2(R_{12}+R_{G2}+x_2)x_4x_5 \\ \qquad\qquad -\Big(M_1R_{G1}+M_2(R_{12}+R_{G2}+x_2)\Big)g\cos x_1 - c_1x_4\Big) \\ F_5(x) = \frac{1}{M_2}\Big(M_2(R_{12}+R_{G2}+x_2)x_4^2 - M_2g\sin x_1 - c_2x_5 + u\Big) \\ F_6(x) = \frac{1}{J_{tot_2}}\Big(-M_3R_{G3}g\sin x_3 - c_3x_6 + T_F\Big) \end{cases} \tag{2.8}$$

2.3 Lagrange multipliers computation

As explained in subsection 1.1.3, Lagrange multipliers are algebraic variables use to model the reaction of the constraints on the system. Therefore, such variables assume precise values depending on the configuration of the system, in order to guarantee the set of algebraic constraints to be instantaneously met.

Constraints $h_1(x)$ and $h_2(x)$ are assumed to be zero at any time instant. Therefore the same shall be also for their time derivatives. Generally speaking, for a set of m constraints, the following conditions shall be met.

$$\begin{cases} h_i(x(t)) = 0 \\ \dot{h}_i(x(t)) = 0 \\ \ddot{h}_i(x(t)) = 0 \\ \qquad\vdots \\ h_i^r(x(t)) = 0 \end{cases} \qquad \forall i \in \{1,\dots,m\} \quad \wedge \quad \forall t \in \mathbb{R}, \quad r \in \mathbb{R} \tag{2.9}$$

These conditions can be used to find an explicit expression for the Lagrangian multipliers through the concept of *relative degree*[2]. Consider a general nonlinear MIMO system as the one described by Equation 2.2. This system has a vectorial relative degree $(r_1,\dots,r_n)$ whose general entry r_i represents the number of times y_i has to be derivated in order to find an explicit dependence on λ.

The explicit computation of the relative degree for the looper is reported in section 2.5 for clarity. However, recall the mechanical nature of the looper. The system is described by two integrators. Therefore, from the algebraic relations describing the constraints, two time differentiations lead to a condition in which system dynamics are involved. As a consequence, the relation $\ddot{h}_i(x(t)) = 0$ includes $(\dot{x}_4,\ \dot{x}_5,\ \dot{x}_6)$ and therefore (λ_1, λ_2). It is straightforward that the relative degree of the system is $r = (2,2)$. Thus, the procedure to find the algebraic relation describing Lagrangian multipliers unfolds as follows.

1. Take the second time derivative of $h_i(x)$. This results in

$$\ddot{h}_i(x) = f_{h_i}(\dot{x}) = f_{h_i}(x_4, x_5, x_6, \dot{x_4}, \dot{x_5}, \dot{x_6}) = 0 \quad \forall i \in \{1,\dots,m\}. \tag{2.10}$$

2. Replace every occurrence of $(\dot{x_4}, \dot{x_5}, \dot{x_6})$ with system dynamics described in Equation 2.5.

[1] All the used variables have been described in subsection 1.2.1 and subsection 1.2.2

[2] For an accurate definition of relative degree see section 2.4

3. Consider the imposed condition $\ddot{h}_i(x) = 0 \quad \forall i \in \{1, \dots, m\}$. The following linear system is obtained:

$$\begin{cases} A_{11}\lambda_1 + \cdots + A_{1m}\lambda_m = C_1 \\ \vdots \\ A_{1m}\lambda_1 + \cdots + A_{mm}\lambda_m = C_m \end{cases} \qquad A_{ij}, C_i, \in \mathbb{R} \quad \forall i, j \in \{1, \dots, m\}, \quad (2.11)$$

where all the coefficients depend on the vector state $x(t)$. Solving this system provides the algebraic relations instantaneously describing $(\lambda_1, \dots, \lambda_m)$ as a function of $x(t)$.

This procedure has been performed on the system in analysis ending up with the following system.

$$\begin{cases} A_1\lambda_1 + A_2\lambda_2 = C_1 \\ B_1\lambda_1 + B_2\lambda_2 = C_2 \end{cases}, \quad (2.12)$$

the solution of which is

$$\begin{cases} \lambda_2 = \frac{C_2A_1 - C_1B_1}{B_2A_1 - A_2B_1} \\ \lambda_1 = \frac{C1 - \lambda_2A_2}{A_1} \end{cases}. \quad (2.13)$$

2.4 Relative degree

This section presents the concept of relative degree. As reported in section 2.3 the relative degree can be interpreted as the number of time system dynamics have to be differentiated in order to find an explicit dependence on the input. Relative degree can be defined for both SISO ans MIMO systems. Consider then a system described by equations of the following form.

$$\begin{aligned} \dot{x} &= f(x) + g(x)\lambda, \\ y &= h(x), \end{aligned} \quad (2.14)$$

where $x(t) \in \mathcal{U} \subseteq \mathbb{R}^n$ denotes the state vector, $\lambda(t) \in \mathbb{R}^m$ denotes the input, and $y(t) \in \mathbb{R}^p$ denotes the output. The relative degree can be defined respectively for SISO ans MIMO systems as described in the following paragraphs.

SISO systems

Consider the system in Equation 2.14.

Definition 3 (Relative Degree)**.** *The nonlinear SISO system 2.14 is said to have* ***relative degree*** r *at point* $\bar{x} \in \mathbb{R}^n$ *if*

i) $L_gL_f^k h(x) = 0 \quad \forall k \in \{0, \dots, r-2\}, \; x \in B_\delta(\bar{x})$

ii) $L_gL_f^{r-1}h(\bar{x}) \neq 0$

The relative degree can be undefined in some points. However the set of points in which it is well defined is a subset of $\mathcal{U}$. For example, consider a system in which $L_g L_f h(x) = \cos x_1$. In this case the relative degree is well-defined for all points except for those where $L_g L_f h(x) = 0$, that is all x such that $x_1 \neq \frac{(2k+1)\pi}{2}, \quad k \in \mathbb{Z}$. Therefore, for the system in example the relative degree is well defined for all $x \mid L_g L_f h(x) \neq 0$.

Definition 3 can be used also for linear systems. Consider a general linear system in state space form.

$$\begin{aligned} \dot{x} &= Ax + B\lambda, \\ y &= Cx. \end{aligned} \tag{2.15}$$

In this case we have $f = A \in \mathbb{R}^{n \times n}$, $g = B \in \mathbb{R}^{n \times m}$, $h = C \in \mathbb{R}^{p \times n}$ and therefore definition 3 reduces to the following conditions.

$$\begin{aligned} L_g L_f^k h(x) &= CA^k B = 0, \qquad \forall k \in \{0, \dots, r-2\} \\ L_g L_f^{r-1} h(x) &= CA^{r-1} B \neq 0, \end{aligned} \tag{2.16}$$

which is consistent with the classical notion of relative degree for linear SISO systems.

The concept of relative degree can be interpreted as the minimum number of time the output shall be differentiated to find an explicit dependence from the input. This claim can be proved through the following procedure.

1. Consider system's output, namely

$$y = h(x) \tag{2.17}$$

2. Compute y time derivative:

$$\dot{y} = \frac{\partial h(x)}{\partial x}\frac{dx}{dt} = \frac{\partial h(x)}{\partial x}[f(x) + g(x)\lambda] = L_f h(x) + L_g h(x)\lambda \tag{2.18}$$

   From definition 3, if $r > 1$ it holds that $L_g h(x) = 0$ and therefore $\dot{y} = L_f h(x)$. This procedure can be iterated through further differentiations.

3. Compute the r^{th} time differentiation of the output, namely

$$y^{(r)} = L_f^r h(x) + L_g L_f^{r-1} h(x)\lambda, \tag{2.19}$$

   which is exactly the result stated in definition 3.

Assume now to check the relative degree in a restricted set, namely a ball $B_\delta(\bar{x})$ of radius δ near a generic point $\bar{x} \in \mathcal{U}$. Assume the following claim to be valid.

$$L_g L_f h(x) = 0 \ \forall x \in B_\delta(\bar{x}) \ and \ \forall k \geq 0 \tag{2.20}$$

In this case no relative degree can be defined. Moreover, the input never affects the output. This is shown by the Taylor expansion of the output, namely

$$y = \sum_{k=0}^{\inf} L_f^k h(\bar{x}) \frac{(x-\bar{x})^k}{k!}. \tag{2.21}$$

Clearly, this Taylor expansion is never affected by the input λ.

MIMO model

The concept of relative degree can be extended to a general nonlinear MIMO model. Such systems end up with a vector of relative degrees.

Definition 4 (Relative Degree)**.** *The nonlinear MIMO system in 2.14 is said to have* ***relative degree*** $(r_1, \ldots, r_m)$ *at point* $\bar{x} \in \mathbb{R}^n$ *if*

i) $L_{g_j} L_f^k h_i(x) = 0 \quad \forall j \in \{1, \ldots, m\} \wedge k < (r_i - 1) \wedge i \in \{1, \ldots, m\} \wedge x \in B_\delta(\bar{x})$

ii) Matrix A(x) is non singular in $x = \bar{x}$*, where*

$$A(x) = \begin{bmatrix} L_{g_1} L_f^{r_1-1} h_1(x) & \ldots & L_{g_m} L_f^{r_1-1} h_1(x) \\ \vdots & \ddots & \vdots \\ L_{g_1} L_f^{r_m-1} h_m(x) & \ldots & L_{g_m} L_f^{r_m-1} h_m(x) \end{bmatrix}$$

As for the MIMO case, each entry of the relative degree vector r_i represents the number of times y_i has to be differentiated in order to find an explicit dependence on λ.

2.5 Looper - relative degree computation

This section goes through the relative degree computation for the system in analysis. As the looper is a MIMO system, the computation is performed accordingly to definition 4.

The system has 2 constraints (h_1, h_2) and 2 input (λ_1, λ_2). Therefore the relative degree will be a vector $r \in \mathbb{R}^2$. Conditions described in definition 4 shall be checked for all the combinations (i, j) such that $i, j \in \{1, 2\}$. The mapping for the system in analysis are described as follows.

$$f = \begin{pmatrix} x_4 \\ x_5 \\ x_6 \\ F_4 \\ F_5 \\ F_6 \end{pmatrix}, \quad g = (g_1 \quad g_2) = \begin{pmatrix} 0 & 0 \\ 0 & 0 \\ 0 & 0 \\ a_{11} & a_{12} \\ a_{21} & a_{22} \\ a_{31} & a_{32} \end{pmatrix}, \quad h = (h_1 \quad h_2), \tag{2.22}$$

where each coefficient a_{ij} is defined accordingly to Equation 2.7. Therefore, for a general pair (i, j), the relative degree computation unfolds as follows.

1. $k = 0$

$$L_{gj}h_i = \begin{bmatrix} \dfrac{\partial h_i}{\partial x_1}, & \dfrac{\partial h_i}{\partial x_2}, & \dfrac{\partial h_i}{\partial x_3}, & 0, & 0, & 0 \end{bmatrix} \times \begin{pmatrix} 0 \\ 0 \\ 0 \\ a_{1j} \\ a_{2j} \\ a_{3j} \end{pmatrix} = 0$$

2. $k = 1$

$$L_f h_i = \begin{bmatrix} \dfrac{\partial h_i}{\partial x_1}, & \dfrac{\partial h_i}{\partial x_2}, & \dfrac{\partial h_i}{\partial x_3}, & 0, & 0, & 0 \end{bmatrix} \times \begin{pmatrix} x_4 \\ x_5 \\ x_6 \\ F_4 \\ F_5 \\ F_6 \end{pmatrix} = w \ : \ \mathbb{R}^6 \to \mathbb{R}$$

$$L_{gj}L_f h_i = \begin{bmatrix} \dfrac{\partial w}{\partial x_1}, & \dfrac{\partial w}{\partial x_2}, & \dfrac{\partial w}{\partial x_3}, & \dfrac{\partial w}{\partial x_4}, & \dfrac{\partial w}{\partial x_5}, & \dfrac{\partial w}{\partial x_6} \end{bmatrix} \times \begin{pmatrix} 0 \\ 0 \\ 0 \\ a_{1j} \\ a_{2j} \\ a_{3j} \end{pmatrix} = v \ : \ \mathbb{R}^6 \to \mathbb{R}$$

This procedure results in different expressions for w and v for each pair (i, j). These shall be analysed accordingly to definition 4. If both map w and v result generally non singular in $\bar{x}$ the relative degree is well defined in such point. The pairs (w, v) are presented and analysed below for all the (i, j) combinations.

1. $i = 1$

$$w_1 = -(R_{12} + R_{23} + x_2)x_4 \sin x_1 + x_5 \cos x_1 - R_{34}x_6 \cos x_3 \tag{2.23}$$

   a $j = 1$

$$v_{11} = -\frac{(R_{12} + R_{23} + x_2)^2 \sin^2 x_1}{J_{tot_1}} - \frac{\cos^2 x_1}{M_2} - \frac{R_{34}^2 \cos^2 x_3}{J_{tot_2}}$$

   b $j = 2$

$$v_{12} = \frac{(R_{12} + R_{23} + x_2)^2 \sin x_1 \cos x_1}{J_{tot_1}} - \frac{\sin x_1 \cos x_1}{M_2} - \frac{R_{34}^2 \sin x_3 \cos x_3}{J_{tot_2}}$$

2. $i = 2$

$$w_2 = (R_{12} + R_{23} + x_2)x_4 \cos x_1 + x_5 \sin x_1 - R_{34}x_6 \sin x_3 \tag{2.24}$$

   a $j = 1$

$$v_{21} = \frac{(R_{12} + R_{23} + x_2)^2 \sin x_1 \cos x_1}{J_{tot_1}} - \frac{\sin x_1 \cos x_1}{M_2} - \frac{R_{34}^2 \sin x_3 \cos x_3}{J_{tot_2}}$$

   b $j = 2$

$$v_{22} = -\frac{(R_{12} + R_{23} + x_2)^2 \cos^2 x_1}{J_{tot_1}} - \frac{\sin^2 x_1}{M_2} - \frac{R_{34}^2 \sin^2 x_3}{J_{tot_2}}$$

Considering a general vector $\bar{x} \in \mathcal{U}$ both (w_1, v_{11}, v_{12}) and (w_2, v_{21}, v_{22}) are non-zero in $\bar{x}$. Therefore, accordingly to condition 1 in definition 4, $r = (2, 2)$ is a candidate relative degree vector. However, condition 2 of definition 4 shall be met as well, namely

$$A = \begin{pmatrix} L_{g1}L_f h_1 & L_{g2}L_f h_1 \\ L_{g2}L_f h_2 & L_{g2}L_f h_2 \end{pmatrix} \tag{2.25}$$

shall be non-singular in $\bar{x}$. The determinant of this matrix is

$$\det(A) = \frac{(R_{12} + R_{23} + x_2)^2}{J_{tot_1} M_2} + \frac{(R_{12} + R_{23} + x_2)^2 R_{34}}{J_{tot_1} J_{tot_2}} \cos^2(x_1 - x_3) + \frac{R_3 4^2}{J_{tot_2} M_2} \sin^2(x_1 - x_3) \tag{2.26}$$

Necessary condition for this expression to be null is

$$R_{12} + R_{23} + x_2 = 0 \tag{2.27}$$

which never happens in standard configurations for this mechanism, as explained in subsection 1.2.3. However, it's useful to consider also the term $\sin(x_1 - x_3)$. By simple geometric considerations it holds that this term is null only if the first and the third link of the mechanism are normal. This situation occurs only when $x_1 = \theta_1^{min}$ or when $x_1 = \theta_1^{max}$. These configurations represent a sort of boundary position for the mechanism.

At the end of this analysis, the vector relative for system Equation 1.44 turns out to be

$$r = (2, 2) \in \mathbb{R}^2. \tag{2.28}$$

2.6 Change of coordinates - nonlinear systems

Systems in state space representation can be transformed in equivalent ones described in different coordinates. The mappings allowing these transformations are called change of coordinates. As far as control theory is concerned, change of coordinates are very useful as they highlight important properties like controllability and observability of the system. They're also used to simplify system's implementation and control.

2.6.1 Diffeomorphism - general overview

Change of coordinates are different for linear and nonlinear systems. Consider a nonlinear system in the form of Equation 2.14, namely

$$\begin{aligned} \dot{x} &= f(x) + g(x)\lambda, \\ y &= h(x). \end{aligned} \tag{2.29}$$

A general change of coordinates is expressed in the following form.

$$z = \Phi(x). \tag{2.30}$$

where $x \in \mathbb{R}^n$ is the vector state and $\Phi : \mathbb{R}^n \to \mathbb{R}^n$ a vector field, namely,

$$\Phi = \begin{pmatrix} \phi_1 \\ \vdots \\ \phi_n \end{pmatrix}. \tag{2.31}$$

Φ is assumed to be invertible. Moreover, both Φ and Φ^{-1} are smooth vector fields. Mappings of this type are called global diffeomorphism. However, global diffeomorphisms are difficult to be found. Therefore, limited mapping are defined over a restricted domain and referred to as local diffeomorphism.

$$\Phi : \mathcal{U} \subseteq \mathbb{R}^n \to \mathbb{R}^n. \tag{2.32}$$

Local diffeomorphism are defined in a neighbourhood of a point of particular interest for the system in analysis. Therefore $\mathcal{U}$ is a set usually containing such point, which from now on will be referred to as $\bar{x} \in \mathbb{R}^n$. The following lemma helps determining whether a function is or is not a local diffeomorphism with respect to a point $\bar{x} \in \mathbb{R}^n$:

Lemma 1. *Assume $\mathcal{U} \subseteq \mathbb{R}^n, \bar{x} \in \mathcal{U}$, and $\Phi : \mathcal{U} \to \mathbb{R}^n$ a smooth vector field. If the Jacobian $J(\Phi(\bar{x}))$ of the mapping Φ in $\bar{x}$ is non-singular, then on a proper choice of $\mathcal{U}$, $\Phi : \mathcal{U} \to \mathbb{R}^n$ is a local diffeomorphism for $\bar{x} \in \mathbb{R}^n$.*

2.6.2 Normal form - SISO system

The normal form of a nonlinear system is a particular kind of diffeomorphism. Such transformation is useful as it simplify the analysis of the system [6]. Consider a general SISO system described by equations of the following form.

$$\begin{aligned} \dot{x} &= f(x) + g(x)\lambda, \\ y &= h(x). \end{aligned} \tag{2.33}$$

Recall the considerations in section 2.4, on the relative degree definition. The following lemma holds.

Lemma 2. *Consider a system in the form of Equation 2.14 and a general point $\bar{x} \in \mathbb{R}^n$. The row vectors*

$$\nabla h(\bar{x}), \nabla L_f h(\bar{x}), \ldots, \nabla L_f^{r-1} h(\bar{x}), \tag{2.34}$$

are linearly independent.

Linear independence of these vectors make them a valid candidate to be a reference frame for the system. Note that this consideration holds if $r < n$, with n the dimension of the state vector. Therefore, the relative degree of a system is related to a partial set of new coordinates in a neighbourhood of the point $\bar{x}$. These considerations are summarized in the following proposition.

Proposition 1. *Consider a system described by equations in the following form.*

$$\begin{aligned} \dot{x} &= f(x) + g(x)\lambda, \\ y &= h(x). \end{aligned} \tag{2.35}$$

Assume such system to have a relative degree r at $\bar{x} \in \mathbb{R}^n$. Therefore $r \leq n$. Set

$$\begin{aligned} \Phi_1 &= h(x), \\ \Phi_2 &= L_f h(x), \\ &\dots \\ \Phi_r &= L_f^{r-1} h(x). \end{aligned} \tag{2.36}$$

If $r < n$ (strictly), it's always possible to find $(n-r)$ functions $(\phi_{r+1}, \dots, \phi_n)$ such that the mapping

$$\Phi = \begin{pmatrix} \phi_1 \\ \dots \\ \phi_n \end{pmatrix} \tag{2.37}$$

has a non-singular Jacobian matrix $J(\Phi(x))$ in $\bar{x}$. Therefore, this mapping represents a local coordinates transformation in a neighbourhood $B_\delta(\bar{x})$ of $\bar{x}$. The additional mappings $(\phi_{r+1}, \dots, \phi_n)$ can assume arbitrary values in $\bar{x}$. Without loss of generality, these can be chosen such that

$$L_g \phi_i(x) = 0 \quad \forall i \in \{r+1, \dots, n\} \ \wedge \ x \in B_\delta(\bar{x}). \tag{2.38}$$

Note that it is not trivial at all to choose $(\phi_{r+1}, \dots, \phi_n)$ such that $L_g \phi_i(x) = 0$. However, even if this condition is not met, the set of mappings is still a valid local diffeomorphism.

The description of the system in this new reference frame is straightforward. The final coordinates transformation is described by equations in the following form.

$$\begin{cases} z_1 = \phi_1(x) \\ \vdots \\ z_n = \phi_n(x) \end{cases} \tag{2.39}$$

The computation of the dynamics of the system unfolds as follows.

1. $i \in \{1, \dots, r-1\}$

$$\begin{aligned} \frac{dz_1}{dt} = \frac{\partial \phi_1}{\partial x}\frac{dx}{dt} = \frac{\partial h}{\partial x}\frac{dx}{dt} = L_f h(x) = \phi_2(x) = z_2, \\ \vdots \\ \frac{dz_{r-1}}{dt} = \frac{\partial \phi_{r-1}}{\partial x}\frac{dx}{dt} = \frac{\partial L_f^{r-2}}{\partial x}\frac{dx}{dt} = L_f^{r-1} h(x) = \phi_r(x) = z_r. \end{aligned} \tag{2.40}$$

2. $i = r$

$$\frac{dz_r}{dt} = \frac{\partial \phi_r}{\partial x}\frac{dx}{dt} = L_f^r h(x) + L_g L_f^{r-1} h(x)\lambda = L_f^r h(\Phi^{-1}(z)) + L_g L_f^{r-1} h(\Phi^{-1}(z))\lambda \tag{2.41}$$

Note that the state vector x has been replaced with its expression depending on z, i.e. $x = \Phi^{-1}(z)$. Moreover, define the following terms.

$$\begin{cases} a(z) = L_g L_f^{r-1} h(\Phi^{-1}(z)) \\ b(z) = L_f^r h(\Phi^{-1}(z)) \end{cases} \tag{2.42}$$

Namely, it holds

$$\dot{z}_r = b(z) + a(z)\lambda. \tag{2.43}$$

Consider definition 3. Note that

$$a(z) \neq 0, \quad z \in \mathbb{R}^n, \tag{2.44}$$

equals the second condition to be met for the relative degree to be defined.

3. $i \in \{r+1, \ldots, n\}$

$$\frac{dz_i}{dt} = \frac{\partial \phi_i}{\partial x}\frac{dx}{dt} = \frac{\partial \phi_i}{\partial x}(f(x) + g(x)\lambda) = L_f \phi_i(x) + L_g \phi_i(x)\lambda \tag{2.45}$$

These last transformations can be simplified if the following holds.

$$\begin{cases} q_i(z) = L_f \phi_i(\Phi^{-1}(z)) \\ p_i(z) = L_g \phi_i(\Phi^{-1}(z)) \end{cases} \qquad \forall i \in \{r+1, \ldots, n\} \tag{2.46}$$

Thus, the whole state space representation of the system in the new set of coordinates is described by equations in the following form.

$$\begin{cases} \dot{z}_1 &= z_2 \\ &\vdots \\ \dot{z}_{r-1} &= z_r \\ \dot{z}_r &= b(z) + a(z)\lambda \\ \dot{z}_{r+1} &= q_{r+1}(z) + p_{r+1}(z)\lambda \\ &\vdots \\ \dot{z}_n &= q_n(z) + p_n(z)\lambda \end{cases} \tag{2.47}$$

Additionally to these equations the output shall be added as well. It is described as a function of the new state variable z. Recalling that $y = h(x)$ it holds $y = z_1$. These equations describing the system are said to be in *normal form*. Note that if the change of coordinates had been designed such that

$$L_g\phi_i(x) = 0, \quad \forall i \in \{r+1, \ldots, n\}, \tag{2.48}$$

the last $(n-r)$ dynamics equations wouldn't have been influenced by the input, namely

$$\begin{cases} \dot{z}_{r+1} &= q_{r+1}(z) \\ &\vdots \\ \dot{z}_n &= q_n(z) \end{cases} \tag{2.49}$$

2.6.3 Normal form - MIMO system

This section traces the procedure to compute the normal form presented in subsection 2.6.2 on general MIMO system. Consider a state space system described by equations in the following form.

$$\begin{aligned} \dot{x} &= f(x) + \sum_{i=0}^{m} g_i(x)\lambda_i \\ y_1 &= h_1(x), \\ &\vdots \\ y_m &= h_m(x), \end{aligned} \tag{2.50}$$

where $(f, g_1, \ldots, g_m)$ are smooth vector fields and $(h_1, \ldots, h_m)$ smooth functions. Note that these equations consists of the expanded version of the system described by Equation 2.14. As in the SISO analysis, the normal form for MIMO systems is developed from the relative degree, which in this case is the vector $r = (r_1, \ldots, r_m)$. The relative degree is computed accordingly to definition 4.

Recall definition 4 for MIMO systems. Consider a general point $\bar{x} \in \mathbb{R}^n$ for which the relative degree vector is well defined. Accordingly to definition 4 the following vector

$$\Big(L_{g_1} L_f^{r_i - 1} h_i(x), \quad \ldots \quad , \quad L_{g_m} L_f^{r_i - 1} h_i(x) \Big), \tag{2.51}$$

is nonsingular in $\bar{x}$ for any value of i in $\{1, \ldots, m\}$. In fact, it consists of the i^{th} row of matrix A which is nonsingular in $\bar{x}$ due to the second condition of definition 4. Therefore, it always exist at least a $j \in \{1, \ldots, m\}$ such that

$$L_{g_j} L_f^{r_i - 1} h_i(x) \neq 0. \tag{2.52}$$

From these considerations the following lemma is stated for MIMO systems.

Lemma 3. *Consider a system in the form of Equation 2.50 and a general point $\bar{x} \in \mathbb{R}^n$. Suppose the system to have a vector relative degree $r = \{r_1, \ldots, r_m\}$ in $\bar{x}$. The row vectors*

$$\begin{gathered}\nabla h_1(\bar{x}), \nabla L_f h_1(\bar{x}), \ldots, \nabla L_f^{r-1} h_1(\bar{x}) \\ \vdots \\ \nabla h_m(\bar{x}), \nabla L_f h_m(\bar{x}), \ldots, \nabla L_f^{r-1} h_m(\bar{x})\end{gathered} \tag{2.53}$$

are linearly independent.

Likewise SISO systems, the property of linear independence of these vectors makes them a good candidate for a coordinate transformation. As for MIMO systems, the approach is to consider each output as a SISO system and apply the related normal transformation. This procedure is summarized in the following proposition.

Proposition 2. *Consider a system in the form of Equation 2.50 and a general point* $\bar{x} \in \mathbb{R}^n$. *Suppose the system to have a vector relative degree* $r = (r_1, \ldots, r_m)$. *It holds*

$$r_{tot} = \sum_{i=1}^{m} r_i \leq n. \tag{2.54}$$

Then, for $i \in \{1, \ldots, m\}$, *set*

$$\begin{aligned}\phi_1^i &= h_i(x), \\ \phi_2^i &= L_f h_i(x), \\ &\vdots \\ \phi_{r_i}^i &= L_f^{r_i - 1} h_i(x).\end{aligned} \tag{2.55}$$

If $r_{tot} \leq n$, *it is always possible to find* $(n - r_{tot})$ *more functions* $(\phi_{r_{tot}+1}, \ldots, \phi_n)$ *such that the mapping*

$$\Phi = col\left(\phi_1^1, \ldots, \phi_{r_1}^1, \ldots, \phi_1^m, \ldots, \phi_{r_m}^m, \ldots, \phi_{r_{tot}+1}, \ldots, \phi_n\right), \tag{2.56}$$

has a Jacobian matrix $J(\Phi(\bar{x}))$ *nonsingular. Therefore, these mappings represents a local coordinate transformation for the system in a neighbourhood of* $\bar{x}$. *The values of the additional mappings can be chosen arbitrarily.*

For the sake of simplicity all the variables transformed by the relations defined through the relative degree are described as ξ_i^j. All the variables transformed by the additional mappings $(\phi_{r_{tot}}, \ldots, \phi_n)$ are described as η_i. Therefore, the final coordinates transformation is described by equations of the following form.

$$\xi = (\xi^1, \ldots, \xi^m) \quad s.t. \quad \forall i \in \{1, \ldots, m\} \tag{2.57}$$

$$\xi_i = \begin{pmatrix} \xi_1^i \\ \xi_2^i \\ \vdots \\ \xi_{r_i} \end{pmatrix} = \begin{pmatrix} \phi_1^i(x) \\ \phi_2^i(x) \\ \vdots \\ \phi_{r_i}^i(x) \end{pmatrix},$$

$$\eta = \begin{pmatrix} \eta_1 \\ \eta_2 \\ \vdots \\ \eta_{n-r_{tot}} \end{pmatrix} = \begin{pmatrix} \phi_{r_{tot}+1}(x) \\ \phi_{r_{tot}+2}(x) \\ \vdots \\ \phi_n(x) \end{pmatrix}.$$

The dynamics of the system are derived following the same procedure reported in subsection 2.6.2 for each subsystem associated to an output h_i. Thus, set

$$\begin{aligned} a_{ij}(\xi,\eta) &= L_{gj}L_f^{r_i-1}h_i(\Phi^{-1}(\xi,\eta)) \quad \forall 1 \leq i,j \leq m, \\ b_i(\xi,\eta) &= L_f^{r_i}h_i(\Phi^{-1}(\xi,\eta)) \quad \forall 1 \leq i \leq m. \end{aligned} \tag{2.58}$$

System dynamics in the new set of coordinates are described by equations in the following form.

$$\begin{aligned} \dot{\xi}_1^i &= \xi_2^i, \\ &\vdots \\ \dot{\xi}_{r_i-1}^i &= \xi_{r_i}^i, \\ \dot{\xi}_{r_i}^i &= b_i(\xi,\eta) + \sum_{j=1}^{m} a_{ij}(\xi,\eta)\lambda_j, \\ y_i &= \xi_1^i, \end{aligned} \tag{2.59}$$

for $1 \leq i \leq m$. The remaining variables, namely $(\eta_1, \ldots, \eta_{n-r_{tot}})$, have the following general structure.

$$\dot{\eta} = q(\xi,\eta) + \sum_{i=1}^{m} p_i(\xi,\eta)\lambda_i = q(\xi,\eta) + p(\xi,\eta)\lambda \tag{2.60}$$

2.6.4 Normal form - zero dynamics

Consider a general MIMO nonlinear system in normal form, namely described by the following equations.

$$\begin{aligned} \dot{\xi}_1^1 &= \xi_2^1, \\ &\vdots \\ \dot{\xi}_{r_1-1}^1 &= \xi_{r_1}^1, \\ \dot{\xi}_{r_1}^1 &= b_1(\xi,\eta) + \sum_{j=1}^{m} a_{1j}(\xi,\eta)\lambda_j, \\ &\vdots \\ \dot{\xi}_1^m &= \xi_2^m, \\ &\vdots \end{aligned} \tag{2.61}$$

$$
\begin{aligned}
\dot{\xi}^m_{r_m-1} &= \xi^m_{r_m}, \\
\dot{\xi}^m_{r_m} &= b_m(\xi,\eta) + \sum_{j=1}^{m} a_{mj}(\xi,\eta)\lambda_j, \\
\dot{\eta}_1 &= q_1(\xi,\eta) + \sum_{i=1}^{m} p_{1i}(\xi,\eta)\lambda_i, \\
&\vdots \\
\dot{\eta}_{(n-r_{tot})} &= q_{(n-r_{tot})}(\xi,\eta) + \sum_{i=1}^{m} p_{(n-r_{tot})i}(\xi,\eta)\lambda_i.
\end{aligned}
$$

Recall that as described in subsection 2.6.3 the output of the system is the whole set of constraints h_i. The following definition can be stated [6].

Definition 5. *(zero dynamics) Consider system 2.60. The dynamics described by*

$$
\dot{\eta} = f_0(0,\eta) = \begin{cases} \dot{\eta}_1 = q_1(0,\eta) + \sum_{i=1}^{m} p_{1i}(0,\eta)\lambda_i \\ \vdots \\ \dot{\eta}_{(n-r_{tot})} = q_{(n-r_{tot})}(0,\eta) + \sum_{i=1}^{m} p_{(n-r_{tot})i}(0,\eta)\lambda_i \end{cases} \tag{2.62}
$$

is called zero dynamics of the system. The system is said to be minimum phase if its zero dynamics have an asymptotically stable equilibrium point in the domain of interest.

From this definition an important theorem can be proved [7].

Theorem 2. *Consider a general system described by the following equations:*

$$
\begin{aligned}
\dot{x} &= f(x) + \sum_{i=0}^{m} g_i(x)\lambda_i, \\
y_1 &= h_1(x), \\
&\vdots \\
y_m &= h_m(x,)
\end{aligned} \tag{2.63}
$$

and its equivalent transformed in normal form, namely

$$
\begin{aligned}
\dot{\xi} &= f_\xi(\xi,\eta), \\
\dot{\eta} &= f_\eta(\xi,\eta),
\end{aligned} \tag{2.64}
$$

where $f : \mathcal{U} \subseteq \mathbb{R}^n \to \mathbb{R}$ and $x \in \mathbb{R}^n$. Assume system Equation 2.63 to have relative degree $0 < r_{tot} \leq n-1$. Stability properties of equilibrium points of system 2.63 are equivalent to stability properties of the zero dynamics 2.64.

2.7 Looper - normal form computation

This section presents the normal form transformation of the system in analysis, namely the looper presented in section 2.2. The choice of such transformation is of the utmost importance for the stability analysis, as it will be explained in chapter 3. Therefore, two different normal form transformations are presented below, whose benefits and drawbacks will be addressed in section 3.2 and in section 3.3.

2.7.1 Normal form - preliminary analysis

Consider the system described by Equation 1.44 and a general point $x \in \mathbb{R}^4$. As reported in section 2.5, the vector relative degree of the looper is $r = (2, 2)$. Recall the notions presented in subsection 2.6.3. The normal form is described by equations of the following form.

$$z = \begin{pmatrix} z_1 \\ z_2 \\ z_3 \\ z_4 \\ z_5 \\ z_6 \end{pmatrix} = \begin{pmatrix} \xi_1^1 \\ \xi_2^1 \\ \xi_1^2 \\ \xi_2^2 \\ \eta_1 \\ \eta_2 \end{pmatrix} = \begin{pmatrix} \phi_1^1(x) \\ \phi_2^1(x) \\ \phi_1^2(x) \\ \phi_2^2(x) \\ \phi_1(x) \\ \phi_2(x) \end{pmatrix}, \tag{2.65}$$

where the vector $(\phi_1^1, \phi_2^1, \phi_1^2, \phi_2^2)$ is defined as follows.

$$\begin{pmatrix} \phi_1^1 \\ \phi_2^1 \\ \phi_1^2 \\ \phi_2^2 \end{pmatrix} = \begin{pmatrix} h_1(x) \\ L_f h_1(x) \\ h_2(x) \\ L_f h_2(x) \end{pmatrix}. \tag{2.66}$$

Consider then the normal form mapping

$$\mathbf{\Phi} = \begin{pmatrix} \phi_1^1 \\ \phi_2^1 \\ \phi_1^2 \\ \phi_2^2 \\ \phi_1 \\ \phi_2 \end{pmatrix}. \tag{2.67}$$

The choice of the pair (ϕ_1, ϕ_2) shall be done in order to meet the condition expressed in proposition 2, namely

$$\det\Big(J(\Phi(x))\Big) \neq 0. \tag{2.68}$$

2.7.2 Normal form - free mappings choice

The following two paragraphs present two possible choices of mappings (ϕ_1, ϕ_2). These mappings result in different considerations on the stability analysis of the system.

Normal form - case 1

The first proposed normal form transformation is described by the following equations.

$$\mathbf{\Phi} = \begin{pmatrix} \phi_1^1 \\ \phi_2^1 \\ \phi_1^2 \\ \phi_2^2 \\ \phi_1 \\ \phi_2 \end{pmatrix} = \begin{pmatrix} h_1(x) \\ L_f h_1(x) \\ h_2(x) \\ L_f h_2(x) \\ x_1 \\ x_6 \end{pmatrix} \tag{2.69}$$

Recall the structure of f and h described in section 2.2, namely

$$\begin{cases} \dot{x}_1 = x_4 \\ \dot{x}_2 = x_5 \\ \dot{x}_3 = x_6 \\ \dot{x}_4 = F_4(x) + a_{11}(x)\lambda_1(x) + a_{21}(x)\lambda_2(x) \\ \dot{x}_5 = F_5(x) + a_{12}(x)\lambda_1(x) + a_{22}(x)\lambda_2(x) \\ \dot{x}_6 = F_6(x) + a_{13}(x)\lambda_1(x) + a_{23}(x)\lambda_2(x) \end{cases}, \tag{2.70}$$

and

$$\begin{cases} h_1(q) = (R_{12} + R_{23} + q_2)\cos q_1 - R_x - R_{34}\sin q_3 = 0 \\ h_2(q) = (R_{12} + R_{23} + q_2)\sin q_1 - R_y + R_{34}\cos q_3 = 0 \end{cases} \tag{2.71}$$

The Jacobian matrix of the proposed diffeomorphism takes the following form.

$$J(\Phi(x)) = \begin{pmatrix} \frac{\partial h_1}{\partial x_1} & \frac{\partial h_1}{\partial x_2} & \frac{\partial h_1}{\partial x_3} & 0 & 0 & 0 \\ \frac{\partial L_f h_1}{\partial x_1} & \frac{\partial L_f h_1}{\partial x_2} & \frac{\partial L_f h_1}{\partial x_3} & \frac{\partial L_f h_1}{\partial x_4} & \frac{\partial L_f h_1}{\partial x_5} & \frac{\partial L_f h_1}{\partial x_6} \\ \frac{\partial h_2}{\partial x_1} & \frac{\partial h_2}{\partial x_2} & \frac{\partial h_2}{\partial x_3} & 0 & 0 & 0 \\ \frac{\partial L_f h_2}{\partial x_1} & \frac{\partial L_f h_2}{\partial x_2} & \frac{\partial L_f h_2}{\partial x_3} & \frac{\partial L_f h_2}{\partial x_4} & \frac{\partial L_f h_2}{\partial x_5} & \frac{\partial L_f h_2}{\partial x_6} \\ 1 & 0 & 0 & 0 & 0 & 0 \\ 0 & 0 & 0 & 0 & 0 & 1 \end{pmatrix} \tag{2.72}$$

The determinant of this Jacobian matrix is in the following form.

$$\det\Big(J(\Phi(x))\Big) = R_{34}(R_{12} + R_{23} + x_2)\sin(x_1 - x_3) \tag{2.73}$$

Recall the considerations on the singularities of the looper reported in subsection 1.2.3. The only configuration making the Jacobian singular occurs when

$$x_1 = x_3, \tag{2.74}$$

namely when the first and the third link of the mechanism are normal. This happens in the joint space boundaries only.

As a result of the previous considerations, the proposed transformation turns out to be a local diffeomorphism for the system in analysis in any point except for $x_1 = \theta_1^{min}$ and $x_1 = \theta_1^{max}$. Therefore, such mapping is also invertible. The inverse transformation is described by the following equations.

$$\Phi^{-1} = \begin{pmatrix} z_5 \\ \phi_{x_2}^{-1}(z) \\ \phi_{x_3}^{-1}(z) \\ \phi_{x_4}^{-1}(z) \\ \phi_{x_5}^{-1}(z) \\ z_6 \end{pmatrix} = \begin{pmatrix} z_5 \\ \frac{z_1+R_x+R_{34}\sin\phi_{x_3}^{-1}(z)}{\cos z_5} - (R_{12}+R_{23}) \\ z_5 - \arccos\left(\frac{(z_3+R_y)\cos z_5-(z_1+R_x)\sin z_5}{R_{34}}\right) \\ \frac{z_4\cos z_5-z_2\sin z_5+R_{34}z_6\sin(\phi_{x_3}^{-1}(z)-z_5)}{R_{12}+R_{23}+\phi_{x_2}^{-1}(z)} \\ \frac{z_2+(R_{12}+R_{23}+\phi_{x_2}^{-1}(z))\phi_{x_4}^{-1}(z)\sin z_5+R_{34}z_6\cos\phi_{x_3}^{-1}(z)}{\cos z_5} \\ z_6 \end{pmatrix} \tag{2.75}$$

Normal form - case 2

The second proposed normal form transformation is described by the following equations:

$$\Phi = \begin{pmatrix} \phi_1^1 \\ \phi_2^1 \\ \phi_1^2 \\ \phi_2^2 \\ \phi_1 \\ \phi_2 \end{pmatrix} = \begin{pmatrix} h_1(x) \\ L_f h_1(x) \\ h_2(x) \\ L_f h_2(x) \\ x_1 \\ x_4 \end{pmatrix} \tag{2.76}$$

Recal the structure of f and h described in Equation 2.70 and Equation 2.71. The Jacobian matrix of this mapping takes the following form.

$$J(\Phi(x)) = \begin{pmatrix} \frac{\partial h_1}{\partial x_1} & \frac{\partial h_1}{\partial x_2} & \frac{\partial h_1}{\partial x_3} & 0 & 0 & 0 \\ \frac{\partial L_f h_1}{\partial x_1} & \frac{\partial L_f h_1}{\partial x_2} & \frac{\partial L_f h_1}{\partial x_3} & \frac{\partial L_f h_1}{\partial x_4} & \frac{\partial L_f h_1}{\partial x_5} & \frac{\partial L_f h_1}{\partial x_6} \\ \frac{\partial h_2}{\partial x_1} & \frac{\partial h_2}{\partial x_2} & \frac{\partial h_2}{\partial x_3} & 0 & 0 & 0 \\ \frac{\partial L_f h_2}{\partial x_1} & \frac{\partial L_f h_2}{\partial x_2} & \frac{\partial L_f h_2}{\partial x_3} & \frac{\partial L_f h_2}{\partial x_4} & \frac{\partial L_f h_2}{\partial x_5} & \frac{\partial L_f h_2}{\partial x_6} \\ 1 & 0 & 0 & 0 & 0 & 0 \\ 0 & 0 & 0 & 1 & 0 & 0 \end{pmatrix} \tag{2.77}$$

The determinant of this Jacobian matrix turns out to be the following.

$$\det\Big(J(\Phi(x))\Big) = -R_{34}^2\sin^2(x_1 - x_3) \tag{2.78}$$

Recall the considerations on the singularities of the looper reported in subsection 1.2.3. The only configuration making the Jacobian singular occurs when

$$x_1 = x_3, \tag{2.79}$$

namely when the first and the third link of the mechanism are normal. This happens in the joint space boundaries only.

As a result of the previous considerations, the proposed transformation turns out to be a local diffeomorphism for the system in analysis in any point except for $x_1 = \theta_1^{min}$ and $x_1 = \theta_1^{max}$. Therefore, such mapping is also invertible. The inverse transformation is described by the following equations.

$$\Phi^{-1} = \begin{pmatrix} z_5 \\ \phi_{x_2}^{-1}(z) \\ \phi_{x_3}^{-1}(z) \\ \phi_{x_4}^{-1}(z) \\ \phi_{x_5}^{-1}(z) \\ z_6 \end{pmatrix} = \begin{pmatrix} z_5 \\ \frac{z_1+R_x+R_{34}\sin\phi_{x_3}^{-1}(z)}{\cos z_5} - (R_{12}+R_{23}) \\ z_5 - \arccos\left(\frac{(z_3+R_y)\cos z_5-(z_1+R_x)\sin z_5}{R_{34}}\right) \\ z_6 \\ \frac{z_2+(R_{12}+R_{23}+\phi_{x_2}^{-1}(z))z_6\sin z_5+R_{34}\phi_{x_6}^{-1}(z)\cos\phi_{x_3}^{-1}(z)}{\cos z_5} \\ \frac{z_4\cos z_5-z_2\sin z_5-(R_{12}+R_{23}+\phi_{x_2}^{-1}(z))z_6}{R_{34}\sin(z_5-\phi_{x_3}^{-1}(z))} \end{pmatrix} \tag{2.80}$$

2.7.3 Normal form - system dynamics

From the algebraic mappings describing the coordinates transformation, system dynamics can be computed. Thus, recalling subsection 2.6.3, set

$$\begin{aligned} a_{11} &= L_{g_1}L_f h_1(\Phi^{-1}(z)), \\ a_{12} &= L_{g_1}L_f h_2(\Phi^{-1}(z)), \\ a_{21} &= L_{g_2}L_f h_1(\Phi^{-1}(z)), \\ a_{22} &= L_{g_2}L_f h_2(\Phi^{-1}(z)), \\ b_1 &= L_f^2 h_1(\Phi^{-1}(z)), \\ b_2 &= L_f^2 h_2(\Phi^{-1}(z)), \\ q_1 &= L_f\Phi_1(\Phi^{-1}(z)) = \phi_{x_4}^{-1}(z), \\ q_2 &= L_f\Phi_2(\Phi^{-1}(z)) = F_4(\Phi^{-1}(z)), \\ p_{11} &= L_{g_1}\Phi_1(\Phi^{-1}(z)) = 0, \\ p_{12} &= L_{g_2}\Phi_1(\Phi^{-1}(z)) = 0. \end{aligned} \tag{2.81}$$

$$\tag{2.82}$$

The last coefficients to be computed are (p_{21}, p_{22}). Such coefficients vary depending on the mapping. Therefore, they are described as follows, accordingly to the coordinates choice presented in subsection 2.7.2.

1. Consider the mapping described in Equation 2.69. It holds

$$\begin{aligned} p_{21} &= L_{g_1}\phi_2(\Phi^{-1}(z)) = \frac{R_{12}+R_{23}+\phi_{x_2}^{-1}(z)}{J_{tot_1}}\sin z_5, \\ p_{22} &= L_{g_2}\phi_2(\Phi^{-1}(z)) = -\frac{R_{12}+R_{23}+\phi_{x_2}^{-1}(z)}{J_{tot_1}}\cos z_5. \end{aligned} \tag{2.83}$$

2. Consider the mapping described in Equation 2.76. It holds.

$$\begin{aligned} p_{21} &= L_{g_1}\phi_2(\Phi^{-1}(z)) = \frac{R_34}{J_{tot_2}}\cos\phi_{x_3}^{-1}(z), \\ p_{22} &= L_{g_2}\phi_2(\Phi^{-1}(z)) = \frac{R_34}{J_{tot_2}}\sin\phi_{x_3}^{-1}(z). \end{aligned} \tag{2.84}$$

Therefore, for both the coordinate transformations, the dynamics of the system are described by equations in the following form.

$$\begin{cases} \dot{\xi}_1^1 = \xi_2^1 \\ \dot{\xi}_2^1 = b_1 + a_{11}\lambda_1 + a_{12}\lambda_2 \\ \dot{\xi}_1^2 = \xi_2^2 \\ \dot{\xi}_2^2 = b_2 + a_{21}\lambda_1 + a_{22}\lambda_2 \\ \dot{\eta}_1 = q_1 + p_{11}\lambda_1 + p_{12}\lambda_2 \\ \dot{\eta}_2 = q_2 + p_{21}\lambda_1 + p_{22}\lambda_2 \end{cases} \tag{2.85}$$

Note that the main difference between mapping 2.69 and 2.76 is that in the latter defines (η_1, η_2) as respectively an angular position and velocity. Therefore, the η dynamics $(\dot{\eta}_1, \dot{\eta}_2)$ represents a mechanical system, whose stability properties can be analysed easier than other kind of systems.

2.7.4 Normal form - Lagrangian multipliers computation

Consider the system described in Equation 2.85. As a matter of fact, the Lagrangian multipliers computed in section 2.3 shall be modified accordingly to the new system of coordinates. Note that the algebraic constraints are represented in the new coordinate system by the pair (ξ_1^1, ξ_1^2). The procedure to compute the Lagrangian multipliers is similar to the one carried on in the original coordinate system. It unfolds as follows.

1. Recall that the vector relative degree is $r = (2, 2)$. Therefore, both the algebraic constraint shall be differentiated twice in order to find an explicit dependence on the input, namely

$$\frac{d^2}{dt}\begin{pmatrix} \xi_1^1 \\ \xi_1^2 \end{pmatrix} = \begin{pmatrix} \dot{\xi}_2^1 \\ \dot{\xi}_2^2 \end{pmatrix} = \begin{pmatrix} b_1 + a_{11}\lambda_1 + a_{12}\lambda_2 \\ b_2 + a_{21}\lambda_1 + a_{22}\lambda_2 \end{pmatrix}. \tag{2.86}$$

2. Constraints derivatives shall be zero at any time. Therefore, the following holds.

$$\begin{cases} b_1 + a_{11}\lambda_1 + a_{12}\lambda_2 = 0 \\ b_2 + a_{21}\lambda_1 + a_{22}\lambda_2 = 0 \end{cases} \tag{2.87}$$

3. The solution of this set of equations provides the solution for the Lagrangian multipliers in the new coordinates system, that is

$$\begin{cases} \lambda_1 = -\frac{b_1 + a_{12}\lambda_2}{a_{11}} \\ \lambda_2 = \frac{b_1 a_{21} - b_2 a_{11}}{a_{11}a_{22} - a_{12}a_{21}} \end{cases} \tag{2.88}$$

Chapter 3

Stability analysis

This chapter presents the study of equilibrium points for the system in analysis, namely the looper. Roughly speaking, the looper consists of an actuated constrained pendulum. Therefore, its free dynamics shall be characterized by two equilibrium point, one of which being stable, the other unstable. However, such points don't always correspond to $\bar{\theta}_2 = 0$ and $\bar{\theta}_2 = \pi$, as in the simple pendulum case. Generally speaking, the equilibrium points of the looper are described as follows.

$$x_{eq_1} = (x_1^{eq_1}, x_2^{eq_1}, x_3^{eq_1}, 0, 0, 0), \quad x_3^{eq_1} \in \left[-\frac{\pi}{2}; \frac{\pi}{2} \right] \tag{3.1}$$

$$x_{eq_2} = (x_1^{eq_2}, x_2^{eq_2}, x_3^{eq_1}, 0, 0, 0), \quad x_3^{eq_2} \in \left[\frac{\pi}{2}; \frac{3\pi}{2} \right] \tag{3.2}$$

Consider again the system described in Figure 1.5. As explained in section 1.2 the steel flows on the upper part of the mechanism, loading the endpoint of the looper. Therefore,it's realistic to assume the operational range of the mechanism to be limited to $\theta_2 \in [-\frac{\pi}{2}; \frac{\pi}{2}]$. As a consequence, the stability analysis of the system is carried on for x_{eq_1} only. For the sake of simplicity from now on x_{eq_1} will be referred to as $\bar{x}$.

The model of the looper has been implemented in MATLAB, considering the set-up described in Table 1.1. In order to find the equilibrium point two different approaches have been used.

1. **Simulation test.** The first and more rough approach to find the equilibrium point of the system consists in running the simulation of the model for a significant amount of time. Due to the presence of friction the simulation asymptotically settles down on a specific state vector, which is assumed to be the equilibrium point $\bar{x}$.

2. **Optimisation test.** This second approach addresses the research of the equilibrium point as constrained optimisation problem. Consider an initial condition x_0 coherent with the assumptions on the algebraic constraints, namely

$$h_i(x_0) = 0, \quad i \in \{1, 2\}. \tag{3.3}$$

   The optimisation process considers at each iteration the output of the model, that is

$$\dot{x} = f(x). \tag{3.4}$$

Then, starting from x_0, the optimisation algorithm minimizes the value of $\dot{x}$ considering Equation 3.3 as an additional constraint to be satisfied at any iteration.

From both these analysis the equilibrium point of the looper results

$$\bar{x} = \begin{bmatrix} 1.0946 & 0.1774 & 0.0955 & 0 & 0 & 0 \end{bmatrix}. \tag{3.5}$$

3.1 Lyapunov stability theory

The stability analysis is developed accordingly to Lyapunov theory of stability. This section shortly recalls the basis of such theory. To develop Lyapunov stability theory consider a general system in the following form.

$$\dot{x} = f(x), \quad f : \mathcal{U} \subseteq \mathbb{R}^n \to \mathbb{R}, \quad x \in \mathcal{U} \tag{3.6}$$

Lyapunov stability Consider $\bar{x} \in \mathcal{U}$ to be an equilibrium point for such system, namely

$$\dot{\bar{x}} = f(\bar{x}) = 0 \tag{3.7}$$

Consider also system initial condition to be $x_0 \in \mathcal{U}$ in $t = t_0$. The following stability definition holds.

Definition 6 (simple stability)**.** *$\bar{x} \in \mathcal{U}$ is said to be stable if*

$$\begin{gathered} \exists \epsilon \geq 0, \quad \exists \delta(\epsilon) \geq 0 \quad s.t. \\ \|x_0 - \bar{x}\| < \delta(\epsilon) \to \|x(t) - \bar{x}\| < \epsilon, \quad \forall t \geq t_0 \end{gathered} \tag{3.8}$$

If the above condition is not satisfied, point $\bar{x}$ is said to be unstable. A more strict kind of stability can be defined.

Definition 7 (local asymptotic stability)**.** *$\bar{x} \in \mathcal{U}$ is said to be locally asymptotically stable (LAS) if*

$$\exists \epsilon \geq 0, \quad \exists \delta(\epsilon) \geq 0 \quad s.t.$$

i) $\|x_0 - \bar{x}\| < \delta(\epsilon) \to \|x(t) - \bar{x}\| < \epsilon, \quad \forall t \geq t_0$

ii) $\lim_{t \to \infty} \|x(t) - \bar{x}\| = 0$

Local asymptotic stability can be extended to the whole system domain.

Definition 8 (global asymptotic stability)**.** *$\bar{x} \in \mathcal{U}$ is said to be globally asymptotically stable (GAS) if*

$$\forall \epsilon \geq 0, \quad \exists \delta(\epsilon) \geq 0 \quad s.t.$$

i) $\|x_0 - \bar{x}\| < \delta(\epsilon) \rightarrow \|x(t) - \bar{x}\| < \epsilon, \quad \forall t \geq t_0$

ii) $\lim_{t \to \infty} \|x(t) - \bar{x}\| = 0$

Note that the difference between LAS and GAS points is the existence of an upper bound for the initial displacement $\|x_0 - \bar{x}\|$. GAS points are said to be globally attractive as any trajectory of the system always tends to them as $t \rightarrow \infty$.

Quadratic forms This paragraph provides a brief introduction on quadratic forms as they are are widely used in Lyapunov theory. Their definition and main properties are summarized in the following definition.

Definition 9 (quadratic form)**.** *Consider a mapping $V : \mathbb{R}^n \rightarrow \mathbb{R}$ such that:*

$$V = x^T P x, \quad P \in \mathbb{R}^{n \times n}, \quad x \in \mathbb{R}^n \tag{3.9}$$

V is said to be a quadratic form in $\mathbb{R}^n$. The following properties hold.

i) Assume $P = P^T$, then

$$V(x) \geq 0 \quad \forall x \in \mathbb{R}^n - \{0\} \tag{3.10}$$

Moreover, it holds

$$\lambda_{min} \|x\|^2 \leq x^T P x \leq \lambda_{max} \|x\|^2, \quad \lambda_{min} = \min(\sigma(P)), \quad \lambda_{max} = \max(\sigma(P)) \tag{3.11}$$

ii) Assume $P = -P^T$, then

$$V(x) \leq 0 \quad \forall x \in \mathbb{R}^n - \{0\} \tag{3.12}$$

Recall also that $V : \mathcal{U} \subseteq \mathbb{R}^n \rightarrow \mathbb{R}$ is said to be positive definite (semi-definite) if $V(x) > 0$ (≥ 0), $\forall x \in \mathcal{U}$. Moreover, V is said to be negative definite (semi-definite) if $-V$ is positive definite (semi-definite).

Lyapunov theorems At this stage, Lyapunov theory can be introduced. The three main theorems for stability analysis are presented below.

Theorem 3 (simple stability)**.** *Consider a general system described by Equation 3.6. Let $\bar{x}$ = be an equilibrium point for such system. Consider also a continuously differentiable mapping $V : \mathcal{U} \subseteq \mathbb{R}^n \rightarrow \mathbb{R}$ such that*

i) $V(0) = 0$

ii) $V(x) > 0, \quad \forall x \in \mathcal{U} - \{0\}$

iii) $\dot{V}(x) \leq 0, \quad \forall x \in \mathcal{U} - \{0\}$

If such conditions are satisfied, $\bar{x}$ is a simply stable point for system 3.6.

Theorem 3 can be modified in order to prove the local asymptotic stability equilibrium points.

Theorem 4 (local asymptotic stability)**.** *Consider a general system described by Equation 3.6. Let $\bar{x} =$ be an equilibrium point for such system. Consider also a continuously differentiable mapping $V : \mathcal{U} \subseteq \mathbb{R}^n \to \mathbb{R}$ such that*

i) $V(0) = 0$

ii) $V(x) > 0, \quad \forall x \in \mathcal{U} - \{0\}$

iii) $\dot{V}(x) < 0, \quad \forall x \in \mathcal{U} - \{0\}$

If such conditions are satisfied, $\bar{x}$ is a locally asymptotic stable point for system 3.6.

Again, Theorem 4 can be extended to prove the global asymptotic stability of equilibrium points. To do so, recall the following definition.

Definition 10. *Consider a mapping $f : \mathbb{R}^n \to \mathbb{R}$. Such mapping is said to be radially unbounded if*

$$\|x\| \to \infty \implies f(x) \to \infty \tag{3.13}$$

The following theorem can be stated.

Theorem 5 (global asymptotic stability)**.** *Consider a general system described by Equation 3.6. Let $\bar{x} =$ be an equilibrium point for such system. Consider also a continuously differentiable mapping $V : \mathcal{U} \subseteq \mathbb{R}^n \to \mathbb{R}$ such that*

i) $V(0) = 0$

ii) $V(x) > 0, \quad \forall x \in \mathcal{U} - \{0\}$

iii) $V(x)$ *is radially unbounded*

iv) $\dot{V}(x) < 0, \quad \forall x \in \mathcal{U} - \{0\}$

If such conditions are satisfied, $\bar{x}$ is a globally asymptotic stable point for system 3.6.

Note that Lyapunov theorems are sufficient yet not necessary conditions for the stability of equilibrium points. That is, even if a specific Lyapunov function V satisfying theorem's requirements can't be found, nothing can be said on the stability of the point.

As for the looper, the stability analysis is performed on the system in normal form. Indeed, different results can be achieved considering different coordinate transformations, as shown in the following paragraphs. The choice of the right coordinate transformation turns out to be crucial for the stability analysis.

3.2 Stability analysis - case 1

This section addresses the stability analysis of the looper in the first normal form choice, namely the one described by Equation 2.69. As explained in subsection 2.6.4, stability properties of a system in normal form can be analysed considering its zero dynamics. Therefore, consider the system described by the following equations.

$$\begin{cases} \dot{\eta}_1 = \phi_{x_4}^{-1}(\eta) \\ \dot{\eta}_2 = F_6(\Phi^{-1}(\eta)) + \frac{R_{12}+R_{23}+\phi_{x_2}^{-1}(\eta)}{J_{tot_1}} \sin\eta_1\lambda_1 + -\frac{R_{12}+R_{23}+\phi_{x_2}^{-1}(\eta)}{J_{tot_1}} \cos\eta_1\lambda_2 \end{cases}, \tag{3.14}$$

which can be also written as

$$\dot{\eta} = \begin{bmatrix} \dot{\eta}_1 \\ \dot{\eta}_2 \end{bmatrix} = \begin{bmatrix} q_{0_1} \\ q_{0_2} \end{bmatrix} = q_0. \tag{3.15}$$

Recalling the considerations presented in chapter 3, the equilibrium point of such system consists of $\bar{x}$ restricted to the η dynamics, namely

$$\bar{\eta} = (\phi_{x_4}(\bar{x_4}), 0) = (\bar{\eta}_1, 0). \tag{3.16}$$

3.2.1 Linearised model

This section studies the stability properties of the linearised model of the looper. The obtained results are then used to infer stability properties on the nonlinear model too.

Consider system 3.15 and compute its linearisation around the equilibrium point $\bar{\eta}$, that is

$$\dot{\eta}_{lin} = q_0\Big|_{\eta=\bar{eta}} + \nabla q_0\Big|_{\eta=\bar{\eta}}(\eta - \bar{\eta}) + o(\eta - \bar{\eta})^2 \tag{3.17}$$

This affine system can always be considered a general linear system through a coordinate transformation, namely

$$\dot{\eta}_{lin} = A(\eta - \bar{\eta}) + o(\eta - \bar{\eta})^2 \tag{3.18}$$

Before dealing with the looper model, the stability analysis approach is described on a general linear system. The stability analysis of linear systems is carried on by means of Theorem 4. Consider then a general system described by equations in the form of

$$\dot{x} = Ax. \tag{3.19}$$

Consider also an equilibrium point $\bar{x} = 0$ and a candidate Lyapunov function $V : \mathcal{D} \subseteq \mathbb{R}^n \to \mathbb{R}$ such that $V = x^T P x$, where $x \in \mathbb{R}^n$ and $P^T = P \in \mathbb{R}^{n\times n}$. Such assumptions are consistent with Theorem 4 and Theorem 5. However, in order to prove the stability of $\bar{x}$, V derivative shall be computed and imposed to be negative semi-definite. This procedure unfolds as follows.

$$\begin{aligned}\frac{dV}{dt} &= x^T P\dot{x} + \dot{x}^T Px = \\ &= x^T PAx + x^T A^T Px = \\ &= x^T (PA + A^T P)x \leq 0\end{aligned} \tag{3.20}$$

According to definition 9, V is a quadratic form, as well as $\dot{V}$. Recall that a quadratic form $V = x^T Px$ is negative definite if P is a skew symmetric matrix. Thus, consider a matrix $Q = Q^T \in \mathbb{R}^{n\times n}$. Consider also the following matrix equation

$$PA + A^T P + Q = 0. \tag{3.21}$$

This is called *Lyapunov equation*. Solving such equation in P ensures $\dot{V} = x^T(PA + A^T P)x < 0$. This proves the local as well as the global asymptotic stability of the equilibrium point $\bar{x} = 0$ considered.

3.2.2 Nonlinear model

The results on the stability of the linear system defined in Equation 3.19 can be extended locally to the related nonlinear system.

Consider a general nonlinear system described by equations of the following form

$$\dot{x} = f(x), \quad x \in \mathbb{R}^n, \tag{3.22}$$

where $f : \mathcal{U} \subseteq \mathbb{R}^n \to \mathbb{R}^n$. Assume also $\bar{x} = 0$ to be an equilibrium point. The question to be addressed is whether the Lyapunov function V defined for the linearised system in subsection 3.2.1 is good to prove the stabiliy of $\bar{x}$ also in the nonlinear framework or not.

In this framework, the nonlinear system can be expressed in terms of the linearised one as follows

$$\dot{x} = \dot{x}_{lin} + hot(x) = Ax + hot(x) \tag{3.23}$$

Therefore, the Lyapunov function derivative analysis becomes the following.

$$\begin{aligned}\frac{dV}{dt} &= x^T P\dot{x} + \dot{x}^T Px = \\ &= x^T P(Ax + hot(x)) + (x^T A^T + hot^T(x))Px = \\ &= x^T PAx + x^T Phot(x) + x^T A^T Px + hot^T(x)Px = \\ &= x^T (PA + A^T P)x + 2x^T Phot(x)\end{aligned} \tag{3.24}$$

By solving the Lyapunov equation as reported in subsection 3.2.1, it holds

$$PA + A^T P = -Q < 0, \quad Q > 0. \tag{3.25}$$

Therefore, the Lyapunov function derivative can be bounded as follows.

$$\dot{V} = -x^T Qx + 2x^T P \leq -x^T Qx + 2\|P\|\|x\|\|hot(x)\| \tag{3.26}$$

Recall now the properties defined for a quadratic form in 9, and more specifically that

$$\lambda_{min}\|x\|^2 \leq x^T P x \leq \lambda_{max}\|x\|^2. \tag{3.27}$$

Therefore, it holds

$$\dot{V} \leq -\lambda_{min}(Q)\|x\| + 2\|P\|\|x\|\|hot(x)\| \tag{3.28}$$

Therefore, in order to have $\dot{V} < 0$, the following condition shall be met.

$$\|hot(x)\| < \frac{\lambda_{min}(Q)\|x\|}{2\|P\|} \tag{3.29}$$

where $\|hot(x)\|$ can be retrieved from Equation 3.23. Thus, the very same Lyapunov function designed for the linear case holds locally also for the nonlinear one. Therefore, only local asymptotic stability of the equilibrium point $\bar{x}$ can be proved.

3.2.3 Results

The procedure described in subsection 3.2.1 and subsection 3.2.2 has been performed on the model of the looper, described in section 2.7.

The nonlinear model and its linearised counterpart are shown in Figure 3.1. The linearisation has been performed around the equilibrium point $\bar{\eta}$.

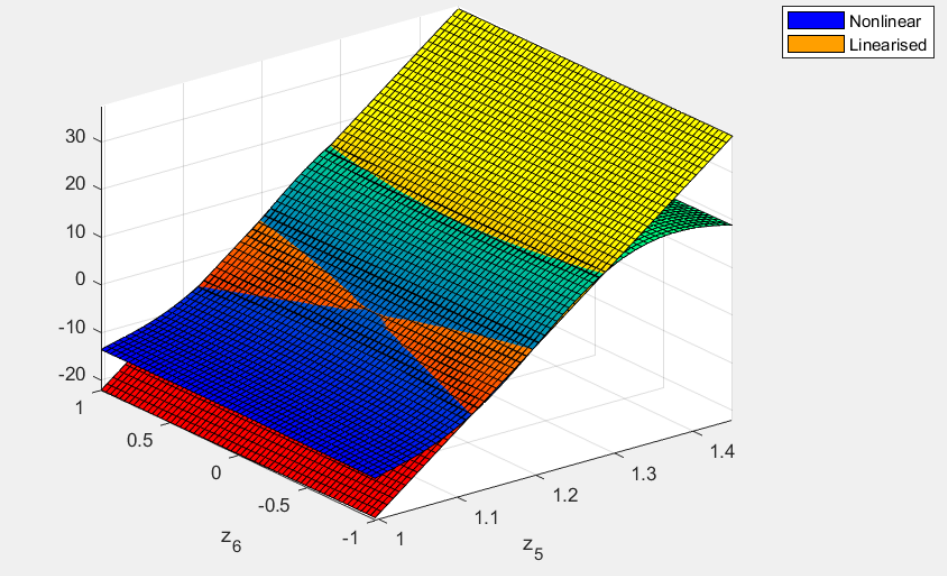

Figure 3.1: Nonlinear model and linearised model of the looper

The Lyapunov equation has been solved considering A as described in subsection 3.2.1 and the following target matrix Q.

$$Q = \begin{bmatrix} 0.0001 & 0 \\ 0 & 0.0002 \end{bmatrix}. \tag{3.30}$$

The solution matrix $\bar{P}$ turns out to be

$$\bar{P} = \begin{bmatrix} 1.4084413 & -0.0000015 \\ -0.0000015 & 0.0031958 \end{bmatrix}. \tag{3.31}$$

The considered Lyapunov function is in the following form.

$$W = (\eta - \bar{\eta})^T \bar{P} (\eta - \bar{\eta}) \tag{3.32}$$

As expected W has a global minimum in $\bar{\eta}$. W is shown in Figure 3.2.

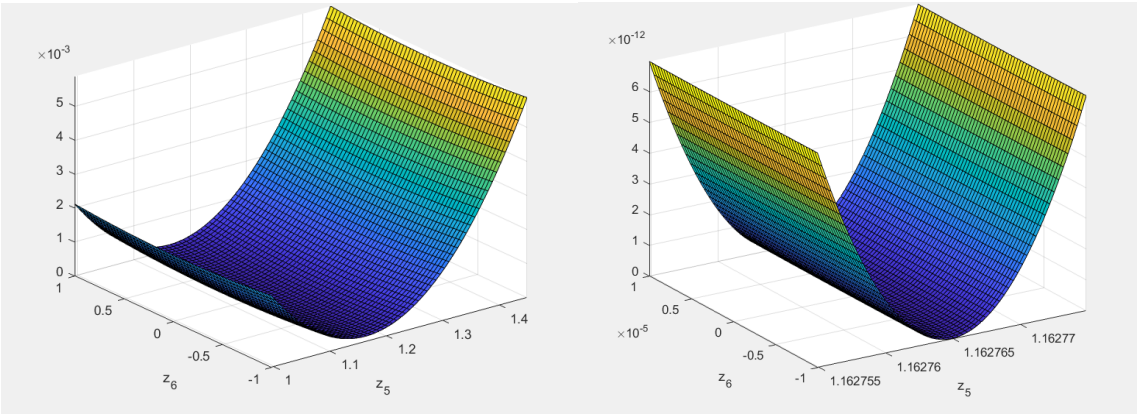

(a) W on whole domain (b) W near $\bar{\eta}$

Figure 3.2: Lyapunov function W

This Lyapunov function has been used to check the local asymptotic stability of $\bar{\eta}$ both for the linear and nonlinear case, namely the following mappings have been defined

$$\begin{aligned} W_{lin} &= (\eta_{lin} - \bar{\eta})^T \bar{P} (\eta_{lin} - \bar{\eta}), \\ W &= (\eta - \bar{\eta})^T \bar{P} (\eta - \bar{\eta}). \end{aligned} \tag{3.33}$$

Both $\dot{W}$ and $\dot{W}_{lin}$ are shown in Figure 3.3. As it can be seen, the condition $\dot{W} < 0$ is satisfied over a limited domain as far as the nonlinear model is concerned, proving the local asymptotic stability of $\bar{\eta}$. In fact, note that in a neighbourhood of $\bar{\eta}$ both $\dot{W}$ and $\dot{W}_{lin}$ are negative definite. Differently, over the whole domain, there exist values of η where $\dot{W} \geq 0$.

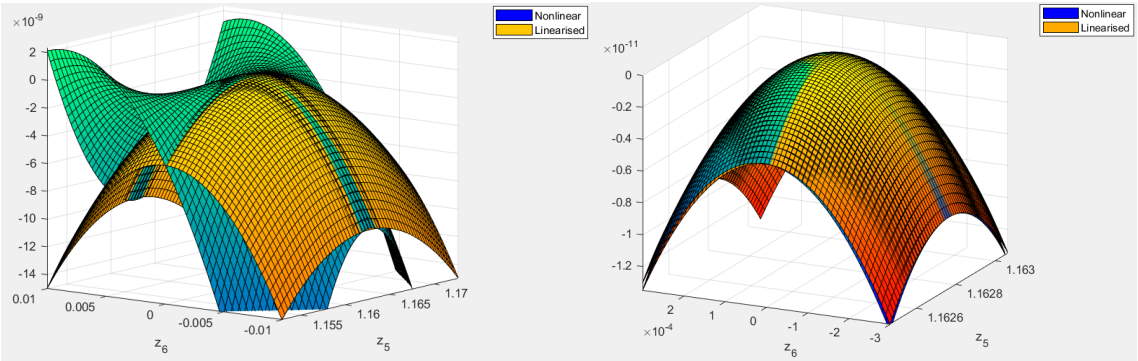

(a) $\dot{W}$ on whole domain (b) $\dot{W}$ near $\bar{\eta}$

Figure 3.3: Lyapunov function W and W_{lin}

The stability analysis of the linear and nonlinear models differs due to the term $\|hot(\eta)\|$. This term has been computed as described in subsection 3.2.2 and referred to as b_{max}. The final condition for the local asymptotic stability is described by the following inequality.

$$\frac{\|hot(\eta)\|}{\|x\|} < b_{max} = 3.550023613765002e-05 \tag{3.34}$$

The comparison between $\frac{\|hot(\eta)\|}{\|x\|}$ and b_{max} is shown in Figure 3.4.

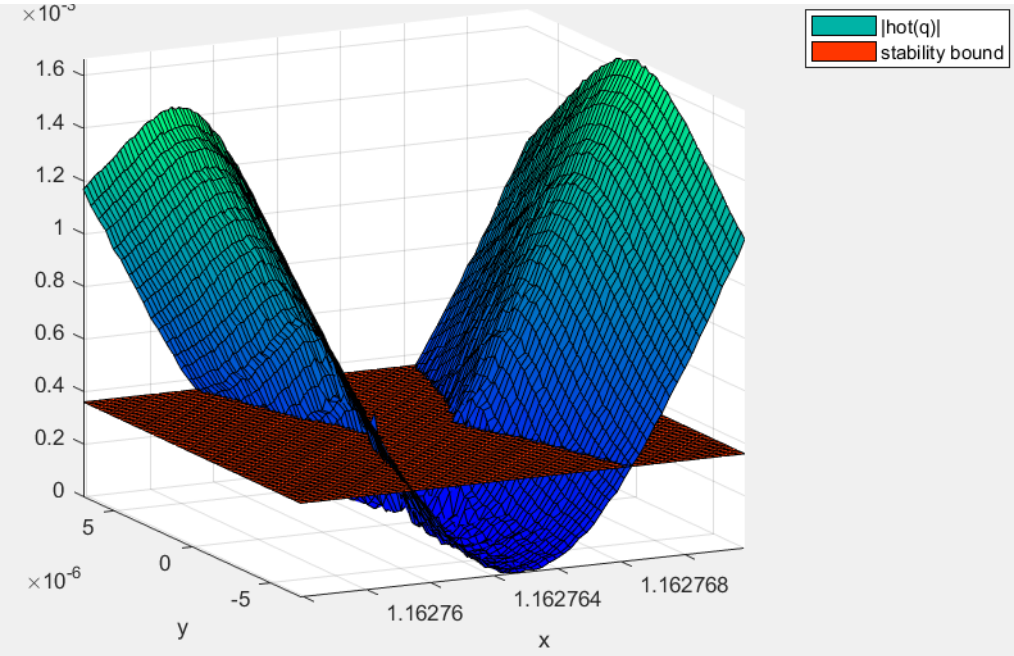

Figure 3.4: Comparison between $\frac{\|hot(\eta)\|}{\|x\|}$ and b_{max}

3.3 Stability analysis - case 2

Consider the second normal form transformation of the looper, presented in section 2.7.2, namely

$$\Phi = \begin{pmatrix} \phi_1^1 \\ \phi_2^1 \\ \phi_1^2 \\ \phi_2^2 \\ \phi_1 \\ \phi_2 \end{pmatrix} = \begin{pmatrix} h_1(x) \\ L_f h_1(x) \\ h_2(x) \\ L_f h_2(x) \\ x_1 \\ x_4 \end{pmatrix} \tag{3.35}$$

In this section the stability analysis is addressed through the looper transformed in this normal form. As discussed, this specific transformation describes the zero dynamics as a mechanical system. The η dynamics of the considered system is described by equations in the following form.

$$\begin{cases} \dot{\eta}_1 = \phi_{x_4}^{-1}(\eta) \\ \dot{\eta}_2 = F_4(\Phi^{-1}(\eta)) + \frac{R_{12}+R_{23}+\phi_{x_2}^{-1}(\eta)}{J_{tot_1}} \sin\eta_1\lambda_1 + -\frac{R_{12}+R_{23}+\phi_{x_2}^{-1}(\eta)}{J_{tot_1}} \cos\eta_1\lambda_2 \end{cases} . \tag{3.36}$$

3.3.1 Simple stability

Generally speaking a scalar mechanical system is described by the following relation

$$\ddot{q} = f(q, \dot{q}), \quad q, \dot{q} \in \mathbb{R}, \tag{3.37}$$

where $f : \mathbb{R}^2 \to \mathbb{R}$. Assume the equilibrium point to be $\bar{q} \in \mathbb{R}$. Define the new variable $\tilde{q} = q - \bar{q}$. Thus, the equilibrium point becomes $\tilde{\bar{q}} = 0$. Consider the Taylor expansion of such system in a neighbourhood of $\tilde{\bar{q}} = 0$. The resulting system is described by the following scalar equation.

$$\ddot{\tilde{q}} = T_0 + T_1\dot{\tilde{q}} + T_2\dot{\tilde{q}}^2 \tag{3.38}$$

where T_0, T_1, T_2 depends on $\tilde{q}$. For the sake of simplicity this dependence will be neglected in the notation from now on. Note that the dynamics of a mechanical system are quadratic in the velocities. Therefore, the system is described exactly by its Taylor expansion.

Consider a positive variable $M(\tilde{q}) > 0 \in \mathbb{R}$ depending on $\tilde{q}$. System 3.40 can be written as:

$$M(q)\ddot{q} + C_1\dot{q} + C_2\dot{q}^2 + G = 0, \tag{3.39}$$

where

$$\begin{aligned} C_1 &= -M(q)T_1, \\ C_2 &= -M(q)T_2, \\ G &= -M(q)T_0. \end{aligned} \tag{3.40}$$

Note that term G doesn't introduce any relation with $\dot{q}$. In fact it is related to the gravitational action on the system. Instead, terms C_1 and C_2 are respectively related to friction and Coriolis terms. These analogies can be stated because of the mechanical nature of the system.

Consider again the equilibrium point $\tilde{\bar{q}} = 0$. In order to prove the stability of such point the following Lyapunov function is defined.

$$V = \frac{1}{2}M(\tilde{q})\dot{\tilde{q}}^2 + \int_{-\infty}^{\tilde{\bar{q}}} G(\xi)d\xi + c, \tag{3.41}$$

where $V : \mathbb{R}^6 \to \mathbb{R}$ and $c \in \mathbb{R}$ is a constant. Recall now the gravitational interpretation of term G. The integral term in V consists of the gravitational potential of the system, which will be addressed as $U(\tilde{q})$. Instead, the first term depends on $\dot{\tilde{q}}$, defining a sort of kinetic energy for the whole system. Moreover, the potential is always defined net of a constant, namely the c term in V. Such constant is assumed to be

$$c = \min_{\tilde{q}} U(\tilde{q}), \quad \tilde{q} \in \mathbb{R}. \tag{3.42}$$

Such minimum coincides with the lowest energy configuration of the system, namely its minimum is reached in $\tilde{\bar{q}} = 0$. Thus, the stability analysis unfolds as follows.

$$\begin{aligned}\dot{V} &= \frac{\partial V}{\partial \tilde{q}}\dot{\tilde{q}} + \frac{\partial V}{\dot{\tilde{q}}}\ddot{\tilde{q}} = \\ &= \frac{1}{2}\left[\frac{\partial M(\tilde{q})}{\partial \tilde{q}}\dot{\tilde{q}}\right]\dot{\tilde{q}}^2 + G\dot{\tilde{q}} + M(\tilde{q})\dot{\tilde{q}}\ddot{\tilde{q}} = \\ &= \frac{1}{2}\left[\frac{\partial M(\tilde{q})}{\partial \tilde{q}}\dot{\tilde{q}}\right]\dot{\tilde{q}}^2 + G\dot{\tilde{q}} + \dot{\tilde{q}}\left[- C_1\dot{\tilde{q}} - C_2\dot{\tilde{q}}^2 - G\right] \\ &= \frac{1}{2}\left[\frac{\partial M(\tilde{q})}{\partial \tilde{q}}\right]\dot{\tilde{q}}^3 + \cancel{G\dot{\tilde{q}}} - C_1\dot{\tilde{q}}^2 - C_2\dot{\tilde{q}}^3 - \cancel{G\dot{\tilde{q}}} = \\ &= \frac{1}{2}\left[\frac{\partial M(\tilde{q})}{\partial \tilde{q}} - C_2\right]\dot{\tilde{q}}^3 - C_1\dot{\tilde{q}}^2 \leq 0.\end{aligned} \tag{3.43}$$

Therefore, in order to impose $\dot{V} \leq 0$, the following conditions shall be satisfied.

$$\frac{\partial M(\tilde{q})}{\partial \tilde{q}} + 2M(\tilde{q})T_2 = 0, \quad \forall \tilde{q} \in \mathbb{R}, \tag{3.44}$$

$$C_1 \geq 0 \quad \forall \tilde{q} \in \mathbb{R}. \tag{3.45}$$

Accordingly to Theorem 4, these conditions ensure the local asymptotic stability of the equilibrium point $\tilde{\tilde{q}} = 0$. In order to meet these conditions a proper choice of $M(\tilde{q})$ shall be made. Given that $\tilde{q} \in \mathbb{R}$, condition 3.44 becomes an ODE whose solution is the following.

$$\frac{dM(\tilde{q})}{d\tilde{q}} + 2M(\tilde{q})T_2 = 0 \implies M(\tilde{q}) = e^{-2\int_{-\infty}^{\tilde{\tilde{q}}} T_2(\xi)d\xi}. \tag{3.46}$$

In the scalar case condition 3.45 shall be met directly checking the sign of C_1 in the domain of the system. Therefore, the choice of this Lyapunov function proves the simple stability of $\tilde{\tilde{q}}$, as $\dot{V}(\tilde{\tilde{q}}) = 0$.

3.3.2 Global asymptotic stability

As reported above, function 3.47 proves only the local asymptotic stability of $\bar{\tilde{q}}$. In order to prove also its global asymptotic stability an additional term is specifically designed for the Lyapunov function V. The additional term is defined as $T = \tilde{q}\dot{\tilde{q}}$. The new Lyapunov function is defined as follows:

$$V_\epsilon = V + \epsilon T = \frac{1}{2}M(\tilde{q})\dot{\tilde{q}}^2 + \int_{\infty}^{\tilde{\tilde{q}}} G(\xi)d\xi + c + \epsilon\tilde{q}\dot{\tilde{q}}, \quad \epsilon \in \mathbb{R}. \tag{3.47}$$

This function still meets the assumptions of Theorem 5. The stability of $\tilde{\tilde{q}}$ depends on $\dot{V}_\epsilon = \dot{V} + \epsilon\dot{T}$. Therefore, in order to prove the global asymptotic stability of $\bar{\tilde{q}}$, the following shall be true.

i) $\dot{V}_\epsilon(\tilde{q}) < 0 \implies \nabla^2\dot{V}_\epsilon(\tilde{\tilde{q}}) < 0.$

ii) $\nabla^2 V_\epsilon(\tilde{\tilde{q}}) > 0.$

Consider the first condition. The derivative of the additional term unfolds as follows.

$$\begin{aligned}\dot{T} &= \frac{\partial T}{\partial \tilde{q}}\dot{\tilde{q}} + \frac{\partial T}{\dot{\tilde{q}}}\ddot{\tilde{q}} = \\ &= \dot{\tilde{q}}^2 + \tilde{q}\ddot{\tilde{q}} = \dot{\tilde{q}}^2 - \frac{C_1}{M}\tilde{q}\dot{\tilde{q}} - \frac{C_2}{M}\dot{\tilde{q}}^2\tilde{q} - \frac{G}{M}\tilde{q}.\end{aligned} \tag{3.48}$$

Assume to choose $M(q)$ accordingly to Equation 3.46. The Lyapunov function derivative turns out to be the following.

$$\dot{V}_\epsilon = -C_1\dot{\tilde{q}}^2 + \epsilon\left(\dot{\tilde{q}}^2 - \frac{C_1}{M}\tilde{q}\dot{\tilde{q}} - \frac{C_2}{M}\dot{\tilde{q}}^2\tilde{q} - \frac{G}{M}\tilde{q}\right), \quad \epsilon \in \mathbb{R}. \tag{3.49}$$

In order to have $\dot{V}_\epsilon < 0$, the following shall be true.

$$\nabla^2\dot{V}_\epsilon(\bar{\tilde{q}}) < 0. \tag{3.50}$$

Recall that the equilibrium point of the system is $\bar{\tilde{q}} = 0$. Through simple computations the condition 3.50 turns out to be

$$\nabla^2\dot{V}_\epsilon(0) = \begin{bmatrix} \frac{1}{M(0)}\frac{-\partial G(0)}{\partial \tilde{q}} & -\frac{C_1(0)}{M(0)} \\ -\frac{C_1(0)}{M(0)} & 2(\epsilon - C_1(0)) \end{bmatrix} < 0. \tag{3.51}$$

On the other hand, by computing $\nabla^2 V_\epsilon(\tilde{q})$, the condition on the Hessian of the Lyapunov function is defined as follows.

$$\nabla^2 V_\epsilon(0) = \begin{bmatrix} \frac{\partial G(0)}{\partial \tilde{q}} & \frac{\epsilon}{2} \\ \frac{\epsilon}{2} & M(\tilde{q})(0) \end{bmatrix} > 0. \tag{3.52}$$

Therefore, a proper choice of ϵ can grant the global asymptotic stability of the equilibrium point $\bar{\tilde{q}} = 0$. Note that the choice of ϵ shall be such that both Equation 3.51 and Equation 3.52 hold. This results in specific bounds on ϵ, different from case to case.

3.3.3 Results

The procedure described in section 3.3 has been performed on the looper, described in section 2.7. The system has an equilibrium point in $\bar{\eta}$.

The Taylor expansion terms T_0, T_1, T_2 are shown Figure 3.5.

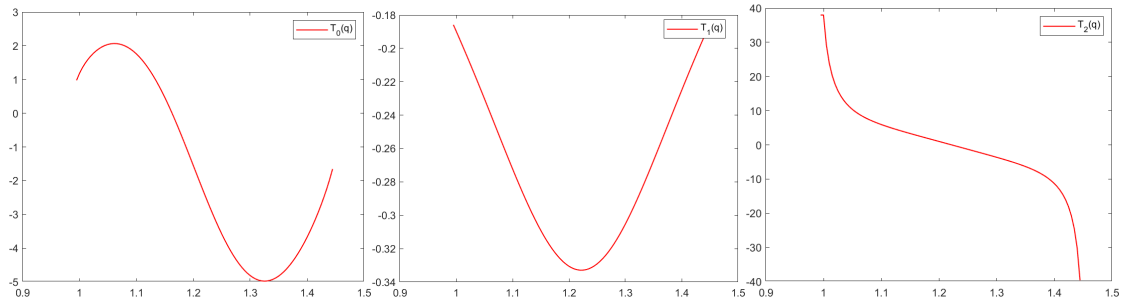

(a) $T_0(\eta)$ term (b) $T_1(\eta)$ term (c) $T_2(\eta)$ term

Figure 3.5: Model's Taylor expansion terms

Recalling the considerations in subsection 3.3.1, $M(\eta)$ has been chosen properly, in order to meet condition 3.44. Note that all these analysis has been carried out numerically instead of in a symbolic way. This because the symbolic computation of Equation 3.44 is heavy computationally speaking. $M(\eta)$ is shown in Figure 3.6.

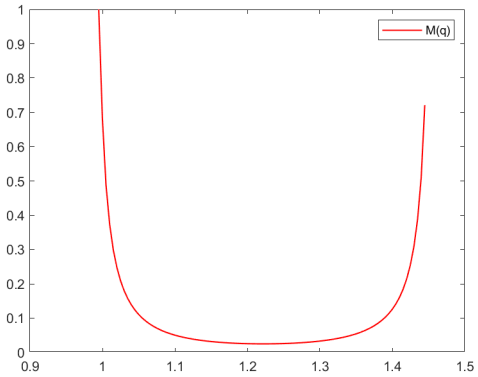

Figure 3.6: $M(\eta)$ - solution of Equation 3.44

From these results, G, C_1, C_2 can be computed. As explained in subsection 3.3.1, terms C_1 and C_2 are related to friction and Coriolis effects. Such terms are presented in Figure 3.7.

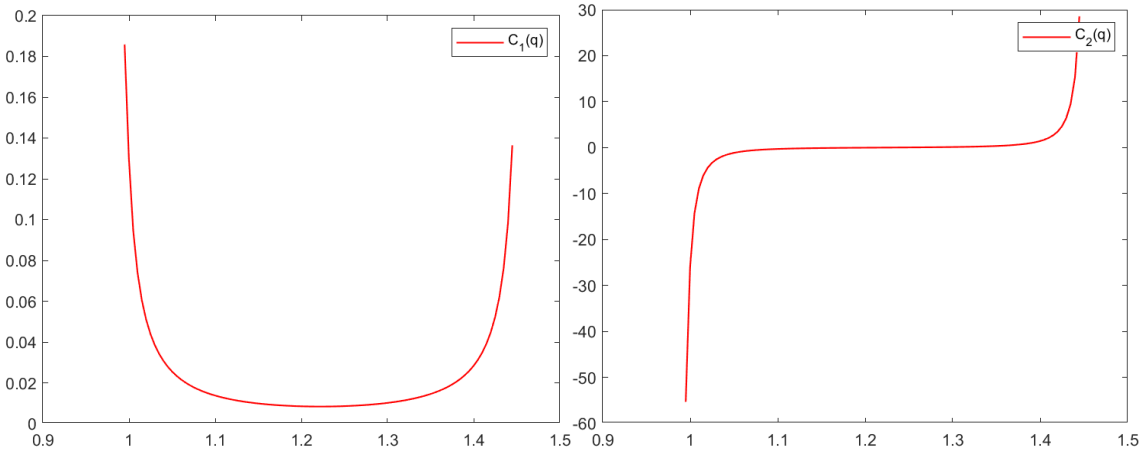

(a) $C_1(\eta)$ term (b) $C_2(\eta)$ term

Figure 3.7: Friction term and Coriolis term

The condition described in Equation 3.44 is checked in Figure 3.8. As explained before, the whole analysis has been carried out numerically and for this reason the computed condition is not exactly zero.

It is interesting to show also term $G = -M(\eta)T_0$. As explained above this term is related to the gravitational action on the system. In fact, as shown in Figure 3.9, it has a zero in $\bar{\eta}$, as reported in Figure 3.9

Therefore, its integral defines the gravitational potential $U(\eta)$ of the system. Consistently, $U(\eta)$ has a minimum in $\bar{\eta}$, as shown in Figure 3.10.

The gravitational potential is always defined net of a constant. As it can be negative, its value could prevent $V(\eta)$ to be positive semi-definite, as required by stability theorems defined in section 3.1. Therefore, in the definition of Lyapunov functions V and V_ϵ, the constant c has been set to

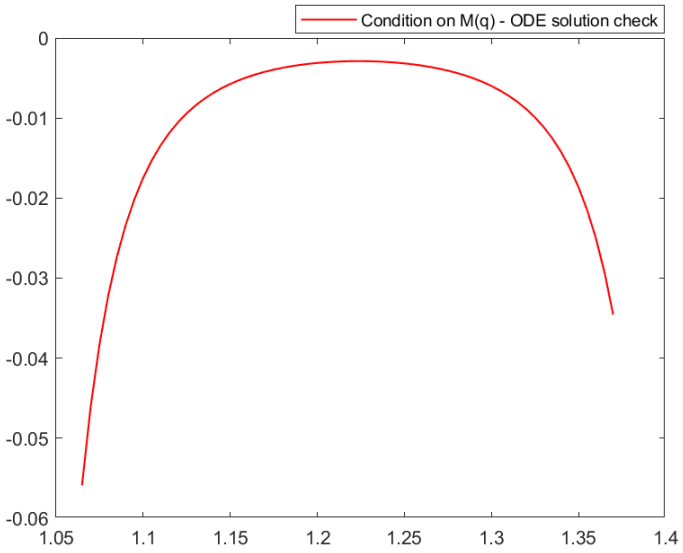

Figure 3.8: Numerical check of condition 3.44

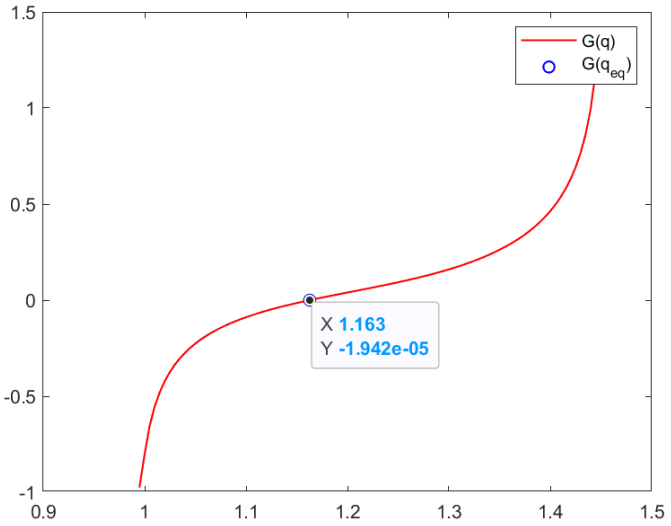

Figure 3.9: Gravitational action on the system and in $\bar{\eta}$

$$c = \| \min_{\eta} U(\eta) \| \tag{3.53}$$

Therefore the two Lyapunov functions are defined as follows:

$$\begin{aligned} V &= \frac{1}{2} M(\eta)\dot{\eta}^2 + U(\eta) + \| \min_{\eta} U(\eta) \| \\ V_\epsilon &= \frac{1}{2} M(\eta)\dot{\eta}^2 + U(\eta) + \| \min_{\eta} U(\eta) \| + \epsilon(\eta - \bar{\eta})\dot{\eta}. \end{aligned} \tag{3.54}$$

The two Lyapunov function are presented in Figure 3.11. Both the plot in the entire domain and on a restricted interval around $\bar{\eta}$ are shown. The equilibrium point $\bar{\eta}$ is highlighted in blue.

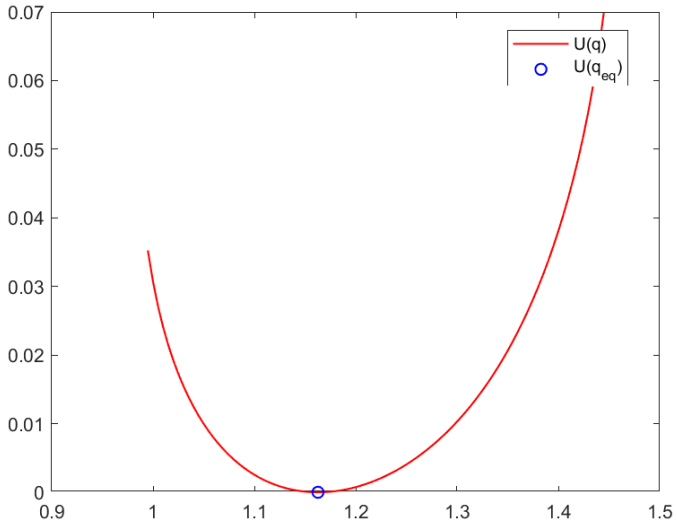

Figure 3.10: Gravitational potential of the system and in $\bar{\eta}$

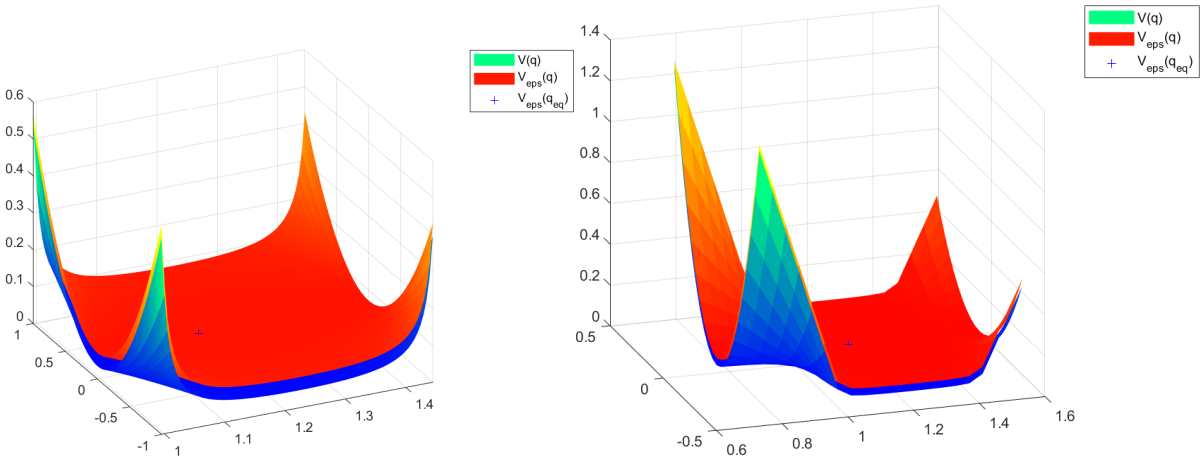

(a) $V(\eta)$ and $V_\epsilon(\eta)$ - domain

(b) $V(\eta)$ and $V_\epsilon(\eta)$ - interval

Figure 3.11: Lyapunov functions $V(\eta)$ and $V_\epsilon(\eta)$

Figure 3.12 presents the same analysis but on the derivative of the Lyapunov functions, namely the conditions proving respectively simple and global asymptotic stability of $\bar{\eta}$.

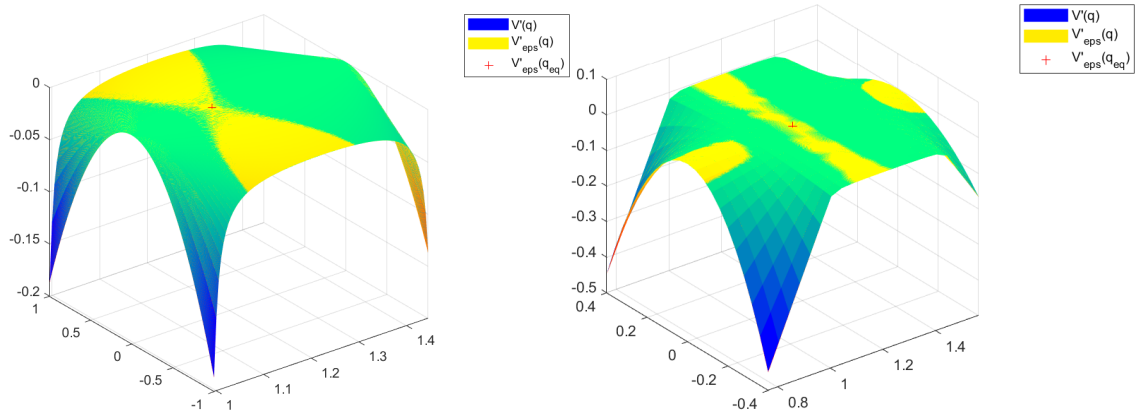

(a) $\dot{V}(\eta)$ and $\dot{V}_\epsilon(\eta)$ - domain

(b) $\dot{V}(\eta)$ and $\dot{V}_\epsilon(\eta)$ - interval

Figure 3.12: Lyapunov functions $\dot{V}(\eta)$ and $\dot{V}_\epsilon(\eta)$

Choice of ϵ

As reported in subsection 3.3.2 global asymptotic stability of $\bar{\eta}$ is proved for a limited range of ϵ values. Indeed, to check the stability of $\bar{\eta}$ both the conditions in Equation 3.3.2 shall be met. More specifically the eigenvalues of those matrices shall be respectively both negative and positive. Such conditions depends on the value of ϵ and are shown in Figure 3.13.

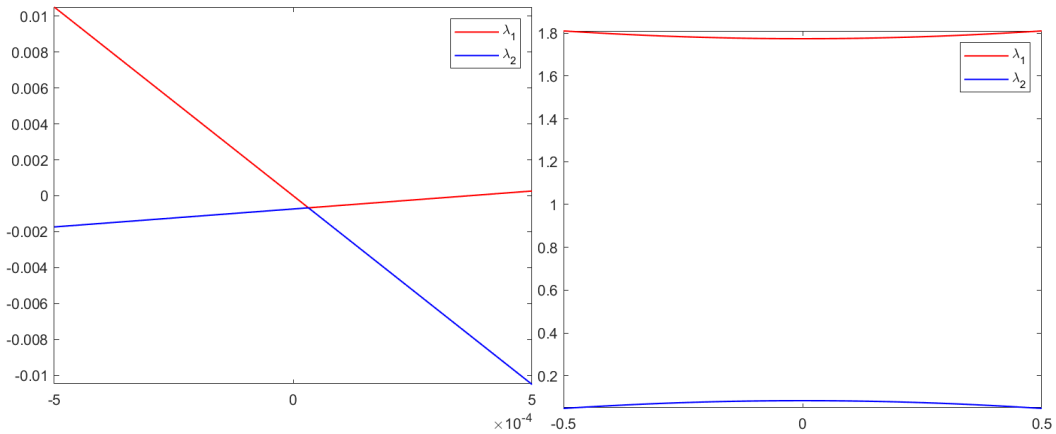

(a) Condition 3.50 (b) Condition 3.3.2

Figure 3.13: Eigenvalues of condition 3.50 and 3.3.2 - dependence on ϵ

Therefore, considering the obtained results, set $\epsilon = 0.0001$. This choice leads to the following results:

i) Condition 3.50

$$\nabla^2 \dot{V}_\epsilon(\bar{\eta}) = H_{\dot{V}} = \begin{bmatrix} -0.0021 & -0.00000043 \\ -0.00000043 & -0.00053 \end{bmatrix} \implies \tag{3.55}$$
$$\implies \sigma(H_{\dot{V}}) = (\lambda_{\dot{V}_1}, \lambda_{\dot{V}_2}) = (-0.0021, -0.00053)$$

ii) Condition 3.3.2

$$\nabla^2 V_\epsilon(\bar{\eta}) = H_V = \begin{bmatrix} 1.773 & 0.00005 \\ 0.00005 & 0.0844 \end{bmatrix} \implies \tag{3.56}$$
$$\implies \sigma(H_V) = (\lambda_{V_1}, \lambda_{V_2}) = (0.0844, 1.773)$$

These results are consistent with the requirements. Therefore, global asymptotic stability of $\bar{\eta}$ is proved.

3.4 Mechanical system - multidof

This section goes through the analysis of multidof mechanical systems. More specifically, after a brief general introduction, it describes the model and the behaviour of the looper in a different configuration compared to the one described so far. In fact, one of the two algebraic constraints is removed and, more specifically, Frame 2 is allowed to slide horizontally. This analysis is presented both for the nonlinear and a linearised version of the model. Moreover, the stability analysis carried on in section 3.3 is introduced on multidof mechanical systems.

The goal of this section is to introduce a potential research field as far as the stability analysis is concerned.

3.4.1 General introduction

For the sake of simplicity this general analysis is performed on a system of the same dimensions of the looper. Consider then the system described by the following equations:

$$\begin{aligned} \ddot{q} &= f(q, \dot{q}) + \nabla h^T(q)\lambda, \\ 0 &= h(q), \end{aligned} \tag{3.57}$$

where $f : \mathbb{R}^6 \to \mathbb{R}^3$, $h : \mathbb{R}^3 \to \mathbb{R}$, $(\ddot{q}, \dot{q}, q) \in \mathbb{R}^3$, $\lambda \in \mathbb{R}$. This system has 3 generalised coordinates and a single algebraic constraint, ending up with a total of two dof.

Assume this system to have an equilibrium point $\bar{q} \in \mathbb{R}^3$. Indeed $\dot{\bar{q}} = 0$. Define $\tilde{q} = q - \bar{q}$. The equilibrium point becomes now $\tilde{\bar{q}} = 0$, with $\dot{\tilde{\bar{q}}} = 0$.

Consider now a global diffeomorphism $\Phi : \mathbb{R}^6 \to \mathbb{R}^6$ and transform the system in normal form. Considering that the system is subjected to a single algebraic constraint h, system dynamics can be described as follows.

$$\begin{aligned} \dot{\xi}_1 &= \xi_2 \\ \dot{\xi}_2 &= b + a\lambda \end{aligned} \tag{3.58}$$

$$\begin{aligned} \dot{\eta}_1 &= q_1 + p_1\lambda \\ \dot{\eta}_2 &= q_2 + p_2\lambda \\ \dot{\eta}_3 &= q_3 + p_3\lambda \\ \dot{\eta}_4 &= q_4 + p_4\lambda. \end{aligned} \tag{3.59}$$

Moreover, considering that a single algebraic constraint acts on the system, the zero dynamics have dimension 4. Therefore, they are described by the following equation.

$$\dot{\eta} = q_0(0, \eta) + p_0(0, \eta)\lambda = f_0(0, \eta), \quad \eta \in \mathbb{R}^4. \tag{3.60}$$

3.4.2 Looper - 2 dof

Consider the looper model described in chapter 1 and assume to relax the set of constraints, namely to remove

$$h_1(q) = (R_{12} + R_{23} + q_2)\cos q_1 - R_x - R_{34}\sin q_3 = 0 \tag{3.61}$$

The resulting 2-dof mechanical system can be described by the following equations.

$$\begin{cases} M_1^{tot}\ddot{q}_1 = F_1(q,\dot{q}) + a_1(q)\lambda(q,\dot{q}) \\ M_2^{tot}\ddot{q}_2 = F_2(q,\dot{q}) + a_2(q)\lambda(q,\dot{q}) \\ M_3^{tot}\ddot{q}_3 = F_3(q,\dot{q}) + a_3(q)\lambda(q,\dot{q}) \\ h(q) = 0 \end{cases} \tag{3.62}$$

where

$$h(q) = (R_{12} + R_{23} + q_2)\sin q_1 - R_y + R_{34}\cos q_3 = 0. \tag{3.63}$$

Consider then the following global diffeomorphism.

$$z = \Phi(x) = \begin{pmatrix} h(x) \\ L_f h_(x) \\ x_1 \\ x_4 \\ x_3 \\ x_6 \end{pmatrix}. \tag{3.64}$$

This diffeomorphism makes the η dynamics to be in the form of a mechanical system. In fact, both (x_1, x_3) describe a position and (x_4, x_6) the respective velocity. Transform now the system in normal form through $\Phi : \mathbb{R}^6 \to \mathbb{R}^6$. The system dynamics turn out to be

$$\begin{cases} \dot{\xi_1} = \xi_2 \\ \dot{\xi_2} = b + a\lambda \\ \dot{\eta_1} = \eta_2 \\ \dot{\eta_2} = q_2 + p_2\lambda \\ \dot{\eta_3} = \eta_4 \\ \dot{\eta_4} = q_4 + p_4\lambda \end{cases} \tag{3.65}$$

Consider the equilibrium point of the system 3.62, namely $\bar{q} \in \mathbb{R}^6$. Note that $\bar{q}$ is computed through the same procedure described in section Equation 3. It holds

$$\bar{q} = \begin{bmatrix} 0.1399 & 10.1541 & 0 & 0 & 0 & 0 \end{bmatrix}. \tag{3.66}$$

This point is transformed through Φ as well, namely

$$\bar{z} = \begin{bmatrix} \phi_1(\bar{q}) \\ \phi_2(\bar{q}) \\ \phi_3(\bar{q}) \\ \phi_4(\bar{q}) \\ \phi_5(\bar{q}) \\ \phi_6(\bar{q}) \end{bmatrix} = \begin{bmatrix} \bar{\xi} \\ \bar{\eta} \end{bmatrix} \in \mathbb{R}^6. \tag{3.67}$$

Consider the 2 dof mechanical system with restricted state variable

$$\eta_r = \begin{bmatrix} \eta_1 \\ \eta_3 \end{bmatrix} \in \mathbb{R}^2. \tag{3.68}$$

Recall now Theorem 2. As a consequence of this theorem, stability properties of the zero dynamics coincides with the ones of the system in original coordinates. The equilibrium point of the η dynamics is $\bar{\eta}$. Consider then the following system.

$$\ddot{\eta}_r = \begin{bmatrix} \ddot{\eta}_1 \\ \ddot{\eta}_3 \end{bmatrix} = q_{0_r}(\eta_r, \dot{\eta}_r) + p_{0_r}(\eta_r, \dot{\eta}_r)\lambda = f_{0_r}(\eta_r, \dot{\eta}_r). \tag{3.69}$$

The restricted equilibrium point becomes $\bar{\eta}_r$. Define also $\tilde{\eta}_r = \eta_r - \bar{\eta}_r$. The equilibrium points becomes $\bar{\tilde{\eta}}_r = 0$. Consider then the linearisation of the system free dynamics near $\bar{\tilde{\eta}}_r$.

$$f_{0_r}(\eta_r, \dot{\eta}_r) = f_{0_r}(\eta_r, \dot{\eta}_r)\Big|_{\bar{\tilde{\eta}}_r} + \nabla_{\eta_r} f_{0_r}(\eta_r, \dot{\eta}_r)\Big|_{\bar{\tilde{\eta}}_r} \cdot \tilde{\eta}_r + \nabla_{\dot{\eta}_r} f_{0_r}(\eta_r, \dot{\eta}_r)\Big|_{\bar{\tilde{\eta}}_r} \cdot \dot{\tilde{\eta}}_r + o(\tilde{\eta_r}^2, \dot{\tilde{\eta}}_r^2) = \tag{3.70}$$

$$= -G\tilde{\eta}_r + -C\dot{\tilde{\eta}}_r + o(\tilde{\eta_r}^2, \dot{\tilde{\eta}}_r^2),$$

where $G, C \in \mathbb{R}^{2\times 2}$. Thus, the final linearised system is described by the following equations:

$$\ddot{\tilde{\eta}}_r + G\tilde{\eta}_r + C\dot{\tilde{\eta}}_r = 0 \tag{3.71}$$

Results

The analysis described in the previous section has been performed on the looper, considering the restricted equilibrium point

$$\bar{\eta}_r = \begin{bmatrix} \bar{\eta}_1 \\ \bar{\eta}_2 \end{bmatrix} = \begin{bmatrix} 0.1399 \\ 0 \end{bmatrix}. \tag{3.72}$$

Figure 3.14 shows the trajectories of both the nonlinear and the linearised system.

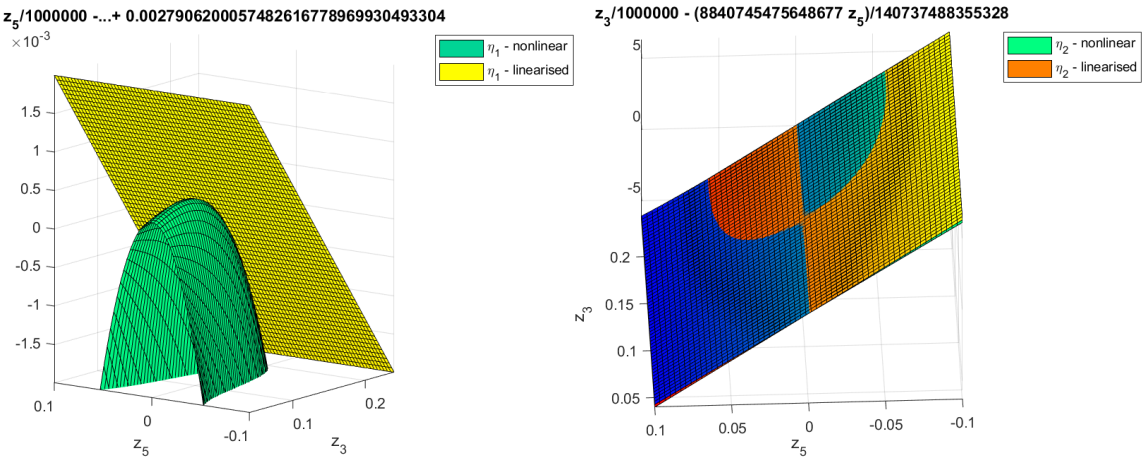

(a) η_1 - linearisation (b) η_3 - linearisation

Figure 3.14: Multi dof system linearisation

In absence of friction the linearised system is described by matrix G_{tot}, namely

$$\dot{\eta} = G_{tot}\eta = \begin{bmatrix} 0 & 1 & 0 & 0 \\ -0.02 & 0 & 0 & 0 \\ 0 & 0 & 0 & 1 \\ 0 & 0 & -62.8173 & 0 \end{bmatrix} \begin{bmatrix} \eta_1 \\ \eta_2 \\ \eta_3 \\ \eta_4 \end{bmatrix}. \tag{3.73}$$

Such system can also be described through Equation 3.71, namely

$$\ddot{\eta}_r = G\eta_r = \begin{bmatrix} -0.0200 & 0 \\ 0 & -62.8173 \end{bmatrix} \begin{bmatrix} \eta_1 \\ \eta_3 \end{bmatrix}. \tag{3.74}$$

In presence of friction, the dissipative terms is described by the following matrix.

$$\dot{\eta} = G_{tot}\eta = \begin{bmatrix} 0 & 0 & 0 & 0 \\ 0 & -0.0147 & 0 & 0 \\ 0 & 0 & 0 & 0 \\ 0 & 0 & 0 & -0.1172 \end{bmatrix} \begin{bmatrix} \eta_1 \\ \eta_2 \\ \eta_3 \\ \eta_4 \end{bmatrix}. \tag{3.75}$$

The friction action can be described also by Equation 3.71, namely

$$\ddot{\eta}_r = C\dot{\eta}_r = \begin{bmatrix} -0.0147 & 0 \\ 0 & -0.1172 \end{bmatrix} \begin{bmatrix} \eta_2 \\ \eta_4 \end{bmatrix}. \tag{3.76}$$

The nonlinear and the linearised systems have been simulated both in presence and absence of friction. The obtained results are shown in Figure 3.15.

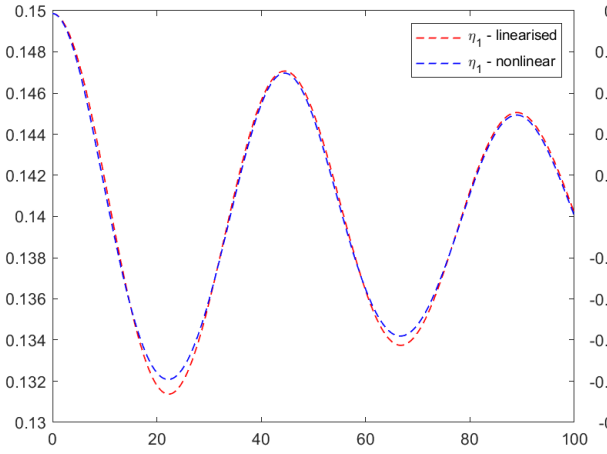

(a) η_1 - friction

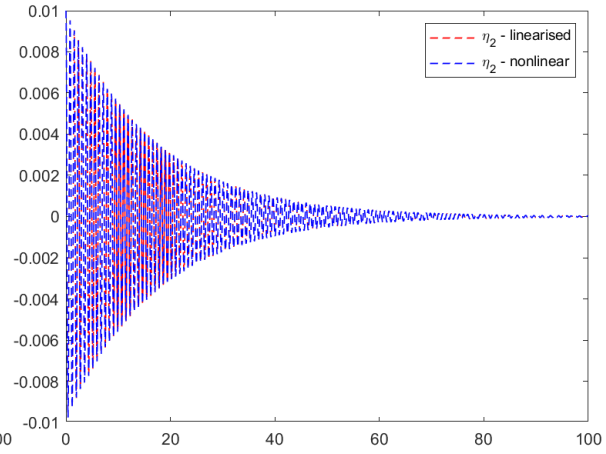

(b) η_3 - friction

Consider the linearised model described in Equation 3.71, namely

$$\ddot{\tilde{\eta}}_r + G\tilde{\eta}_r + C\dot{\tilde{\eta}}_r = 0 \tag{3.77}$$

The stability analysis of this system can be addressed as described in subsection 3.3.1. However, in a multidof system the variable $M(q)$ is a matrix, not a scalar anymore. This introduces several considerations. One among the others, recall that $M(q)$ shall be chosen in order to satisfy condition 3.44, namely

$$\frac{\partial M(\tilde{q})}{\partial \tilde{q}} + 2M(\tilde{q})T_2 = 0, \quad \forall \tilde{q} \in \mathbb{R} \tag{3.78}$$

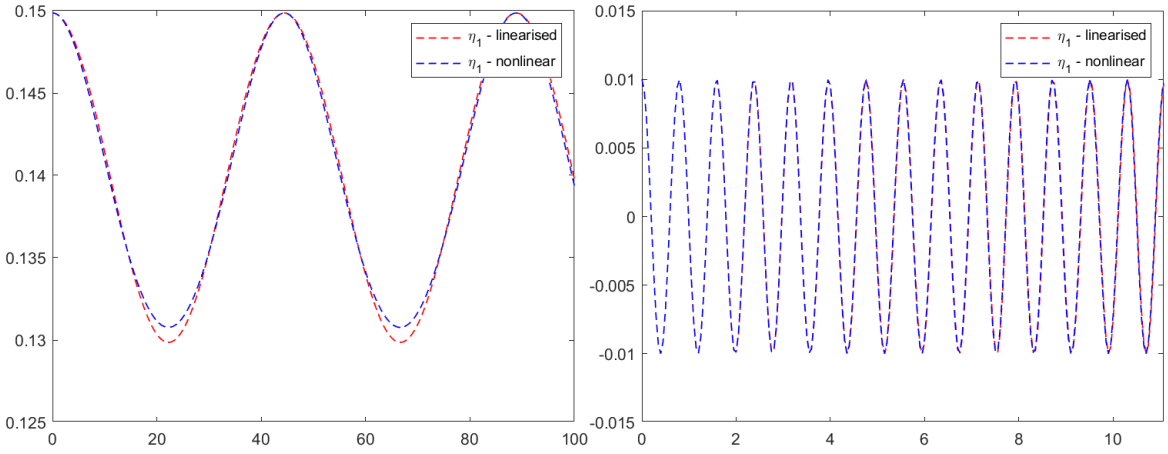

(c) η_1 - no friction

(d) η_3 - no friction

Figure 3.15: Multi dof system linearisation - simulation results

In the case of a multidof system, this procedure implies the solution of a system of PDEs. The study of the necessary and sufficient conditions for this requirement to be met are not investigated in this thesis. However, this could be an interesting topic to be treated more in detail.

Chapter 4

Control on numerical integration of DAE

This chapter addresses the issues rising during the numerical integration of DAE. Once the dynamics of a DAE system have been computed as described in chapter 2, their simulation is usually carried on through numerical integration schemes. However, as presented in [8],the accuracy of such integration schemes is poor in general. This issue is referred to as *drifting*. Therefore, this chapter unfolds with a first introduction on such phenomenon and then with two control schemes specifically crafted to solve it.

4.1 Drifting - general introduction

Consider a general mechanical system composed of $\bar{n}$ mass points, with $\bar{n} \in \mathbb{N}$. The dynamics of such system are described by the following equations [8].

$$m_i \ddot{x}_i - F_i = 0, \quad i \in \{1, \dots, n\}, \tag{4.1}$$

where x_i is the position of the mass m_i, and F_i the external forces. Assume also such system as subjected to a constraint $h(x)$. At this time no assumptions are made on the constraint, namely it could be both holonomic and non-holonomic[1]. The described setting mimics a general system of DAE as the one defined in Equation 2.2 and here expressed in semi-explicit form, namely

$$\begin{aligned} \dot{x} &= f(x,u) + g(x)\lambda, \\ 0 &= h(x). \end{aligned} \tag{4.2}$$

Consider now a general constraint described by the following relations.

$$\begin{aligned} h &= N(x, \dot{x}, t), \\ \dot{h} &= \Psi(N, x, \dot{x}, t). \end{aligned} \tag{4.3}$$

The differential system in Equation 4.2 together with the set of initial conditions imply that $N = 0$, namely the constraint is initially satisfied. Theoretically speaking, this condition should be met during the entire evolution of the system.

[1] Recall the definition of holonomic and non-holonomic constraints in subsection 1.1.2

However, Equation 4.3 could be unstable in the sense of Lyapunov[2]. Consider an initial condition $N_0 = \epsilon \neq 0$. This initial condition is wrong and propagates on the time evolution of $(x, \dot{x})$. This may lead to an unstable behaviour of $N(x, \dot{x}, t)$. For instance, assume Equation 4.3 to represent an holonomic constraint. Thus its dynamics are described by

$$\ddot{h} = \ddot{N}(x, \dot{x}, \ddot{x}, t). \tag{4.4}$$

Assume also that the numerical integration at a certain time instant $t^\star$ yields

$$\begin{aligned} \tilde{N}(t^\star) &= \sigma, \\ \dot{\tilde{N}}(t^\star) &= \epsilon. \end{aligned} \tag{4.5}$$

Such values deviate from the exact ones, which are

$$\begin{aligned} \tilde{N}(t^\star) &= 0, \\ \dot{\tilde{N}}(t^\star) &= 0. \end{aligned} \tag{4.6}$$

Assume the differential equation solution to be described by the general relation

$$N = \Theta(N, \dot{N}). \tag{4.7}$$

Generally speaking, the numerical integration returns $N(t^\star) = \Theta(\epsilon, \sigma) \neq 0$, introducing further errors in the following integration steps. These errors make the algebraic constraint to be not satisfied, ending in wrong system dynamics evolution.

The drifting effect is negligible if the simulation runs for a limited time range. The more the simulation runs, the more the dynamics are affected by drifting. In Figure 4.1 drifting effects are presented on the looper over a time range of $10s$ and $100s$.

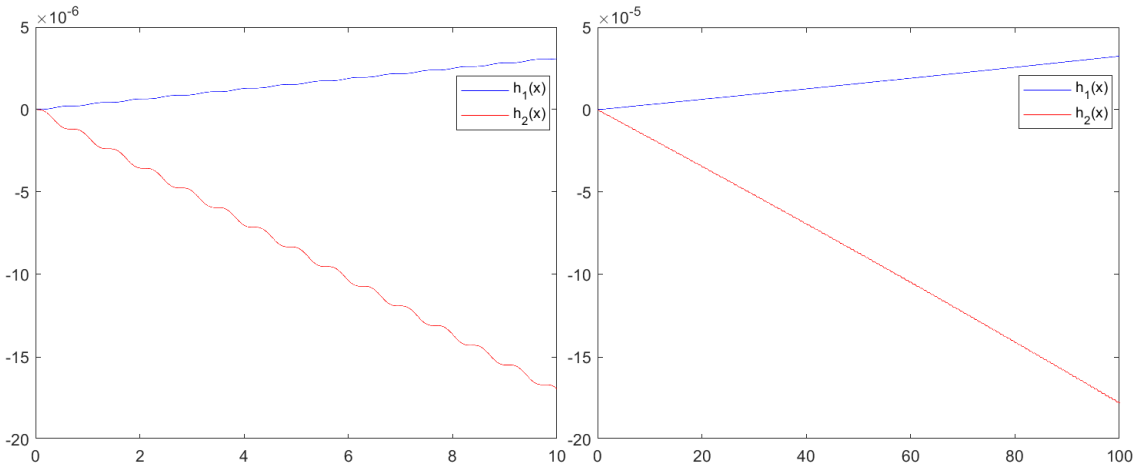

(a) Drifting - 10 s

(b) Drifting - 100 s

Figure 4.1: Drifting example on looper constraints $h_1(x)$ and $h_2(x)$

[2]For Lyapunov stability theory see section 3.1

Simulations in Figure 4.1 have been run considering the initial condition x_0 to be coherent with the algebraic constraints $h_1(x)$ and $h_2(x)$, namely

$$h_0 = h(x_0) = 0, \quad x_0 \in \mathbb{R}^n. \tag{4.8}$$

In Figure 4.2 the system has been simulated starting from

$$\bar{x}_0 = x_0 + \delta. \tag{4.9}$$

This disturbed initial condition results in a greater drifting effect.

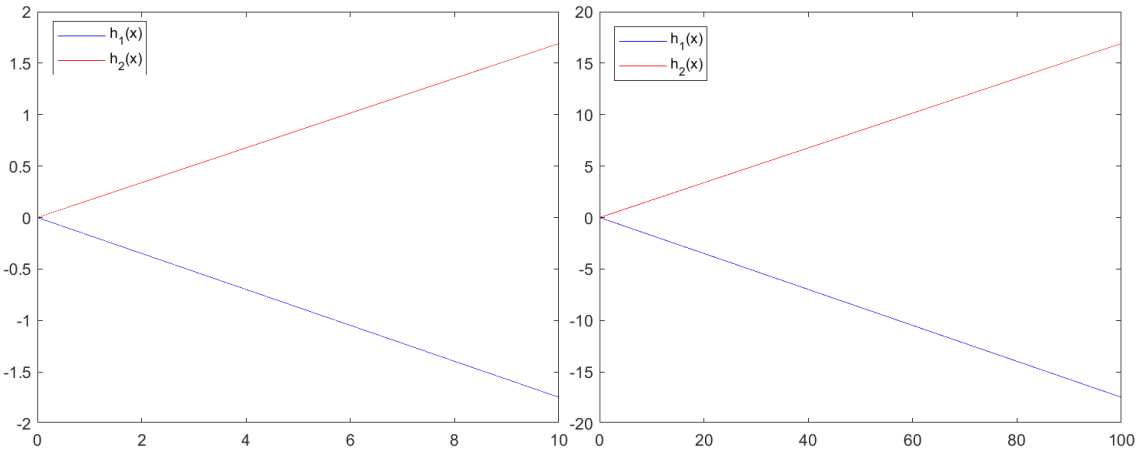

(a) Drifting - 10 s - disturbed (b) Drifting - 100 s - disturbed

Figure 4.2: Drift example on looper constraints $h_1(x)$ and $h_2(x)$ - disturbed initial condition

The effect on the dynamics of the system are shown in Figure 4.3. Clearly, the right behaviour is described by the oscillation of the looper around its equilibrium point, namely the one depicted in the right section of Figure 4.3.

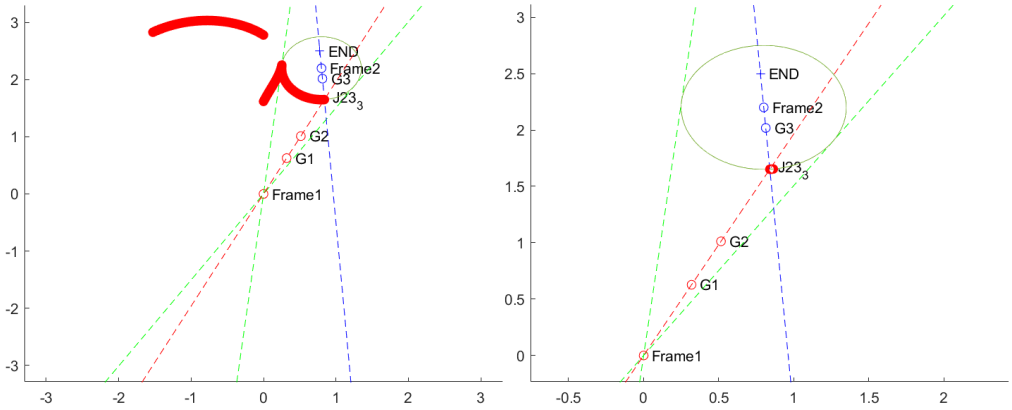

(a) Dynamics - drifting (b) Dynamics - no drifting

Figure 4.3: Drift effect on system's dynamics

Different integration schemes introduce different errors. Figure 4.4 presents the drifting on constraint $h_1(x)$ resulting from three different integration schemes.

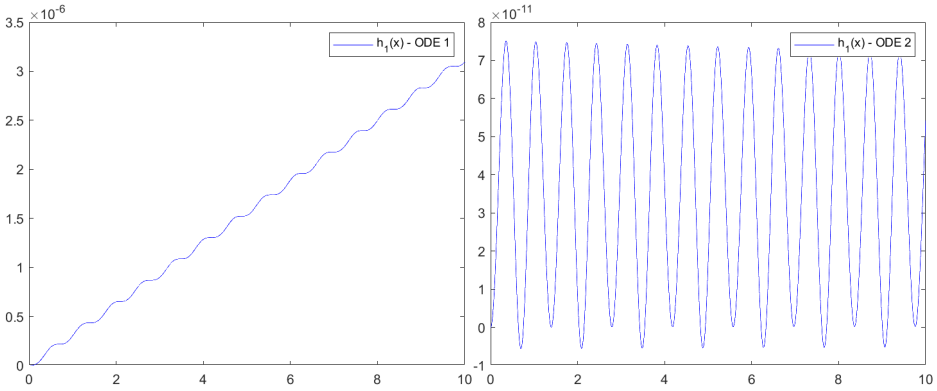

(a) Drift - 10 s
ODE 1 (forward Euler method)

(b) Drift - 10 s
ODE 2 (non-adaptive method of order 2)

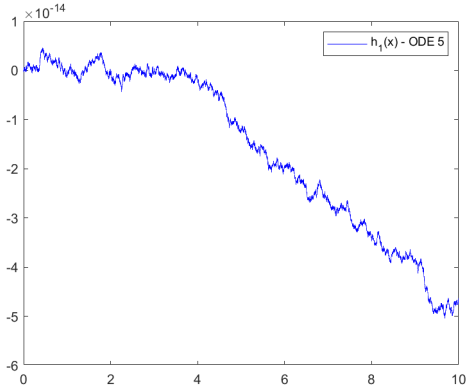

(c) Drift - 10 s
ODE 5 (non-adaptive method of order 5)

Figure 4.4: Drift example on looper constraints - different numerical integration methods

4.2 Stabilisation - Baumgarte method

This section addresses a first method to correct the drifting effect. Consider a set of holonomic constraints, that is the exact case handled in the looper analysis. As described in section 4.1 the dynamics of the constraint shall be zero at any time but due to integration errors this doesn't happen. Baumgarte method [8] modifies the dynamics of the constraint in order to impose the following 2^{nd} order system.

$$\ddot{h} = \ddot{\tilde{N}} + 2\alpha\dot{\tilde{N}} + \beta^2\tilde{N} = 0, \quad \alpha > 0. \tag{4.10}$$

The aggregate term $(2\alpha\dot{\tilde{N}} + \beta^2\tilde{N})$ acts as control term achieving the stability of the DAE system.

This method is stated with the system in the original coordinates. By applying one of the diffeomorphisms defined in subsection 2.7.2 the controlled dynamics of Baumgarte algorithm are described by equations in the following form.

$$\dot{\xi}^j_{r_i} = \sum_{k=1}^{r_i} \alpha^j_k \xi^j_k, \quad i \in \{1, \dots, r_i\}, j \in \{1, \dots, m\}, \tag{4.11}$$
$$\dot{\eta} = q(\xi, \eta) + p(\xi, \eta)\lambda,$$

where the coefficients α^j_k, can be stacked in a single vector such that

$$\alpha = [\alpha^1_1, \dots, \alpha^m_{r_m}] = [\alpha_1, \dots, \alpha_{r_{tot}}]. \tag{4.12}$$

These coefficients shall be chosen such that the roots of the following polynomial have all negative part.

$$\sigma(\tau) = \sum_{j=1}^{r_{tot}} \alpha_j \tau^j, \quad \tau \in \mathbb{R} \tag{4.13}$$

Consider now the model of the looper in normal form, namely the system described by the following equations.

$$\begin{cases} \dot{\xi}^1_1 = \xi^1_2 \\ \dot{\xi}^1_2 = b_1 + a_{11}\lambda_1 + a_{12}\lambda_2 \\ \dot{\xi}^2_1 = \xi^2_2 \\ \dot{\xi}^2_2 = b_2 + a_{21}\lambda_1 + a_{22}\lambda_2 \\ \dot{\eta}_1 = q_1 + p_{11}\lambda_1 + p_{12}\lambda_2 \\ \dot{\eta}_2 = q_2 + p_{21}\lambda_1 + p_{22}\lambda_2 \end{cases} \tag{4.14}$$

Baumgarte algorithm modifies such dynamics as follows.

$$\begin{cases} \dot{\xi}^1_1 = \xi^1_2 \\ \dot{\xi}^1_2 = b_1 + a_{11}\lambda_1 + a_{12}\lambda_2 - \alpha_1\xi^1_1 - \alpha_2\xi^1_2 \\ \dot{\xi}^2_1 = \xi^2_2 \\ \dot{\xi}^2_2 = b_2 + a_{21}\lambda_1 + a_{22}\lambda_2 - \alpha_3\xi^2_1 - \alpha_4\xi^2_2 \\ \dot{\eta}_1 = q_1 + p_{11}\lambda_1 + p_{12}\lambda_2 \\ \dot{\eta}_2 = q_2 + p_{21}\lambda_1 + p_{22}\lambda_2 \end{cases} \tag{4.15}$$

where $[\alpha_1, \alpha_2, \alpha_3, \alpha_4]$ satisfy condition expresses by Equation 4.13.

Baumgarte algorithm has been tested on the looper. The coefficients have been chosen to be

$$[\alpha_1, \alpha_2, \alpha_3, \alpha_4] = (28, 284, 1232, 1920), \tag{4.16}$$

defining a polynomial with roots $(-10, -8, -6, -4)$, satisfying condition 4.13.

4.2.1 Looper - Results

This paragraph presents some results on the looper model. A random disturb δ is considered on the initial condition x_0, with order of magnitude $1e^{-2}$. Therefore the initial condition is defined as described in Equation 4.9. The drifting correction on the algebraic constraints is shown in Figure 4.5.

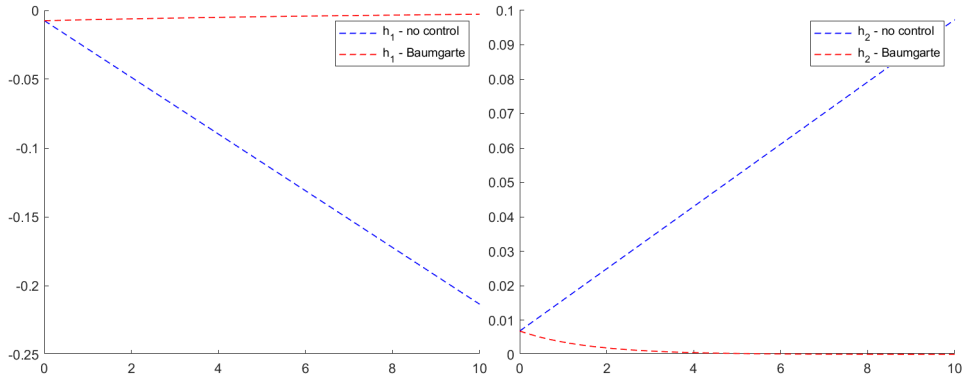

(a) h_1 - drifting correction (b) h_2 - drifting correction

Figure 4.5: Drifting correction through Baumgarte algorithm - algebraic constraints

Instead, Figure 4.6 shows the effect of drifting on the state variables and the correction operated by Baumgarte algorithm. Note that, due to the initial disturb on x_0, drifting is significant even after only $10s$.

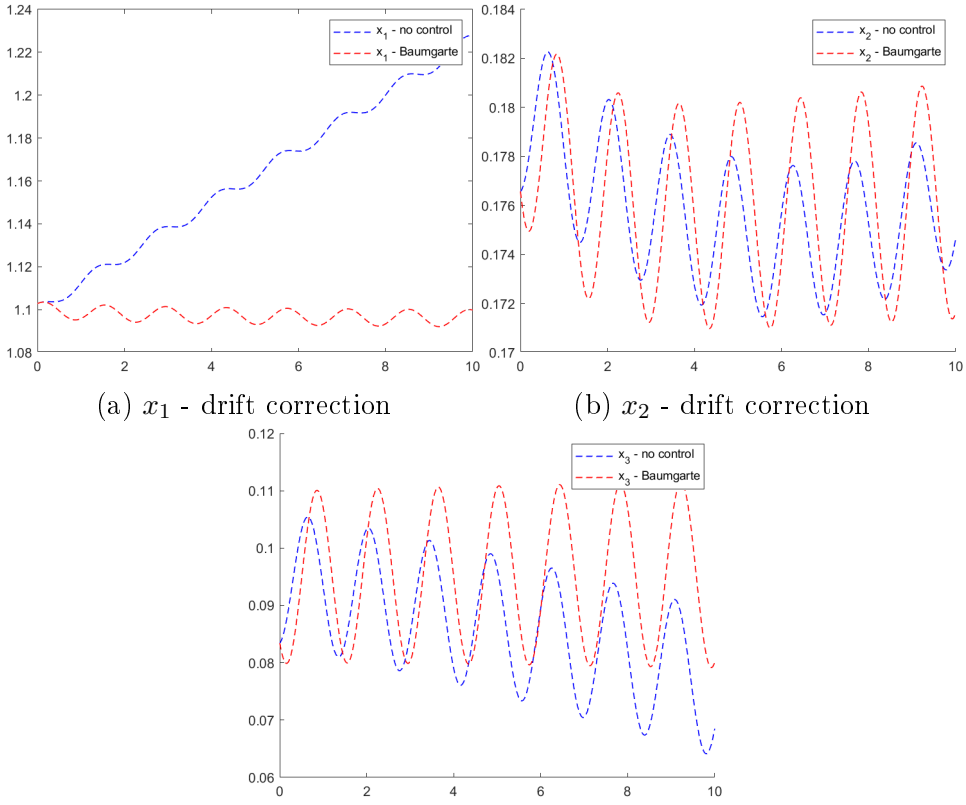

(a) x_1 - drift correction (b) x_2 - drift correction

(c) x_3 - drift correction

Figure 4.6: Drift correction through Baumgarte algorithm - state variables

4.3 Stabilisation - Nonlinear method

Depending on the structure of the system in analysis, Baumgarte algorithm may perform poorly or even end up in trajectories with finite escape time (see [7]). This occurs often in holonomic systems of which the looper is an example. Mainly for this reason a different stabilisation has been proposed. This section presents the theoretical background of such method, discusses the implementation and shows simulation results. All the following arguments are presented in [7].

4.3.1 General overview

Consider a general nonlinear MIMO system subjected to algebraic constraints. Assume to have a global diffeomorphism defined over its domain and then transform the system in its normal form. The system in analysis is described by equations in the form of 2.59 and 2.60, namely

$$\begin{aligned}
\dot{\xi}_1^i &= \xi_2^i, \\
&\vdots \\
\dot{\xi}_{r_i-1}^i &= \xi_{r_i}^i, \\
\dot{\xi}_{r_i}^i &= b_i(\xi,\eta) + \sum_{j=1}^{m} a_{ij}(\xi,\eta)\lambda_j, \quad \forall i \in \{1,\dots,m\}, \\
\dot{\eta} &= q(\xi,\eta) + \sum_{i=1}^{m} p_i(\xi,\eta)\lambda_i = q(\xi,\eta) + p(\xi,\eta)\lambda, \quad \xi = [\xi_1^1,\dots,\xi_{r_m}^m].
\end{aligned} \tag{4.17}$$

The solution manifold of such system is defined as

$$\mathcal{M} = \{(\xi^T,\eta^T)^T : \xi = 0\} \tag{4.18}$$

Note that if in general $\xi(t) \neq 0$ the trajectories of system 4.17 differ from the expected manifold in which $\xi(t) = 0$. As explained in section 4.1 this may happen due to numerical integration errors. Therefore, it is useful to describe system dynamics considering also these drifting elements. Indeed, under proper smoothness assumptions, the η subsystem of Equation 4.17 can be rewritten as

$$\dot{\eta} = q(\xi,\eta) = q_0(0,\eta) + \sum_{j=1}^{m}\sum_{i=1}^{r_i} q_{ij}(\xi,\eta)\xi_i^j = q_0(0,\eta) + Q(\xi,\eta)\xi^T, \tag{4.19}$$

where $q_0(0,\eta)$ is the system zero dynamics and $q_{ij} : \mathbb{R}^{r_i} \to \mathbb{R}^{n-r_{tot}}$ are smooth mappings $\forall i \in \{1,\dots,r_i\}, j \in \{1,\dots,m\}$. This model shows how disturbances introduced by the drifting effect affect system dynamics. Such disturbances could lead to finite escape time trajectories but also to erroneous equilibrium points.

System dynamics are now described by the following equations:

$$
\begin{aligned}
\dot{\xi}_1^i &= \xi_2^i, \\
&\vdots \\
\dot{\xi}_{r_i-1}^i &= \xi_{r_i}^i, \\
\dot{\xi}_{r_i}^i &= b_i(\xi,\eta) + \sum_{j=1}^{m} a_{ij}(\xi,\eta)\lambda_j, \quad \forall i \in \{1,\dots,m\}, \\
\dot{\eta} &= q(\xi,\eta) = q_0(0,\eta) + \sum_{j=1}^{m}\sum_{i=1}^{r_i} q_{ij}(\xi,\eta)\xi_i^j.
\end{aligned}
\tag{4.20}
$$

Clearly, if the system evolves correctly, both system 4.17 and 4.20 lay on the zero dynamics manifold, namely $\mathcal{M}$.

4.3.2 Stabilisation approach

Consider the following modified version of system 4.20.

$$
\begin{aligned}
\dot{\xi}_1^i &= \xi_2^i + k_1^i(\xi,\eta)\xi_1^i \\
&\vdots, \\
\dot{\xi}_{r_i-1}^i &= \xi_{r_i}^i + k_{r_{i-1}}^i(\xi,\eta)\xi_{r_i-1}^i, \\
\dot{\xi}_{r_i}^i &= b_i(\xi,\eta) + \sum_{j=1}^{m} a_{ij}(\xi,\eta)\lambda_j + k_{r_i}^i(\xi,\eta)\xi_{r_i}^i \quad \forall i \in \{1,\dots,m\}, \\
\dot{\eta} &= q(\xi,\eta) = q_0(0,\eta) + \sum_{j=1}^{m}\sum_{i=1}^{r_i} q_{ij}(\xi,\eta)\xi_i^j,
\end{aligned}
\tag{4.21}
$$

where $\xi_i^j \in \mathbb{R}$ and

$$
k_i^j(\xi,\eta) = -\frac{\delta^2}{2}\|q_{ij}(\xi,\eta)\|^2 - \epsilon, \tag{4.22}
$$

for $i,j \in \{1,\dots,m\}$, with $\delta,\epsilon > 0$. The control terms $k_i^j(\xi,\eta)$ have been added in order to steer the ξ dynamics to zero, keeping system trajectories on the solution manifold $\mathcal{M}$.

As control terms have been added it is of the utmost importance that the solutions of the original system 4.17 and of the controlled 4.21 coincide. Such result is ensured by the following lemma [7].

Lemma 4. *Consider system 4.17 and 4.21. Assume system 4.17 to have a well defined relative degree $r = (r_1,\dots,r_m)$. Suppose also (ξ_0,η_0) to belong to the solution manifold $\mathcal{M}$ defined in Equation 4.18. Then, any solution of 4.17 is a solution of 4.21 and viceversa.*

As a consequence of this result the trajectories of system 4.17 and 4.21 are the same. Therefore, if the solution manifold $\mathcal{M}$ was modified to be attractive on 4.21, the consequence would be valid also on 4.17. This result is stated by the following theorem [7].

Theorem 6. *Consider system 4.21. Assume there exist a positive definite and radially unbounded function $W(\eta)$ such that both the following hold*

$$C_1: \quad \frac{\partial W(\eta)}{\partial \eta} q_0(\eta) \leq \gamma W(\eta) + \gamma_0, \quad \gamma, \gamma_0 \in \mathbb{R} \tag{4.23}$$

$$C_2: \quad \sup_{\eta \in \mathbb{R}^{n-r_{tot}}} \frac{\| \frac{\partial W(\eta)}{\partial \eta} \|^2}{W(\eta)} \leq \overline{W} < +\infty, \quad \overline{W} \in \mathbb{R} \tag{4.24}$$

Then, there exists $\bar{\delta}, \bar{\epsilon} > 0$ such that for all $\delta > \bar{\delta}$ and $\epsilon > \bar{\epsilon}$ the control terms defined in 4.22 ensure that:

i) $\eta(t)$ and $\xi(t)$ exist for all $\eta_0 \in \mathbb{R}^{n-r_{tot}}$, $\xi_0 \in \mathbb{R}^{r_{tot}}$, and $t \geq 0$.

ii) $\lim_{t \to \infty} \xi(t) = 0$, for all $\xi_0 \in \mathbb{R}^{r_{tot}}$.

Theorem 6 presents global results proving $\mathcal{M}$ to be attractive. However, it requires to find a mapping $W(\eta)$ meeting conditions 4.23 and 4.24 globally, that could be difficult. Therefore, Theorem 6 is stated in a local fashion, adding some interesting considerations on the stability of η trajectories.

Theorem 7. *Consider system 4.21. Assume such system to have a locally asymptotic stable equilibrium point in $\bar{q} = (\bar{\xi}, \bar{\eta})$. Let $\mathcal{B} \subseteq \mathbb{R}^{n-r_{tot}}$ be a closed set which contains $\bar{\eta}$. Assume there exist a positive definite and radially unbounded function $W(\eta)$ such that both the following hold*

$$C_1: \quad \frac{\partial W(\eta)}{\partial \eta} q_0(\eta) \leq \gamma W(\eta) + \gamma_0, \quad \gamma < 0, \gamma_0 = 0, \forall \eta \in \mathcal{B} \tag{4.25}$$

$$C_2: \quad \sup_{\eta \in \mathcal{B}} \frac{\| \frac{\partial W(\eta)}{\partial \eta} \|^2}{W(\eta)} \leq \overline{W} < +\infty, \quad \overline{W} > 0 \tag{4.26}$$

Then, there exists a neighbourhood $U \subseteq \mathbb{R}^n$ of the equilibrium point $(\bar{\xi}, \bar{\eta})$ and $\bar{\delta}, \bar{\epsilon} > 0$ such that for all $\delta > \bar{\delta}$ and $\epsilon > \bar{\epsilon}$ in 4.22 the following hold:

i) $\eta(t)$ and $\xi(t)$ exist for all $(\eta_0, \xi_0) \in U$, and $t \geq 0$.

ii) $\lim_{t \to \infty} \xi(t) = 0$, for all $(\eta_0, \xi_0) \in U$.

iii) $\lim_{t \to \infty} \eta(t) = \bar{\eta}$, for all $(\eta_0, \xi_0) \in U$.

if Theorem 7 holds globally the following remark holds:

Remark 1. *Consider the setting defined in Theorem 7. If $\mathcal{B} = \mathbb{R}^{n-r_{tot}}$ and $W(\eta)$ is radially unbounded, the whole set of statements in Theorem 7 holds globally.*

4.3.3 Discretization scheme

Assume $\mathcal{M}$ to be attractive accordingly to one among Theorem 6, Theorem 7, or Remark 1. Consider the controlled scheme described in Equation 4.21. In order to implement such control method, a discretization scheme is needed. Indeed, different discretization schemes imply different behaviours as far as the drifting effect is concerned. Consider the following discretization scheme.

$$\begin{aligned} \frac{\xi_i^{j+} - \xi_i^j}{T} &= k_i^j(\xi, \eta)\xi_i^j, \\ \frac{\eta_k^+ - \eta_k}{T} &= \rho_T^k(q_0^k) + \sum_{j=1}^{m}\sum_{i=1}^{r_i} q_{ij}(\xi, \eta)\xi_i^j, \end{aligned} \tag{4.27}$$

where $i \in \{1, \dots, r_i\}, j \in \{1, \dots, m\}, k \in \{i, \dots, n - r_{tot}\}$, and $\rho_T^i : \mathbb{R} \to \mathbb{R}$. Moreover, consider (k_i^j, q_0^i) as defined in Equation 4.22 and Equation 4.21. Consider the following expression.

$$\lim_{T \to 0} \rho_T^k(q_0^k) = q_0^k, \quad \forall k \in \{i, \dots, n - r_{tot}\}. \tag{4.28}$$

If $T \to 0$ and Equation 4.28 holds, system Equation 4.27 coincides with Equation 4.21. Moreover, if

$$\rho_T^k(q_0^k) = q_0^k, \quad \forall k \in \{i, \dots, n - r_{tot}\}, \tag{4.29}$$

the discretization scheme presented in Equation 4.27 consists of a simple forward Euler method for the integration of ODEs (ODE1 method). ODE1 is one of the simplest yet less accurate integration methods. Thus, the drifting effect introduced by this method is significant.

In this framework, the results obtained in subsection 4.3.2 can be stated in a discretized fashion, providing a constructive procedure to implement the control scheme described in Equation 4.21. Consider then the discretized system 4.27. The following holds [7].

Theorem 8. *Consider system 4.27 and its equilibrium point $\bar{q} = (\bar{\xi}, \bar{\eta})$. Assume $(\xi_0, \eta_0) \in \mathcal{U} \subseteq \mathbb{R}^n$ where $\mathcal{U}$ is a compact set containing $\bar{q}$. Then, for all T such that*

$$0 < T < \frac{2}{\max\limits_{j=1,\dots,m}\left(\max\limits_{i=1,\dots,r_i}\left(\max\limits_{(\xi,\eta)\in U} -k_i^j(\xi, \eta)\right)\right)} \tag{4.30}$$

the following holds:

i) $(\xi(t), \eta(t))$ *exist for all* $(\xi_0, \eta_0) \in \mathbb{R}^n$

ii) $\lim\limits_{t \to \infty} \xi(t) = 0$, *for all* $(\xi_0, \eta_0) \in \mathcal{U}$.

This theorem reframes results of Theorem 6 considering the sampling time needed for the discretization scheme. The same reasoning can be carried on for Theorem 7 [7].

Theorem 9. *Assume now the results of Theorem 7 to be valid for the equilibrium point $\bar{q}$. Let $\mathcal{U} \subseteq \mathbb{R}^n$ be a closed set containing $\bar{q}$. Consider the discretization scheme presented in system 4.27. Assume there exists $\overline{\overline{T}}$ such that*

$$\max_{(\xi,\eta)\in U} \frac{(q_0(\eta) + Q(\xi,\eta))^T H_T(\xi,\eta) q_0(\eta) + Q(\xi,\eta))}{W(\eta) + \xi^T \xi} \leq \hat{W} < +\infty, \tag{4.31}$$

for all $0 \leq T \leq \overline{\overline{T}}$, where

$$H_T(\xi,\eta) = \begin{bmatrix} \frac{\partial^2 W(\eta^+)}{\partial^2 \eta_1^+} & \cdots & \frac{\partial^2 W(\eta^+)}{\partial \eta_1^+ \partial \eta_{n-r_{tot}}^+} \\ \vdots & \ddots & \vdots \\ \frac{\partial^2 W(\eta^+)}{\partial \eta_{n-r_{tot}} \partial \eta_1^+} & \cdots & \frac{\partial^2 W(\eta^+)}{\partial^2 \eta_{n-r_{tot}}^+} \end{bmatrix}. \tag{4.32}$$

Define $\alpha = \frac{1}{2}$. Let the sampling time be

$$T \leq \min\left(\alpha \overline{T}, \overline{\overline{T}} \min\left(1, \frac{|\gamma^{\bar{\delta}^2} + \overline{W}|}{\bar{\delta}^2 \hat{W}}\right)\right). \tag{4.33}$$

where $(\bar{\delta}, \gamma)$ have been chosen accordingly to Theorem 7. By choosing T accordingly to Equation 4.33, there exists a neighbourhood of the equilibrium point $\tilde{\mathcal{U}} \subseteq \mathcal{U}$ in which the following hold.

i) $\eta(t)$ and $\xi(t)$ exist for all $(\eta_0, \xi_0) \in \tilde{\mathcal{U}}$, and $t \geq 0$.

ii) $\lim_{t\to\infty} \xi(t) = 0$, for all $(\eta_0, \xi_0) \in \tilde{\mathcal{U}}$.

iii) $\lim_{t\to\infty} \eta(t) = \bar{\eta}$, for all $(\eta_0, \xi_0) \in \tilde{\mathcal{U}}$.

Note that results on the local or global attractivity of $\mathcal{M}$ are a direct consequence of $W(\eta)$ properties, accordingly to Theorem 7 and Remark 1.

Algorithm implementation

The discretization represents the last step in the control scheme described by Equation 4.21. The following sequence recalls all the procedure described until now.

Data

---

1. Consider a general system of DAE described by equations in the form of 2.14. Assume such system to have a locally asymptotic equilibrium point $\bar{x}$. Moreover, assume such system to have a well defined relative degree $r = (r_1, \ldots, r_m)$.
2. Consider x_0 such that $h(x_0) = 0$.
3. Consider a function W meeting the assumptions of Theorem 7.

Algorithm output

Consider the discretization presented in Equation 4.27. The output of the control scheme is x^+ such that both Theorem 8 and Theorem 9 hold.

Algorithm

The following steps shall be computed on the current state vector x:

1. **Step 1.** Consider a local diffeomorphism $\Phi : \mathcal{U} \subseteq \mathbb{R}^n \to \mathbb{R}^n$ valid in x. Through such mapping transform the current state vector in normal form coordinates, namely set $q = (\xi, \eta) = \Phi(x)$.

2. **Step 2.** From the system in normal form, compute the mappings q_{ij} such that

$$\dot{\eta} = q(\xi, \eta) = q_0(0, \eta) + \sum_{j=1}^{m} \sum_{i=1}^{r_i} q_{ij}(\xi, \eta) \xi_i^j. \tag{4.34}$$

3. **Step 3.** Select a compact set $\mathcal{B} \subseteq \mathbb{R}^{n-r_{tot}}$ and compute the parameters $\gamma < 0$ and $\overline{W}$ satisfying conditions 4.25 and 4.26 with $\gamma_0 = 0$.

4. **Step 4.** Check the following conditions:
   IF $\gamma < 0$ **AND** $\gamma_0 = 0$
   Select:

$$\begin{aligned} &\epsilon \geq -\gamma - \beta, \quad \beta \in [0, -\gamma], \\ &\delta < \bar{\delta} = \frac{1}{2\beta} \overline{W}, \quad \beta \in [0, -\gamma]. \end{aligned} \tag{4.35}$$

   ELSE
   Select:

$$\begin{aligned} &\epsilon > 0, \\ &\delta < \bar{\delta} = \frac{1}{2\beta} \overline{W}, \quad \beta > 0. \end{aligned} \tag{4.36}$$

5. **Step 5.** Compute $\overline{T}$ and $\overline{\overline{T}}$ such that condition 4.33 and 4.31 are satisfied.

6. **Step 6.** Check the following conditions:
   IF $\gamma < 0$ **AND** $\gamma_0 = 0$
   Select T according to Equation 4.33

   ELSE
   Select $T \leq \overline{T}$

7. **Step 7.** Accordingly to the choices made in the previous steps, update the state vector as defined in Equation 4.27.

8. **Step 8.** Set $x^+ = \Phi^{-1}(\xi^+, \eta^+)$.

4.3.4 Looper - Algorithm implementation

The procedure described in subsection 4.3.2 has been applied on the system in analysis, namely the looper. Recall the stability analysis carried on in section 3.2 and section 3.3. The system has been proved to have a globally asymptotic stable equilibrium point $\bar{x} = (\bar{q}_1, \bar{q}_2\bar{q}_3, 0, 0, 0) \in \mathcal{U} \subseteq \mathbb{R}^n$, where $\mathcal{U}$ defines the joint space of the system. This section presents the implementation of each step of the algorithm described in subsection 4.3.3.

Data

The system considered is the one described by Equation 1.44, namely

$$\begin{cases} M_1^{tot}\ddot{q}_1 = F_1(q,\dot{q}) + a_{11}(q)\lambda_1(q,\dot{q}) + a_{21}(q)\lambda_2(q,\dot{q}) \\ M_2^{tot}\ddot{q}_2 = F_2(q,\dot{q}) + a_{12}(q)\lambda_1(q,\dot{q}) + a_{22}(q)\lambda_2(q,\dot{q}) \\ M_3^{tot}\ddot{q}_3 = F_3(q,\dot{q}) + a_{13}(q)\lambda_1(q,\dot{q}) + a_{23}(q)\lambda_2(q,\dot{q}) \\ h_1(q) = 0 \\ h_2(q) = 0 \end{cases} \tag{4.37}$$

Note that here (q_1, q_2, q_3) are the generalised coordinates used to describe the system. Accordingly to section 2.7 such system has a well defined relative degree $r = (r_1, r_2) = (2, 2)$. Recall the stability analysis in section 3.2 and section 3.3.

Consider now the diffeomorphism defined in Equation 2.76. Transform system 4.37 accordingly to such diffeomorphism. The transformed equilibrium point is

$$\bar{q} = (0, \bar{\eta}) \in \mathbb{R}^6. \tag{4.38}$$

Recall the stability analysis performed in subsection 3.3.1. Both the Lyapunov functions $V(\eta)$ and $V_\epsilon(\eta)$ represent a good candidate for the mapping $W(\eta)$ mentioned in subsection 4.3.2. Again, the choice of the normal form transformation turns out to be decisive as it defines the main properties of mapping $W(\eta)$. The main goal of this analysis is to prove the solution manifold $\mathcal{M}$ to be attractive on the controlled system defined in Equation 4.21.

Consider the equilibrium $\bar{q} = (0, \bar{\eta})$ and restrict it to $\bar{\eta}$. This is done because W depends only on η. Set $W_1(\eta) = V(\eta)$ and $W_2(\eta) = V_\epsilon(\eta)$ as a candidate mapping, where $V(\eta)$ is defined accordingly to Equation 3.41 and V_ϵ accordingly to Equation 3.47, namely

$$W_1 = \frac{1}{2}M(\eta)\dot{\eta}^2 + \int_0^\eta G(\tau)d\tau + c \tag{4.39}$$

$$W_2 = \frac{1}{2}M(\eta)\dot{\eta}^2 + \int_0^\eta G(\tau)d\tau + c + \epsilon(\eta - \bar{\eta})\dot{\eta}, \quad \epsilon \in \mathbb{R}. \tag{4.40}$$

Note that both $W_1(\eta)$ and $W_2(\eta)$ are defined around the equilibrium point $\bar{\eta} \neq 0$ instead of $\tilde{\eta} = 0$ as in Equation 3.41 and Equation 3.47. In Figure 4.7 both W_1 and W_2 are presented, along with their derivative $\dot{W}_1$ and $\dot{W}_2$.

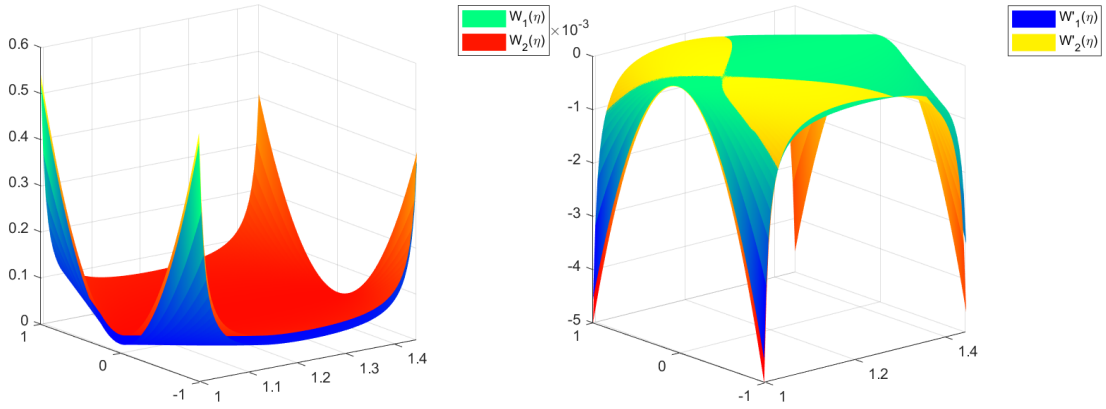

(a) W_1 and W_2 comparison (b) $\dot{W}_1$ and $\dot{W}_2$ comparison

Figure 4.7: Comparison between the two candidates functions W_1 and W_2 and their derivatives

By setting $\epsilon = 0.0001$ as reported in subsection 3.3.1, from the numerical analysis it turns out that

$$\begin{aligned} \max_{\eta \in \mathcal{B}} \dot{W}_1(\eta) &= 0, \\ \max_{\eta \in \mathcal{B}} \dot{W}_2(\eta) &= -2 \cdot 10^{-10} < 0. \end{aligned} \tag{4.41}$$

As expected W_1 proves local asymptotic stability while W_2 global asymptotic stability of $\bar{\eta}$. W_1 and W_2 can be used to check the assumptions defined in Theorem 7. From the stability analysis the looper is known to have a globally asymptotic stable equilibrium point in $(0, \bar{\eta})$. It is always possible to define a subset $\mathcal{B} \subseteq \mathbb{R}^{n-r_{tot}}$ containing $\bar{\eta}$. Moreover, as shown in Figure 4.7, both W_1 and W_2 are radially unbounded, namely

$$\lim_{\|\eta\| \to \infty} W_i(\eta) = \infty. \tag{4.42}$$

Consider now conditions 4.25 and 4.26. Figure 4.8 compares condition 4.25 on both W_1 and W_2.

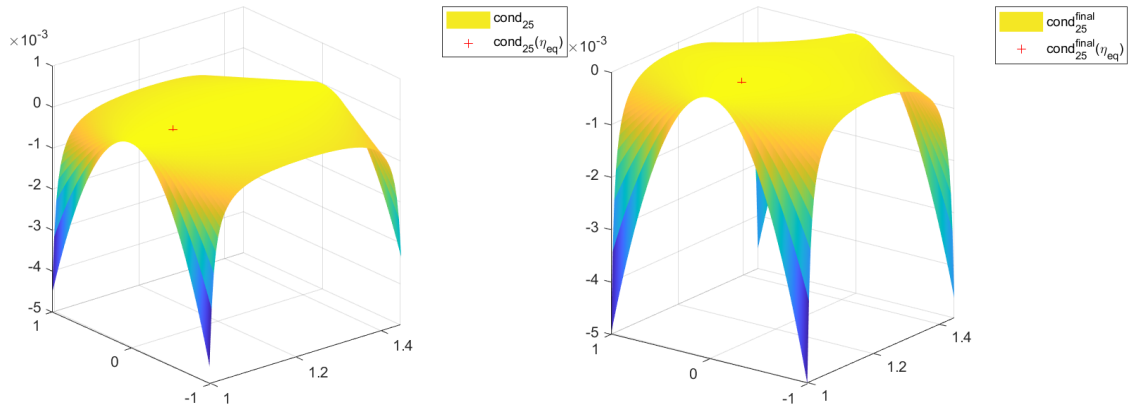

(a) Condition 4.25 on W_1 (b) Condition 4.25 on W_2

Figure 4.8: Comparison between condition 4.25 on both W_1 and W_2

Consider now $\mathcal{B} = \mathcal{U}_\eta \subseteq \mathbb{R}^{n-r_{tot}}$, coinciding with the whole joint space of the looper η dynamics, defined in subsection 1.2.1. Set $\gamma = -1 \cdot 10^{-10}$ and compute condition 4.25 on both W_1 and W_2, namely $C_1^{W_1}$ and $C_1^{W_2}$. The numerical analysis returns the following results.

$$\begin{aligned} \max_{\eta \in \mathcal{B}} C_1^{W_1}(\eta) &= 2 \cdot 10^{-10} > 0, \\ \max_{\eta \in \mathcal{B}} C_1^{W_2}(\eta) &= -2 \cdot 10^{-10} < 0. \end{aligned} \tag{4.43}$$

Therefore, there exist points in $\mathcal{B}$ in which $C_1^{W_1} > 0$. Thus W_1 meets condition 4.25 only locally near the equilibrium point $\bar{\eta}$ while W_2 satisfies the same globally in $\mathcal{B}$. W_1 and W_2 behaviour near $\bar{\eta}$ is presented in the contour plots in Figure 4.9.

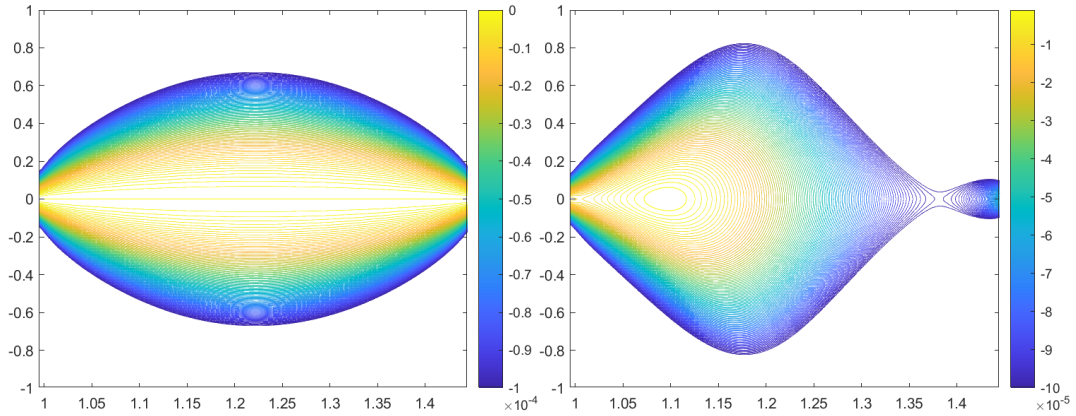

(a) Contour plot of condition 4.25 on W_1 (b) Contour plot of condition 4.25 on W_2

Figure 4.9: Comparison between the contour plots of condition 4.25 for both W_1 and W_2

Figure 4.10 presents instead the comparison between condition 4.26 on both W_1 and W_2.

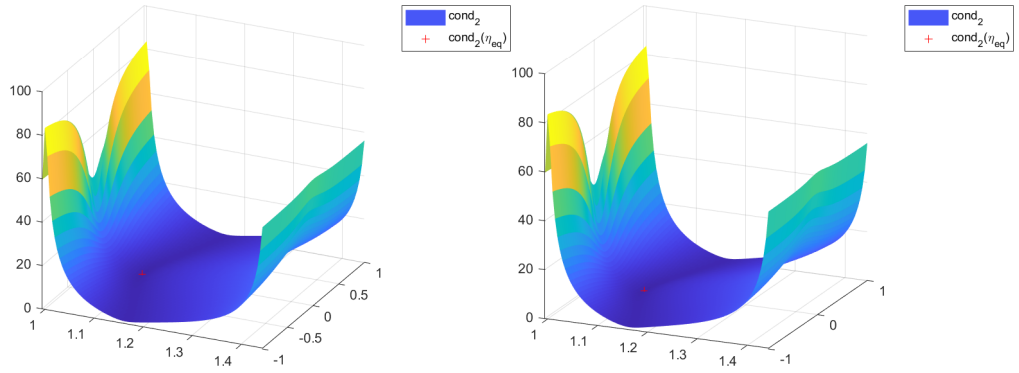

(a) Condition 4.26 on W_1 (b) Condition 4.26 on W_2

Figure 4.10: Comparison between condition 4.26 on both W_1 and W_2

Clearly, both W_1 and W_2 meet condition 4.26, in fact, from numerical analysis, the following holds.

$$\overline{W}_1 = \max_{\eta \in \mathcal{B}} C_2^{W_1}(\eta) = \overline{W}_2 = \max_{\eta \in \mathcal{B}} C_2^{W_2}(\eta) = 83.6255 \tag{4.44}$$

This analysis points out that both W_1 and W_2 meet all the conditions of Theorem 7, proving the local asymptotic stability of $\bar{\eta}$ on the controlled system described in Equation 4.21. However, mapping W_2 meets conditions 4.25 and 4.25 also globally in $\mathcal{B} = \mathcal{U}_\eta$. Therefore, for W_2, Remark 1 holds, proving $\bar{\eta}$ to be a global asymptotic equilibrium point for the controlled system Equation 4.21. Thus, this prove $\mathcal{M}$ to be attractive on the whole joint space domain $\mathcal{B} = \mathcal{U}_\eta$.

At the end of this analysis the set up described in section **Data** of subsection 4.3.3 is correctly defined. In fact, the system is provided with an asymptotic equilibrium point and with a well defined relative degree. Moreover, two W mappings have been found both meeting the requirements of Theorem 7 and even Remark 1.

Algorithm - Step 1

Recall the stability analysis in subsection 3.3.2. The diffeomorphism defined in Equation 2.76 transform the system in a normal form whose zero dynamics behaves as a mechanical system with a globally asymptotic equilibrium point, namely $\bar{q}$. Recall that

$$z = \begin{bmatrix} z_1 \\ z_2 \\ z_3 \\ z_4 \\ z_5 \\ z_6 \end{bmatrix} = \begin{bmatrix} \xi_1^1 \\ \xi_2^1 \\ \xi_1^2 \\ \xi_2^2 \\ \eta_1 \\ \eta_2 \end{bmatrix} \tag{4.45}$$

Therefore the considered diffeomorphism for the looper is described by equations in the following form.

$$\Phi = \begin{pmatrix} \phi_1^1 \\ \phi_2^1 \\ \phi_1^2 \\ \phi_2^2 \\ \phi_1 \\ \phi_2 \end{pmatrix} = \begin{pmatrix} h_1(x) \\ L_f h_1(x) \\ h_2(x) \\ L_f h_2(x) \\ x_1 \\ x_4 \end{pmatrix} \tag{4.46}$$

The inverse transformation is described by the following equations.

$$\Phi^{-1} = \begin{pmatrix} z_5 \\ \phi_{x_2}^{-1}(z) \\ \phi_{x_3}^{-1}(z) \\ \phi_{x_4}^{-1}(z) \\ \phi_{x_5}^{-1}(z) \\ z_6 \end{pmatrix} = \begin{pmatrix} z_5 \\ \frac{z_1 + R_x + R_{34} \sin \phi_{x_3}^{-1}(z)}{\cos z_5} - (R_{12} + R_{23}) \\ z_5 - \arccos\left(\frac{(z_3 + R_y)\cos z_5 - (z_1 + R_x)\sin z_5}{R_{34}} \right) \\ z_6 \\ \frac{z_2 + (R_{12} + R_{23} + \phi_{x_2}^{-1}(z)) z_6 \sin z_5 + R_{34} \phi_{x_6}^{-1}(z) \cos \phi_{x_3}^{-1}(z)}{\cos z_5} \\ \frac{z_4 \cos z_5 - z_2 \sin z_5 - (R_{12} + R_{23} + \phi_{x_2}^{-1}(z)) z_6}{R_{34} \sin(z_5 - \phi_{x_3}^{-1}(z))} \end{pmatrix} \tag{4.47}$$

This diffeomorphism is well defined over the whole joint space of the looper, except for the boundary configurations, namely $q_1 = \theta_1^{min}$ and $q_1 = \theta_1^{max}$ (See subsection 1.2.3).

Algorithm - Step 2

Consider the system transformed in normal form, whose dynamics are described by equations in the following form.

$$\begin{cases} \dot{\xi}_1^1 = \xi_2^1 \\ \dot{\xi}_2^1 = b_1 + a_{11}\lambda_1 + a_{12}\lambda_2 \\ \dot{\xi}_1^2 = \xi_2^2 \\ \dot{\xi}_2^2 = b_2 + a_{21}\lambda_1 + a_{22}\lambda_2 \\ \dot{\eta}_1 = q_1 + p_{11}\lambda_1 + p_{12}\lambda_2 \\ \dot{\eta}_2 = q_2 + p_{21}\lambda_1 + p_{22}\lambda_2 \end{cases} \tag{4.48}$$

The η dynamics of this system can be written in the following form.

$$\dot{\eta} = q(\xi, \eta) = q_0(0, \eta) + Q(\xi, \eta)\xi = q_0(0, \eta) + \sum_{j=1}^{m}\sum_{i=1}^{r_i} q_{ij}(\xi, \eta)\xi_i^j. \tag{4.49}$$

The q_{ij} terms shall be computed from the original mapping $q(\xi, \eta)$. To do so consider the general mapping $Q(\xi, \eta)$ defined as follows.

$$Q(\xi, \eta)\xi = q(\xi, \eta) - q_0(0, \eta). \tag{4.50}$$

By means of this formulation the system can be written in the following form.

$$\begin{aligned} \begin{bmatrix} q_1 \\ q_2 \end{bmatrix} &= \begin{bmatrix} q_1^0 \\ q_2^0 \end{bmatrix} + \begin{bmatrix} q_1^{11} & q_1^{12} \\ q_1^{21} & q_1^{22} \end{bmatrix} \begin{bmatrix} \xi_1^1 \\ \xi_2^1 \end{bmatrix} + \begin{bmatrix} q_2^{11} & q_2^{12} \\ q_2^{21} & q_2^{22} \end{bmatrix} \begin{bmatrix} \xi_1^2 \\ \xi_2^2 \end{bmatrix} \\ &= \begin{bmatrix} q_1^0 \\ q_2^0 \end{bmatrix} + \begin{bmatrix} q_1^{11} & q_1^{12} \\ q_1^{21} & q_1^{22} \end{bmatrix} \begin{bmatrix} z_1 \\ z_2 \end{bmatrix} + \begin{bmatrix} q_2^{11} & q_2^{12} \\ q_2^{21} & q_2^{22} \end{bmatrix} \begin{bmatrix} z_3 \\ z_4 \end{bmatrix} \end{aligned} \tag{4.51}$$

where (q_1, q_2) and (q_0^1, q_0^2) are respectively the mappings for the η general and zero dynamics. The procedure to compute the q_k^{ij} is developed as follows.

1. Consider the general mapping

$$q_1 = x_4(\Phi^{-1}(z)) = z_6 = \eta_2 \tag{4.52}$$

   Accordingly to the diffeomorphism defined in Equation 4.46 and Equation 4.47 there is no dependence on ξ_i^j and therefore $q_1^{ij} = 0, \quad \forall i, j \in \{1, 2\}$.

2. Consider the general mapping

$$q_2(z) = f_4 + p_{21}\lambda_1 + p_{22}\lambda_2 \tag{4.53}$$

Generally speaking, the dependence between q_1 and (z_1, z_2, z_3, z_4) is defined by a nonlinear mapping. However, consider the expanded version of the relation described in Equation 4.51, namely,

$$q_2 = q_2^0 + q_1^{21} z_1 + q_1^{22} z_2 + q_2^{21} z_3 + q_2^{22} z_4. \tag{4.54}$$

Assume to know the zero dynamics q_2^0 and three linear mappings, for instance $(q_1^{21}, q_1^{22}, q_2^{22})$. The last mapping q_2^{21} can be computed as

$$q_2^{21} = \frac{q_2 - q_2^0 - q_1^{21} z_1 - q_1^{22} z_2 - q_2^{22} z_4}{z_3}. \tag{4.55}$$

Note that in general, nothing prevent z_3 to be null during the simulation. On the contrary, as $z_3 = h_2(x)$, its desired value is exactly 0. Thus, $z_3 = 0$ would cause a zero division. Therefore, in the practical implementation, a saturation is applied on z_3, namely

$$|z_3| \leq \bar{z}_3 \tag{4.56}$$

This solution shall be taken into account during the algorithm performance evaluation, which will be addressed in section 4.4.

Note that even if the linear mappings $(q_1^{21}, q_1^{22}, q_2^{22})$ don't describe the exact relation with q_2, the final mapping is correct because q_2^{21} embodies all the previously neglected terms.

The following computations are presented in order to derive these mappings. Recall the computation of λ_i carried on in subsection 2.7.4. It holds

$$\begin{cases} \lambda_1 = -\frac{b_1 + a_{12}\lambda_2}{a_{11}} \\ \lambda_2 = \frac{b_1 a_{21} - b_2 a_{11}}{a_{11}a_{22} - a_{12}a_{21}} \end{cases} \tag{4.57}$$

From Equation 4.53, consider the $p_2\lambda_2$ term. It holds

$$\begin{aligned} p_2\lambda_2 &= p_2 \left[\frac{x_2 x_4^2 \sin x_1 \cos^2 x_1}{M_2} + T_{junk} \right] \frac{1}{D_{\lambda_2}} = \\ &= p_2 \left[\frac{z_1}{\cos x_1} + T_{junk} \right] \left[\frac{x_4^2 \sin x_1 \cos^2 x_1}{M_2} + T_{junk} \right] \frac{1}{D_{\lambda_2}} = \\ &= z_1 \left[p_2 \frac{x_4^2 \sin x_1 \cos x_1}{M_2 D_{\lambda_2}} + T_{junk} \right] = \\ &= q_1^{21} z_1 + T_{junk} z_1 \end{aligned} \tag{4.58}$$

where $D_{\lambda_2} = (a_{11}a_{22} - a_{12}a_{21})$ and T_{junk} represents the remaining part of the nonlinear relation between $p_2\lambda_2$ and z_1. Note that any mapping depends on the vector state z by means of the diffeomorphism defined in Equation 4.46 and Equation 4.47. The same computations can be done to extract q_1^{22} and q_2^{22}. The final mappings are described by the following equations.

$$
\begin{aligned}
q_1^{21} &= \left[p_2 \frac{x_4^2 \sin x_1 \cos x_1}{M_2 D_{\lambda_2}} \right], \\
q_1^{22} &= \left[p_2 \frac{2x_4^2 \sin^2 x_1}{M_2 D_{\lambda_2}} \right], \\
q_2^{22} &= \left[p_2 \frac{2x_4 \sin^2 x_1 \cos^2 x_2 \cos x_3}{M_2 D_{\lambda_2}} \right].
\end{aligned} \tag{4.59}
$$

Therefore, q_2^{21} is computed as reported in Equation 4.55. The final description of the η dynamics turns out to be

$$
\begin{bmatrix} \dot{\eta}_1 \\ \dot{\eta}_2 \end{bmatrix} \begin{bmatrix} q_1 \\ q_2 \end{bmatrix} = \begin{bmatrix} q_1^0 \\ q_2^0 \end{bmatrix} + \begin{bmatrix} 0 & 0 \\ q_1^{21} & q_1^{22} \end{bmatrix} \begin{bmatrix} z_1 \\ z_2 \end{bmatrix} + \begin{bmatrix} 0 & 0 \\ q_2^{21} & q_2^{22} \end{bmatrix} \begin{bmatrix} z_3 \\ z_4 \end{bmatrix}, \tag{4.60}
$$

Lastly, note that each linear mapping depends on p_2. Recall that the Lagrangian multipliers description is invariant with respect to the choice of the diffeomorphism. Therefore, the mappings would remain the same if transformation 2.69 was used, except for the formulation of the coefficient p_2.

Algorithm - Step 3

The next step in the nonlinear stabilisation algorithm consists in selecting a compact set $\mathcal{B} \in \mathbb{R}^{n-r_{tot}}$ containing the equilibrium point $\bar{\eta}$. Once this set has been defined, consider it as the domain of the W mapping defined in section 4.3.4.

Considering the results of analysis carried on in section 4.3.4, consider $\mathcal{B} = \mathcal{U}_\eta \subseteq \mathbb{R}^{n-r_{tot}}$, namely the whole system joint space, restricted to the η state variables.

Consider then the following W mapping, previously defined in section 4.3.4.

$$
W = \frac{1}{2} M(\eta) \dot{\eta}^2 + \int_0^\eta G(\tau) d\tau + c + \epsilon(\eta - \bar{\eta})\dot{\eta}, \quad \epsilon \in \mathbb{R}. \tag{4.61}
$$

From the analysis performed in section 4.3.4 it holds that the pair

$$
\begin{aligned}
\gamma &= -1 \cdot 10^{-10} \\
\gamma_0 &= 0,
\end{aligned} \tag{4.62}
$$

satisfies both conditions 4.25 and 4.26 over the whole set $\mathcal{B}$, with $\overline{W} = 83.6255$. With this choice, step 3 of the algorithm is completed.

Algorithm - Step 4

Considering the values of γ and γ_0 described in section 4.3.4 the following choices have been done.

$$
\begin{aligned}
&\beta = 5 \cdot 10^{-11} \in [0, 1 \cdot 10^{-10}], \\
&\epsilon = 3 \geq \bar{\epsilon} = -\gamma - \beta = 5 \cdot 10^{-11}, \\
&\delta = 0.9 < \bar{\delta} = \frac{1}{2\beta} \overline{W} = 8.36 \cdot 10^{11}.
\end{aligned} \tag{4.63}
$$

Algorithm - Step 5

As reported in the algorithm described insubsection 4.3.2, $\overline{T}$ and $\overline{\overline{T}}$ shall be computed. Consider the conditions described in Equation 4.30 and in Equation 4.31. $\overline{T}$ and $\overline{\overline{T}}$ shall be chosen such that the following hold.

$$0 < T < \overline{T} = \frac{2}{\max\limits_{j=1,\dots,m}\left(\max\limits_{i=1,\dots,r_i}\left(\max\limits_{(\xi,\eta)\in U} -k_i^j(\xi,\eta)\right)\right)} \tag{4.64}$$

,

$$\overline{\overline{T}} = \max_{(\xi,\eta)\in U} \frac{(q_0(\eta)+Q(\xi,\eta))^T H_T(\xi,\eta) q_0(\eta)+Q(\xi,\eta))}{W(\eta)+\xi^T\xi} \leq \hat{W} < +\infty.$$

The research of the maxima has been performed over the domain $\mathcal{B}$ through a grid search on (ξ,η) with an accuracy of $\Delta = 0.01$. The obtained values are reported below.

$$\begin{aligned} \overline{T} &= 6 \cdot 10^{-30} \\ \overline{\overline{T}} &= 0.1 \end{aligned} \tag{4.65}$$

Algorithm - Step 6

From the values of $\overline{T}$ and $\overline{\overline{T}}$ the final sampling time shall be computed accordingly to Equation 4.33, namely

$$T \leq \min\left(\alpha\overline{T}, \overline{\overline{T}} \min\left(1, \frac{|\gamma^{\bar{\delta}^2} + \overline{W}|}{\bar{\delta}^2 \hat{W}}\right)\right), \tag{4.66}$$

with $\alpha = \frac{1}{2}$. Therefore, $T = 2.7 \cdot 10^{-30}$.

The selected sampling time turns out to be very small. This because the margin on condition 4.26 ensured by γ is very tiny. Consequently, all the bounds end up in strict conditions. Indeed, the selected sampling time ensures the effectiveness of the algorithm from a theoretical background. However, consider the formulation of Theorem 9. All the conditions imposed on T are sufficient but not necessary to prove $\mathcal{M}$ to be attractive. Therefore, a different (more relaxed) sampling time T doesn't necessarily prevent the algorithm to steer the system onto the trajectories defined by the solution manifold $\mathcal{M}$. Consequently, for the numeric analysis of the algorithm performance on the looper, the sampling time has been set to

$$T = 1 \cdot 10^{-3}. \tag{4.67}$$

Algorithm - Step 7

This step is straightforward as the state vector $q = (\xi, \eta)$ is updated accordingly to Equation 4.27, namely

$$\frac{\xi_i^{j+} - \xi_i^j}{T} = k_i^j(\xi, \eta)\xi_i^j, \tag{4.68}$$
$$\frac{\eta_k^+ - \eta_k}{T} = \rho_T^k(q_0^k) + \sum_{j=1}^{m}\sum_{i=1}^{r_i} q_{ij}(\xi, \eta)\xi_i^j.$$

Algorithm - Step 8

The last step of the discretized control scheme defined in subsection 4.3.2 applies the inverse transformation described in Equation 4.47. By doing so the state vector is expressed in the original coordinates. Therefore, it holds

$$x^+ = \Phi^{-1}(\xi^+, \eta^+). \tag{4.69}$$

4.4 Looper - results

This section presents the algorithm performances on the looper, compared to Baumgarte approach.

In Figure 4.11 the performances of the nonlinear stabilizer and the Baumgarte algorithm are compared, assuming no disturb on the initial condition.

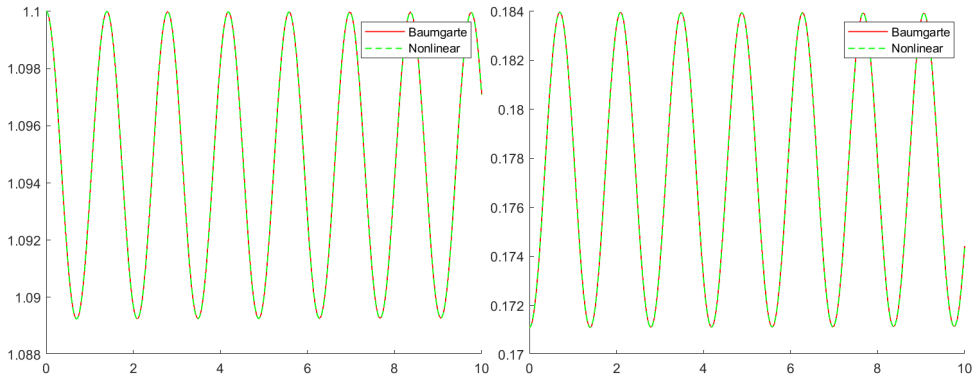

(a) Comparison on x_1 (b) Comparison on x_2

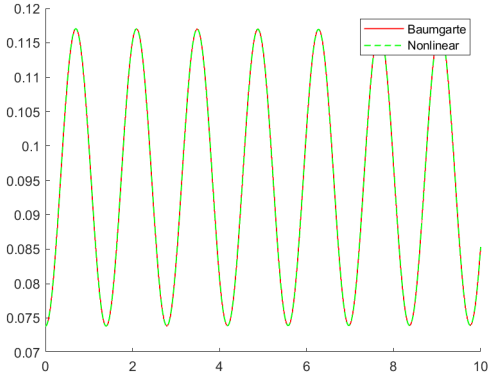

(c) Comparison on x_3

Figure 4.11: Comparison between condition the nonlinear stabilizer and Baumgarte algorithm - state variable and no disturb

Clearly, the performances are almost the same. The real effectiveness of the algorithms shall be tested considering a disturb on the initial condition. Therefore,

a random disturb is introduced in the initial condition x_0, as described in Equation 4.9. Such disturb is generated adding a random value to the initial state vector of the system. Therefore, the initial condition is described by the following relation.

$$\begin{aligned} \tilde{x}_0 &= x_0 + \delta_0, \quad \delta_0 \in \mathbb{R}^6, \quad ||\delta_{0_i}|| \leq \bar{\delta} \in \mathbb{R} \\ \tilde{z}_0 &= \Phi(\tilde{x}_0) \end{aligned} \tag{4.70}$$

Consider the simple case in which $\bar{\delta} = 0.001$. The results of the simulations are shown in Figure 4.12.

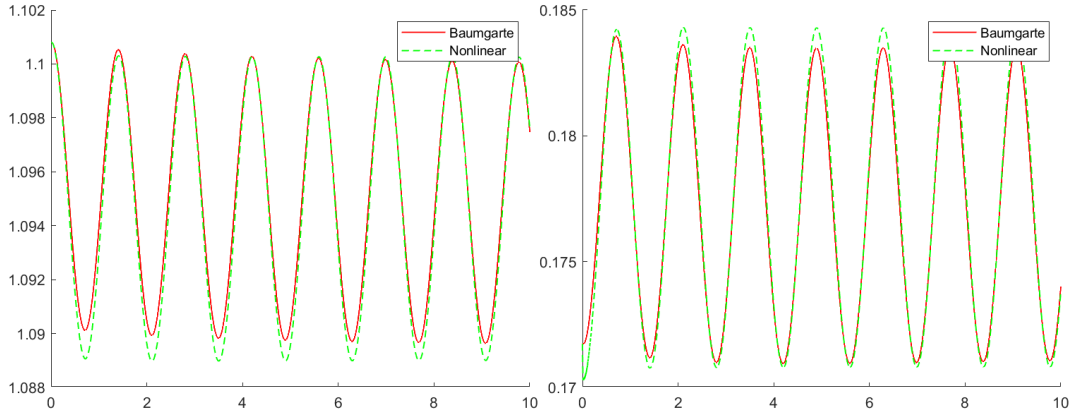

(a) Comparison on x_1

(b) Comparison on x_2

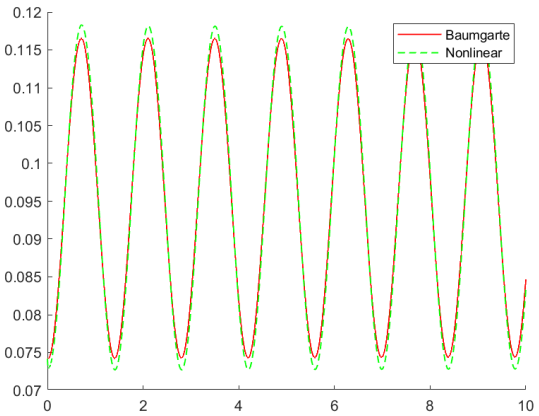

(c) Comparison on x_3

Figure 4.12: Comparison between condition the nonlinear stabilizer and Baumgarte algorithm - state variable and disturb with amplitude $\delta = 0.001$

The results on the algebraic constraints h_1, h_2 are instead shown in Figure 4.13. As the figure depicts, the nonlinear stabilizer corrects the disturb way more quickly than the Baumgarte algorithm. This ends up in different dynamics of the system as shown by the oscillation amplitude in Figure 4.12.

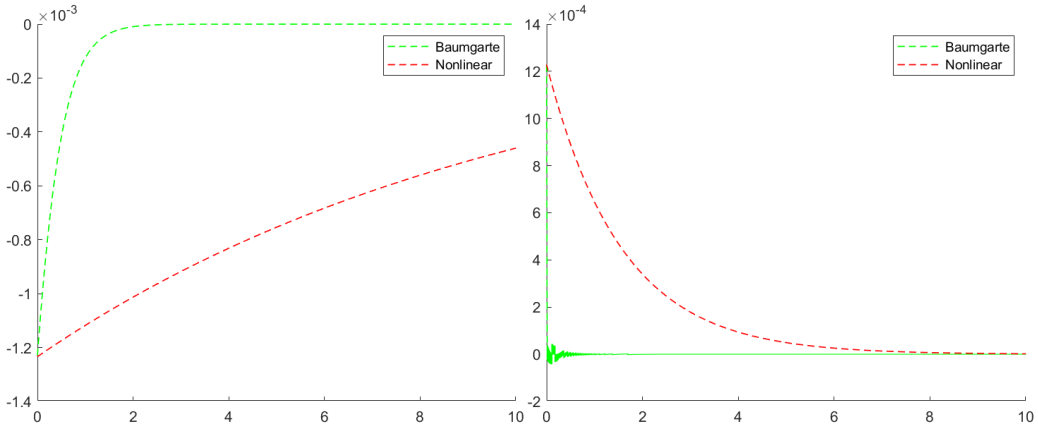

(a) Comparison on h_1 (b) Comparison on h_2

Figure 4.13: Comparison between condition the nonlinear stabilizer and Baumgarte algorithm - constraints correction

However, note the discontinuous trend on the stabilization of h_2. Recall section 4.3.4. Any spike present in the nonlinear algorithm simulation is due to the saturation on z_3 defined in Equation 4.56. More specifically, the threshold has been set to $\bar{z}_3 = 0.005$. The effect of the saturation, as expected, is evident in the control of h_2, namely the physical interpretation of z_3 variable. Such numerical effect is evident in constraint h_2 in Figure 4.13. Such numerical issues make it difficult to test the actual performance of the algorithm. For this reason the whole model, with both Baumgarte and the nonlinear stabilization schemes have been implemented in SIMULINK. This because this tool allows to reach a higher accuracy during the numerical integration. The results of the very same simulation run on SIMULINK are shown in Figure 4.14.

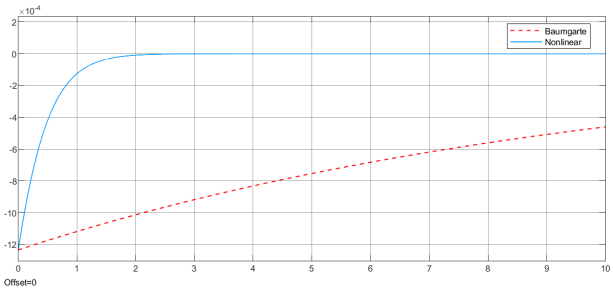

(a) Comparison on h_1

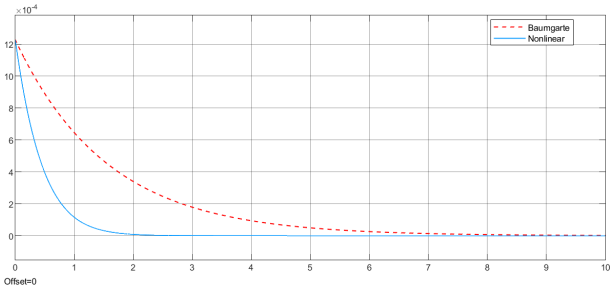

(b) Comparison on h_2

Figure 4.14: Comparison between condition the nonlinear stabilizer and Baumgarte algorithm - constraints on SIMULINK

As the figure shows, the numerical effects of the saturation on z_3 are mitigated by the higher accuracy of the solver used by SIMULINK. Note that the solver method is still ODE1. Therefore, in order to test the algorithm performances in the best possible set-up, the SIMULINK model will be used from now on.

Robustness analysis

Both the algorithms has been tested on different disturbance amplitudes, in order to check their robustness. Assuming the disturbance amplitude to be at most $\bar{\delta} = 0.1$, the nonlinear stabilizer performs better compared to the Baumgarte algorithm, as reported in Figure 4.15

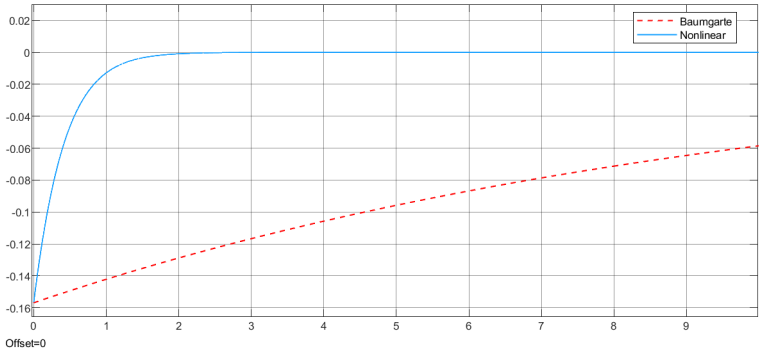

(a) Comparison on h_1

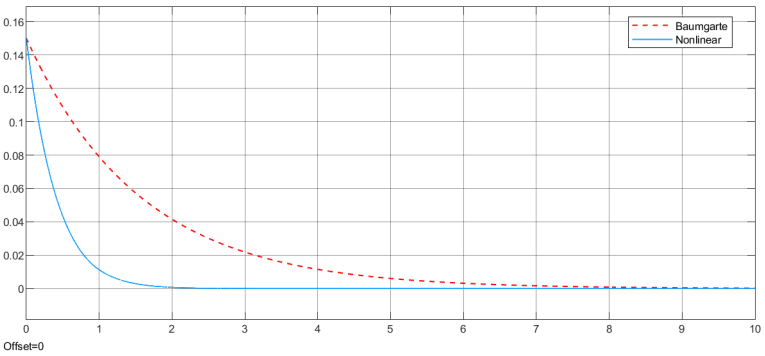

(b) Comparison on h_2

Figure 4.15: Comparison between condition the nonlinear stabilizer and Baumgarte algorithm - constraints on SIMULINK

Again, the error in the algebraic constraint is corrected more quickly by the nonlinear stabilization scheme. Such error implies different dynamics on the Looper, as depicted in Figure 4.16.

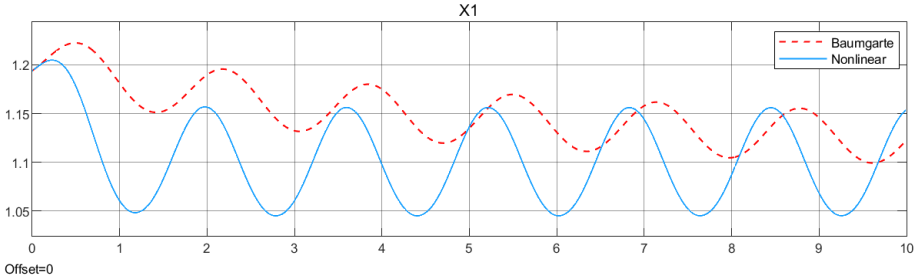

(a) Comparison on x_1

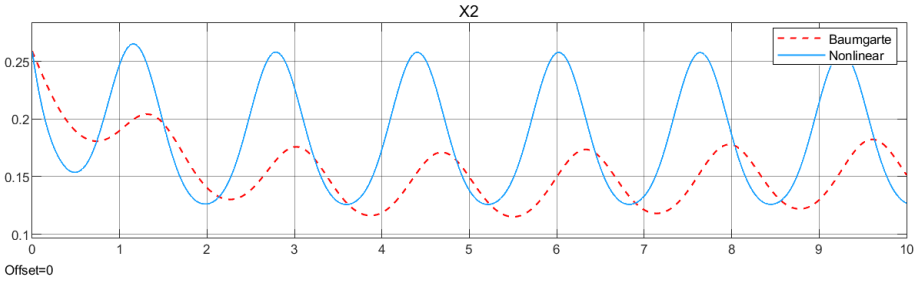

(b) Comparison on x_2

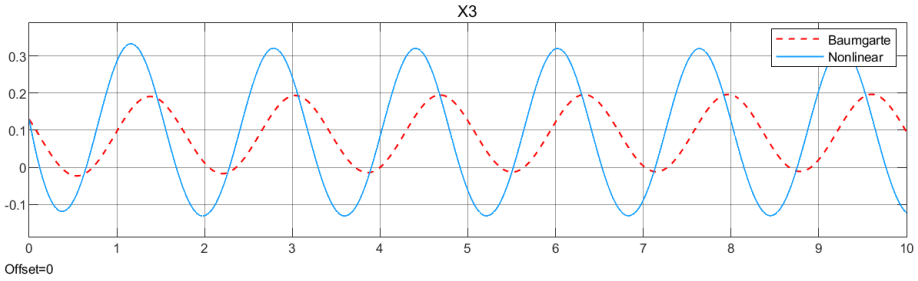

(c) Comparison on x_3

Figure 4.16: Comparison between condition the nonlinear stabilizer and Baumgarte algorithm - state variable

Clearly, both the algorithms are able to correct disturbances of a limited entity. If the nonlinear stabilizer performed better generally speaking, the Baumgarte approach is more robust in terms of disturbs. In fact, from the numerical analysis, the nonlinear stabilizer is able to correct disturbances up to $\bar{\delta} = 0.8$ while the Baumgarte algorithm still works on that disturbance, even if the stabilization time rises significantly.

Finally, consider the disturbance definition in Equation 4.70. As for the physics of the system, it makes no sense to perturb the initial position of the looper as this would imply an impossible initial configuration of the mechanical system. Yet, the links could be stressed in an unnatural way. Thus, a disturbed initial condition on velocities is useful to study the mechanism. Therefore, the disturbance δ is set in order to affect only (x_4, x_5, x_6), namely $\delta_i = 0$ for all $i = \{1, 2, 3\}$. The results of the simulation are shown in Figure 4.17.

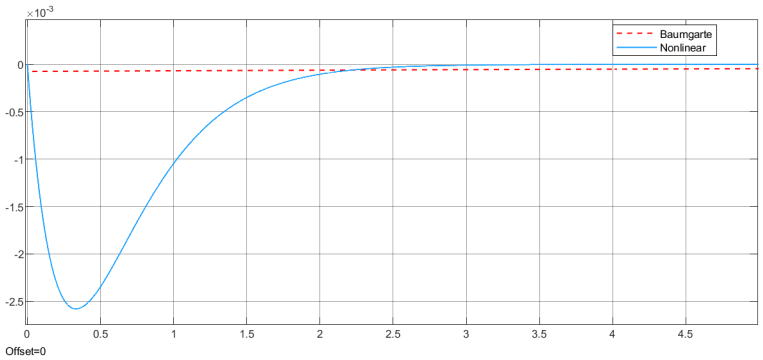

(a) Comparison on h_1

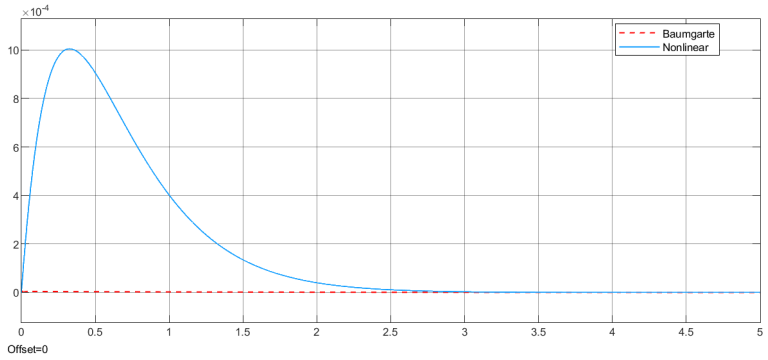

(b) Comparison on h_2

Figure 4.17: Comparison between condition the nonlinear stabilizer and Baumgarte algorithm - constraints on SIMULINK

As shown in the figure, the control effect on h_i presents an overshoot. This is because of the structure of the controller, namely

$$k_i^j(\xi, \eta) = -\frac{\delta^2}{2}\|q_{ij}(\xi, \eta)\|^2 - \epsilon. \tag{4.71}$$

Indeed, a coherent initial condition such that $h_i(0) = 0$ is perturbed by the proportional structure of the controller itself. This is a drawback highlighted by the structure of the specific system in analysis.

Conclusions

This thesis went through a complete analysis of a 1 dof mechanical system, namely the looper. The main steps are summarized in the following sequence, as well as the main results.

- **Modelling.** Chapter 1 of the the thesis presents a general modelling technique for constrained mechanical system, namely the Lagrange multipliers method. Then, the model of the looper is described, along with a general analysis of the joint space, and some considerations on the mechanism singularities. Chapter 2 describes the state space representation of the looper and its main properties like the relative degree. Lastly, two different change of coordinates are computed, in order to transform the system in normal form. Different interpretations of the resulting zero dynamics are presented, depending on the transformation used.

- **Stability analysis.** Chapter 3 goes through the stability analysis of the looper. After a brief introduction on Lyapunov stability theory, local and global asymptotic stability of an equilibrium point are proved through respectively the first and the second coordinate transformation described in chapter 2. The stability analysis is performed through two different approaches, both based on Lyapunov stability theory.

- **Control.** Chapter 4 presents the drifting issue and two possible solutions, namely Baumgarte approach and a nonlinear stabilizer. Both the algorithms shows good performances. The nonlinear stabilizer performs better in terms of speed of convergence while Baumgarte algorithm turns out to be more reliable in terms of robustness to initial disturbances.

- **Possible developments.** The main results of this thesis deals with the stability analysis and the design of control algorithms for nonlinear mechanical systems. Two main topics could be further investigated.

    1. The nonlinear stabilization method presented in chapter 4 could be extended in order to use it as a more general control design procedure.
    2. The stability analysis proposed in chapter 3 could be tested on multidof mechanical systems, as briefly introduced in subsection 3.4.2.

List of Figures

Bibliography

[1] Claudio Melchiorri. *Slides fot Industrial Robotics*. 2015. Chap. Elements of kinematics and dynamics of Industrial Robots (cit. on pp. 3, 4).

[2] Rocco Vertechy. *Slides for Mechanics of machines for Automation*. 2017. Chap. 1,5,6 (cit. on pp. 4, 5).

[3] Haim Baruh. *Applied dynamics*. CRC Press, 2015. Chap. 8 (cit. on pp. 5, 6).

[4] Asano Kazuya et.al. "Hot strip mill tension-looper control based on decentralization and coordination". In: (1999) (cit. on p. 9).

[5] C.W. Gear. "Differential-Algebraic equation index transformations". In: (1988) (cit. on p. 21).

[6] Alberto Isidori. *Nonlinear Control Systems*. Springer, 1995. Chap. 4 (cit. on pp. 29, 35).

[7] Pierluigi Di Franco et.al. "A globally stable algorithm for the integration of high-index differential-algebraic systems". In: (2018) (cit. on pp. 1, 35, 68, 69, 71).

[8] J Baumgarte. "Stabilization of constraints and integrals of motion in dynamical systems". In: (1971) (cit. on pp. 1, 62, 65).